LBL-11497
GREMP-11
SSS-R-80-4313
UC-66

Reservoir Simulation Studies: Wairakei Geothermal Field, New Zealand

FINAL REPORT

J. W. Pritchett, L. F. Rice and S. K. Garg

JANUARY 1980

Geothermal Reservoir Engineering Management Program

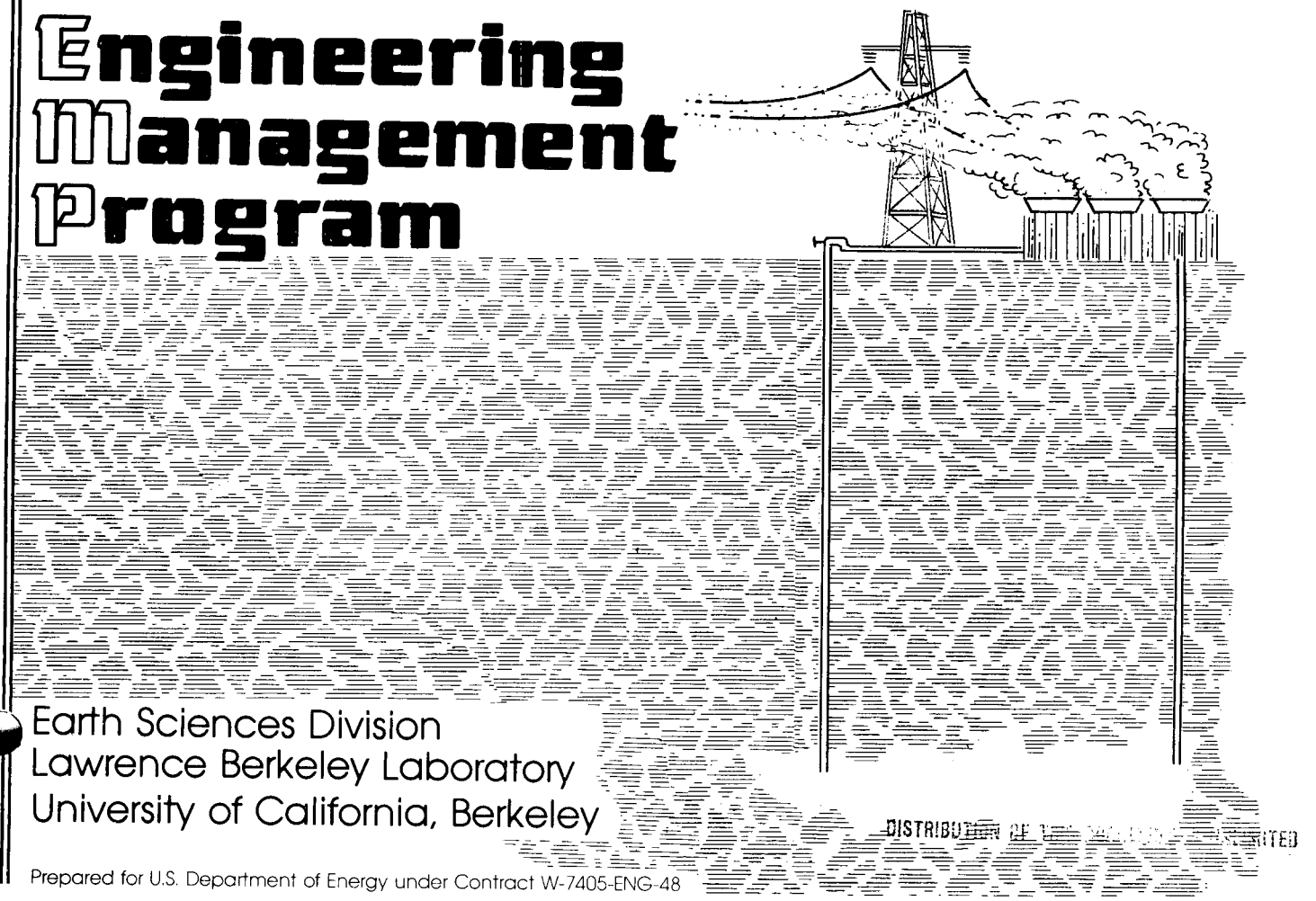

Earth Sciences Division
Lawrence Berkeley Laboratory
University of California, Berkeley

Prepared for U.S. Department of Energy under Contract W-7405-ENG-48

DISCLAIMER

Printed in the United States of America
Available from
National Technical Information Service
U.S. Department of Commerce
5285 Port Royal Road
Springfield, VA 22161
Price Code: A06

LBL-11497

GREMP-11

SSS-R-80-4313

RESERVOIR SIMULATION STUDIES: WAIRAKEI GEOTHERMAL FIELD, NEW ZEALAND

FINAL REPORT

J. W. PRITCHETT
L. F. RICE
S. K. GARG

PREPARED FOR:

UNIVERSITY OF CALIFORNIA
LAWRENCE BERKELEY LABORATORY
BERKELEY, CALIFORNIA 94720

PURCHASE ORDER NO. 3024102

THIS WORK WAS SPONSORED BY THE
U. S. DEPARTMENT OF ENERGY
DIVISION OF GEOTHERMAL ENERGY

JANUARY 1980

ACKNOWLEDGEMENTS

This report was prepared by Systems Science and Software, La Jolla, California under Lawrence Berkeley Laboratory (LBL) Purchase Order No. 3024102 and includes the results of research done through January, 1980. The subject research is pursuant to the LBL contract with the U. S. Department of Energy, Division of Geothermal Energy for Geothermal Reservoir Engineering Research. It was administered under the technical direction of K. Goyal, J. Howard, M. O'Sullivan, N. Narasimhan, and W. Schwarz. Mr. Paul Marshall was the Contract Administrator for LBL, under Contract W-7405-ENG-48.

This manuscript was printed from originals provided by the author.

TABLE OF CONTENTS

ABSTRACT

Numerical reservoir simulation techniques were used to perform a history-match of the Wairakei geothermal system in New Zealand. First, a one-dimensional (vertical) model was chosen; realistic stratigraphy was incorporated and the known production history was imposed. The effects of surface and deep recharge were included. Good matches were obtained, both for the reservoir pressure decline history and changes in average discharge enthalpy with time. Next, multidimensional effects were incorporated by treating a two-dimensional vertical section. Again, good history matches were obtained, although computed late-time discharge enthalpies were slightly high. It is believed that this disparity arises from inherently three-dimensional effects. Predictive calculations using the two-dimensional model suggest that continued future production will cause little additional reservoir pressure drop, but that thermal degradation will occur. Finally, ground subsidence data at Wairakei was examined. It was concluded that traditional elastic pore-collapse models based on classical soil-mechanics concepts are inadequate to explain the observed surface deformation. We speculate that the measured subsidence may be due to structural effects such as aseismic slippage of a buried reservoir boundary fault.

I. INTRODUCTION

This report presents the results of a one-year effort to model the Wairakei geothermal field in New Zealand. This project is an extension of work previously performed by Systems, Science and Software (S^3) in which a comprehensive data bank pertaining to the character, performance and response to production of the system was compiled (Pritchett et al. [1978]). The data collected in the prior phase of the effort forms the basis for the modeling study reported herein.

Using the reservoir data bank as a foundation, the modeling effort employed S^3's MUSHRM geothermal simulator to follow changes in the system with time. The conceptual model was developed in an evolutionary fashion. Starting with the existing geological and hydrological description of the system which has been assembled over the years by previous investigators, a preliminary model was devised and the MUSHRM simulator was used to calculate the consequences of that particular conceptualization. Then, differences between computed and observed reservoir response were noted and used to improve the original model. In this iterative manner, a self-consistent description of the reservoir was developed which can reproduce the known facts concerning the response of the system to production.

In the present effort, we began with a simple one-dimensional (vertical) description of the system, and followed the iterative procedure outlined above until a

satisfactory match with observations was obtained. Next, a two-dimensional vertical cross-section was considered; once again, an iterative sequence of computer simulations was performed until adequate agreement was obtained. Finally, a fully three-dimensional simulation was attempted. Unfortunately, limitations of time and funds precluded the completion of the iterative process for the three-dimensional case; therefore, in this report we will not, therefore, present the results of the three-dimensional simulations which we performed.

The first problem to be faced in the development of a model for Wairakei (whether 1-D, 2-D or 3-D) is to determine an initial (pre-production) state for the system which is self-consistent in the sense that it comprises a steady (or nearly steady) solution to the basic reservoir mechanics equations and is also consistent with early measurements. For Wairakei, although plentiful data exist concerning the character of the system after substantial production had occurred, data concerning the virgin state of the field is exceedingly sparse. Accordingly, to estimate the initial conditions, it was necessary to supplement the meager supply of known facts with extrapolations backward in time. In addition, estimates for initial heat flow, natural mass discharge, and initial reservoir pressure have been presented by several prior investigators.

Nonetheless, the initial state of the reservoir at Wairakei cannot be uniquely defined based on early measurements alone. In other words, it is possible to develop numerous different models of the reservoir in the pre-production state, all of which amount to steady

solutions of the governing equations which agree with the limited data set available, but which differ substantially among themselves. That is, each of these different pre-production states, if used as initial conditions for a production simulation, would produce a different reservoir response history. Therefore, an adequate reservoir model must match not only the early data but the known production history (pressures, discharge enthalpies, etc.) as well.

As discussed above, the authors chose to first perform a series of one-dimensional calculations to model the gross features of the system. This of course is an elementary idealized model. However, due to the observed horizontal uniformity of pressure response in the system, it was believed that it could provide information about the global characteristics of the system. This assumption proved to be correct, particularly with respect to recharge and the distribution of production from the grid system. This one-dimensional model satisfactorily reproduced the pressure and enthalpy histories of the field.

Additional complexity was then introduced by considering a two-dimensional vertical cross section. This model of the system was undertaken in an attempt to better define the spatial distribution of key parameters in the reservoir. The two-dimensional model yielded excellent agreement between the calculated and observed pressure histories. The enthalpy history proved to be somewhat less satisfactory. However, the authors believe that the discrepancy between observed and calculated enthalpies could be remedied by a three-dimensional model

of the system. Therefore, a three-dimensional model was undertaken. Of course, as additional dimensions are added to the problem, the difficulty of assigning appropriate parameters to the numerical simulator is increased. In many cases extrapolations of existing data were made to fill out the full three-dimensional grid. As discussed previously, the development of the three-dimensional model was terminated due to time and money constraints.

Chapter II of the report presents a brief history of the Wairakei system. Chapter III discusses the geology of the region. Chapter IV provides information about the pre-exploitation conditions of the system. Chapters V and VI present the results of the one and two-dimensional calculations, respectively. Chapter VII examines the subsidence which has occurred as a result of fluid production from Wairakei. Chapter VIII presents a summary of our conclusions and recommendations for future work.

II. DEVELOPMENT OF THE WAIRAKEI GEOTHERMAL FIELD

The development of the Wairakei field began in 1950 with a joint effort by Ministry of Works (MOW) and the Department of Scientific and Industrial Research (DSIR) to assess the geothermal potential of the Wairakei region of the thermal belt of New Zealand's North Island. Prior to this development, the region had been used primarily for recreational purposes. The study by MOW and DSIR concluded that some potential existed for electric power production. The demand for electrical power led to the commencement of the drilling of a sequence of shallow holes between Geyser Valley and Waiora Valley. These shallow bores demonstrated the presence of a substantial resource. In 1953 a deeper drilling plan was undertaken. It soon demonstrated even a larger resource than had originally been estimated.

In 1955 the decision to construct a 69 megawatt power plant was made and by 1957 the first stage of that plant was under construction. Estimates of ultimate power potential as high as 240 MW were made (Grindley [1957, 1965]). However, due to concern over possible unacceptable reservoir pressure drop and premature depletion, the decision was made to limit power production to somewhat less than its estimated potential. Wairakei has, therefore, been producing approximately 140 MW of electric power since the mid-1960's.

There are a total of 141 bores in the Wairakei/Tauhara region. Twelve of these are shallow pressure/temperature monitor holes and four are deep bores located in Tauhara. There has been essentially no production from

these sixteen holes. Of the remaining 125 bores, 26 consist of the "200 series" bores which were generally considered to be investigative holes when drilled. In fact, many of them have proved to be potentially very good producers. Of the 200-series, however, all but bore 216 are a considerable distance from the power plant, and hence have not been used for fluid production.

Of the remaining 99 bores, 65 have produced over their lifetime (defined herein as January 1, 1953 - December 31, 1976) a total of fluid in excess of 5×10^9 pounds per well. These 65 bores account for about 95 percent of the total fluid production from the Wairakei/ Tauhara system. The total mass production over the life of the field was 2329×10^9 pounds of fluid with an average discharge enthalpy of 481.64 BTU/pound.

Drilling activity at Wairakei ceased in 1968. Since that time, average mass production rates have been declining at about 4 percent per year. Bore field pressures have dropped more than 350 psi over the life of the field. Temperatures have also declined. Even though there has been somewhat of a degradation of the reservoir over its life, the generating capacity of the system has been maintained by improving the thermal efficiency of the power plant.

The Wairakei system is an ongoing operating facility which, even though it is being depleted, should last for many years to come. It has been a unique adventure, certainly in its inception. It was only the second geothermal power system to be constructed in the world -- the first ever to tap a liquid-dominated resource. Much has been written about this system. Here we do not intend

to reiterate those comments, but will instead describe our attempts to model the history of the reservoir so as to gain understanding about Wairakei in particular, and liquid-dominated systems in general. The historical data (1953-1976) assembled by Pritchett, et al. [1978] has played a major role in this effort. It would certainly be useful for the reader to acquaint himself with that information. In this report, data presentation has been limited to that which is directly relevant to the reservoir engineering analysis which we performed.

III. GEOLOGICAL STRUCTURE

The Wairakei geothermal field lies to the west of the Waikato River and to the north of Lake Taupo. The Tauhara geothermal region lies to the south-southeast of the Wairakei field. As discussed by Pritchett, et al. [1978], pressure evidence indicates that the Tauhara region is part of the same aquifer system as the Wairakei field.

The geology of the Wairakei geothermal region has been described by Grange [1937] and in much greater detail by Grindley [1965] and Healy [1965]. The geology of the Tauhara region has also been discussed by Grindley, et al. [1966]. A summary of these results is presented in Pritchett, et al. [1978]. In this section, discussion will be limited to that necessary to give a geologic picture of the region of interest for the reservoir engineering modelling efforts performed.

The Wairakei/Tauhara geothermal region lies in an active volcanic belt which extends from Mount Ruapehu south of Lake Taupo in a north-easterly direction to White Island in the Bay of Plenty. The volcanic region extends for 150 miles and is between 10 and 20 miles wide. The volcanic zone includes most of the active faults and hydrothermal areas as well as all the active volcanoes in the region. The Wairakei/Tauhara hydrothermal system is underlain by a nearly horizontal Quaternary acidic volcanic sequence. Grindley [1965, 1966, 1974] and Rishworth [1967] have examined the stratigraphic sequences at Wairakei and Tauhara and have found them to be in close

correlation. Their findings are also discussed in Pritchett, et al. [1978]. In general, the stratigraphic sequence of the region consists of the following formations (in order of increasing depth): Holocene pumice cover, Wairakei breccia, Huka Falls formation, Haparangi rhyolite, Waiora formation, Waiora Valley Andesites, Wairakei ignimbrites, and the Ohakuri group. A discussion of each of these formations is presented by Pritchett, et al. [1978]. It is important to note that there exist at least two aquifers in the above sequence, the Wairakei breccia and the Waiora formation. The Wairakei breccia is a shallow groundwater aquifer which is not used for power production due to its low temperature. The bulk of the mass produced is generally believed to come from the Waiora aquifer, and in particular from the interfaces between the Waiora, Ignimbrite and Andesite formations. These interfaces are believed to be highly fractured regions, thus accounting for the productivity of the wells which intersect them. In fact, most of the wells at Wairakei are located in regions of high permeability associated with major faults and fractures. Nevertheless, it is believed that the reservoir as a whole behaves like a porous medium (Mercer, et al. [1975]). In the main production region, the Waiora formation begins about 600-700 feet below the present land surface and is approximately 1500 feet thick. In the southeast and eastern regions of the field where the underlying ignimbrite formation dips steeply, the Waiora formation is up to 3000 feet thick. The boundary between the Waiora and the Wairakei ignimbrites is not well defined; fracture zones and the irregular surface of the unconformity between the ignimbrites and the aquifer provide a region

of locally high permeability. The Wairakei ignimbrite is a rock of low primary permeability. However, it is extensively faulted, and it is generally believed that these fault zones in the ignimbrites serve as conduits for hot water recharge to the Waiora aquifer from below. Recharge and discharge to the Waiora aquifer from above take place through the overlying Huka Falls formation, again a formation of relatively low primary permeability. The Huka Falls above and the Ignimbrites below act as aquitards for the Waiora formation, the region of primary fluid production from the field. A deeper third aquifer may also exist in the Ohakuri group below the ignimbrites. However, very little information about this formation is available since it has only been encountered in two boreholes at Wairakei.

Figure 3.1 is a general map of the area showing cross-sectional lines corresponding to Figures 3.3 through 3.7. The legend for Figures 3.3 through 3.7 is given in Figure 3.2. The cross-section presented in Figures 3.3 through 3.6 show the stratigraphy through the Wairakei region and Figure 3.7 presents a cross-section of the Tauhara region. A more complete set of cross-sections of the entire region is presented in Pritchett, et al. [1978].

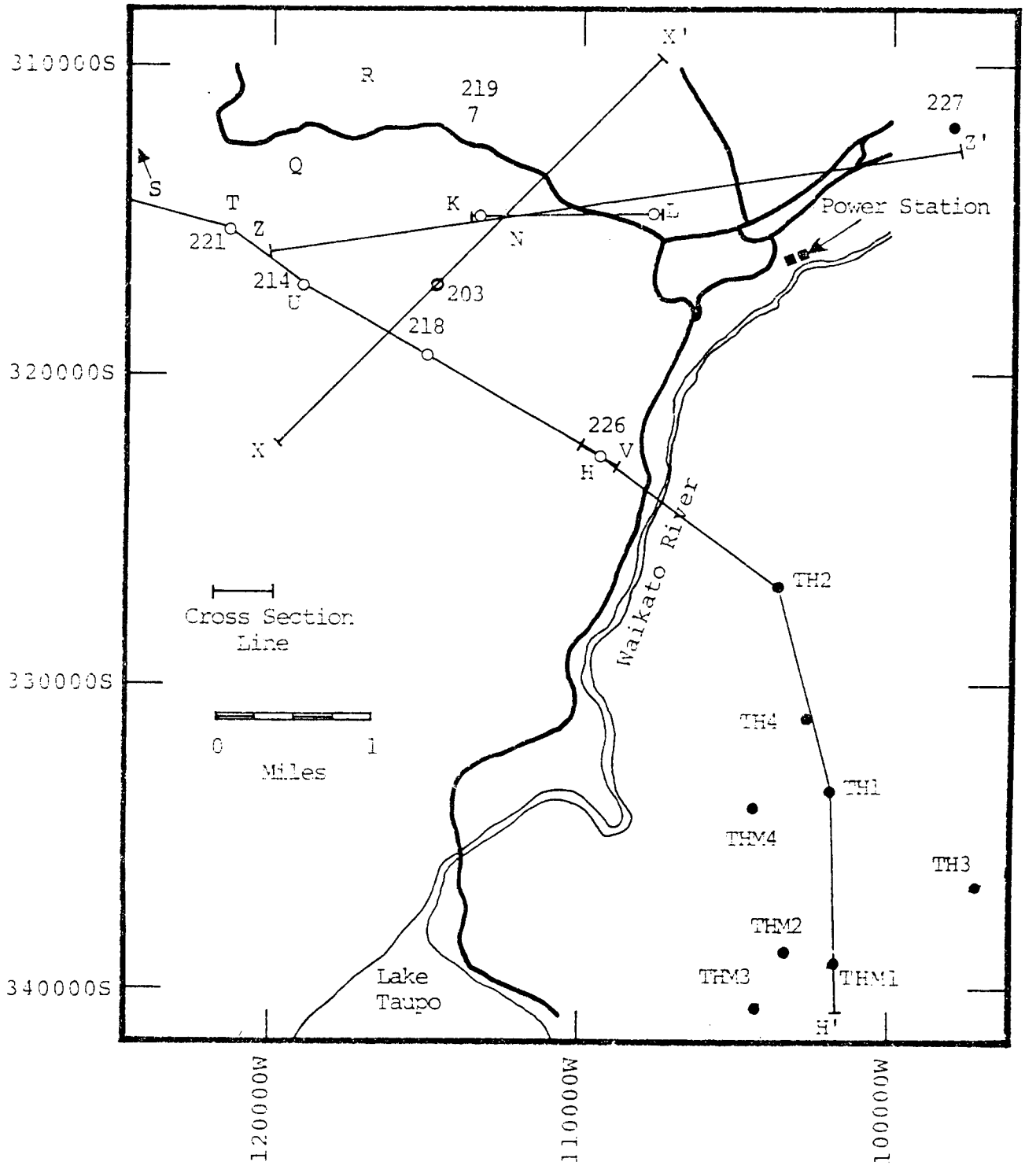

Figure 3.1. Locations of cross-sections shown in Figures 3.3 through 3.7.

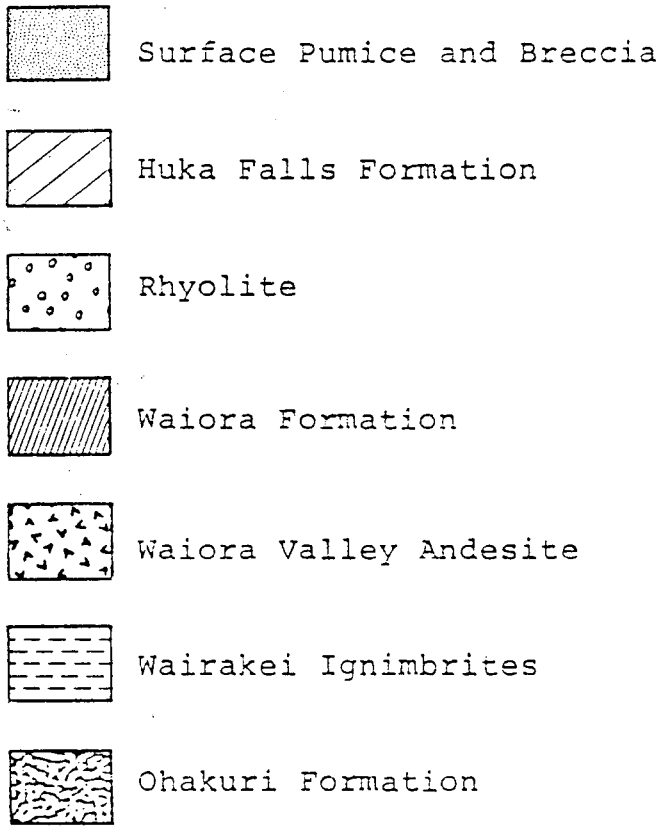

Figure 3.2. Legend for cross-sections in Figures 3.3 through 3.7.

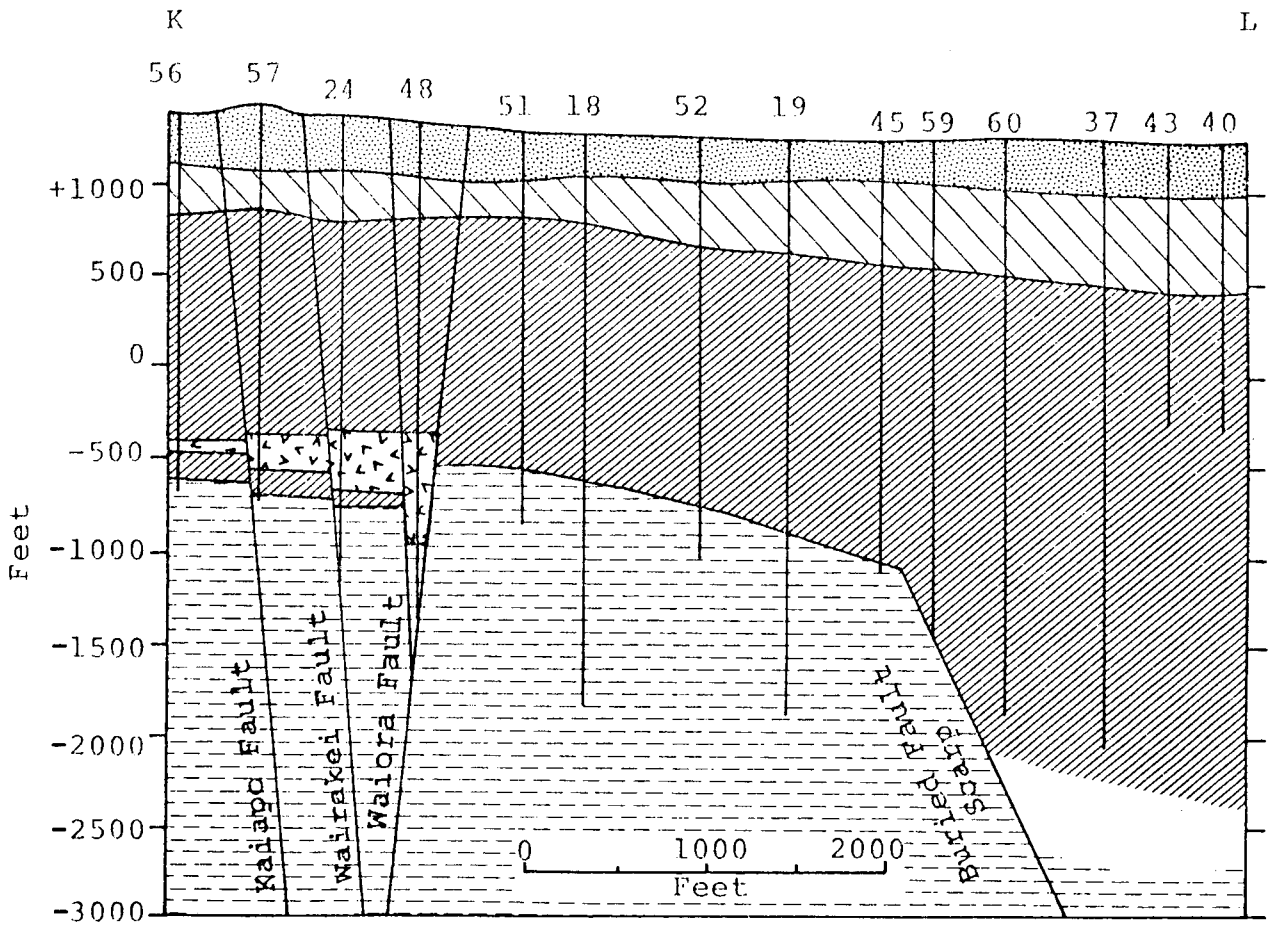

Figure 3.3. Section KL [after Grindley, 1965].

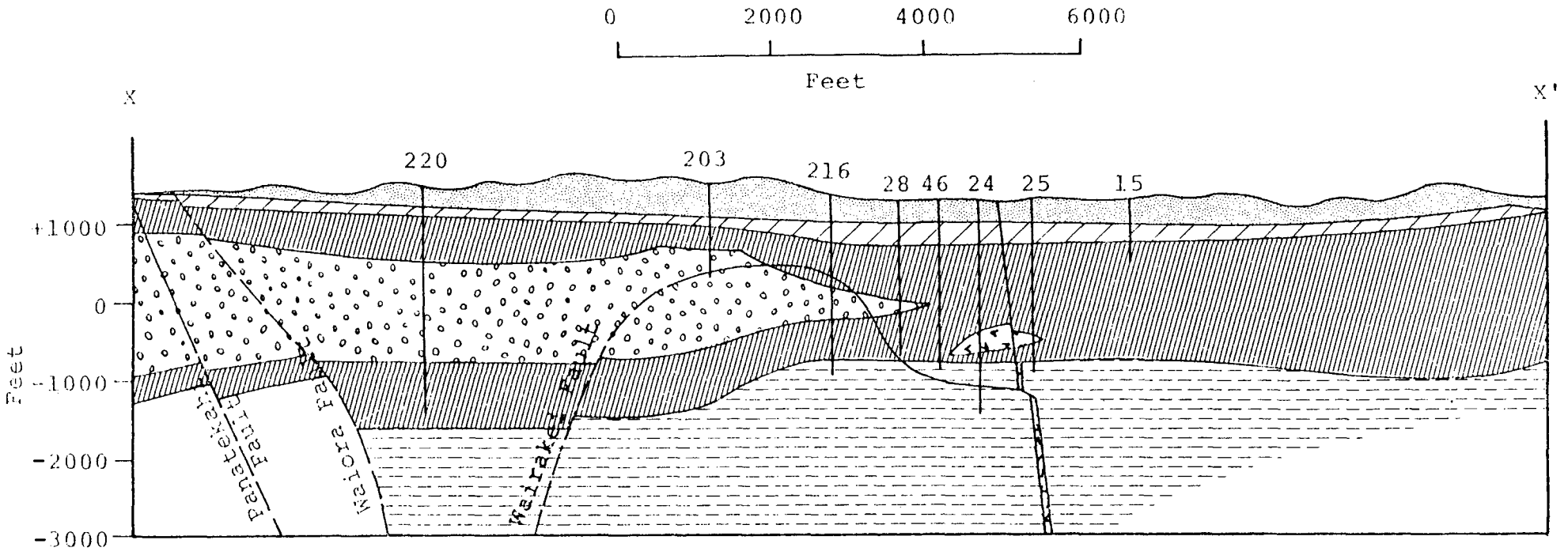

Figure 3.4. Section XX' [after Grindley, 1965].

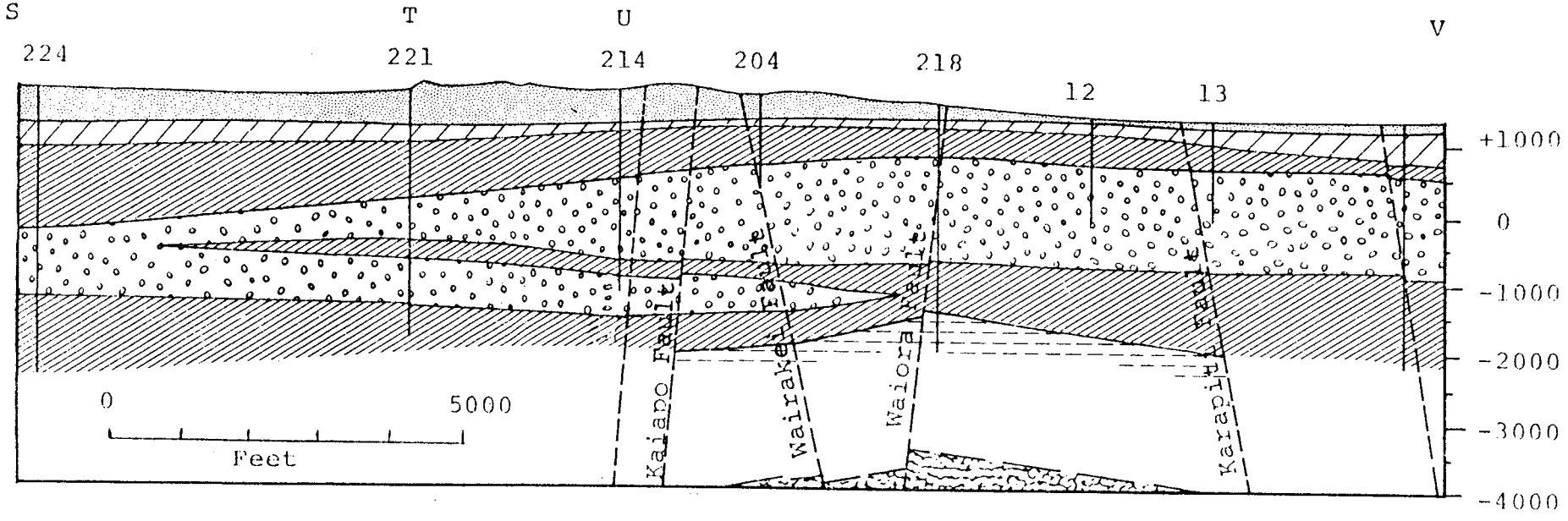

Figure 3.5. Section STUV [after Grindley, 1965].

SSS-R-80-4313

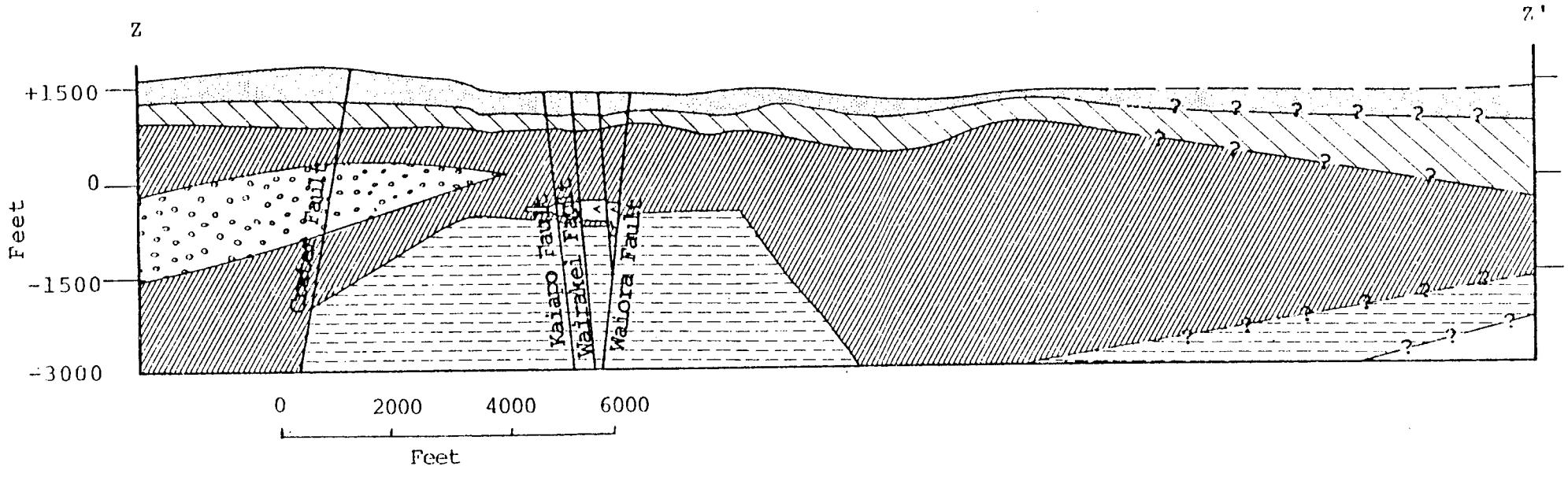

Figure 3.6. Section ZZ' [after Pritchett, et al., 1976, and including log data for bore 227].

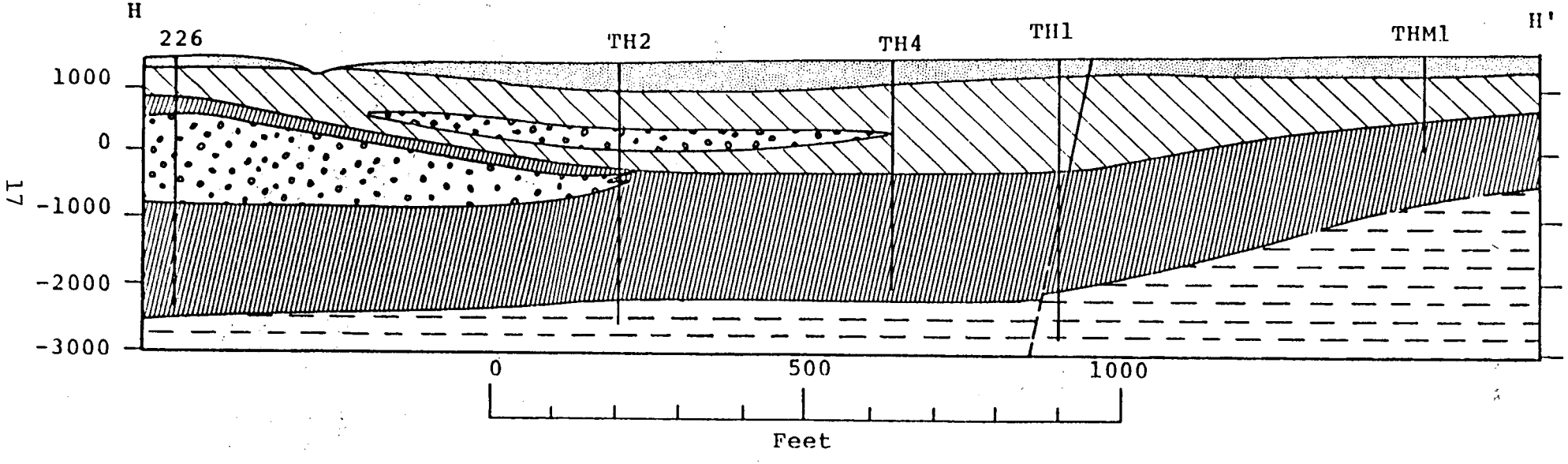

Figure 3.7. Section HH' [after Grindley, et al., 1966].

IV. INITIAL STATE OF THE WAIRAKEI SYSTEM

To make calculations of the response of a geothermal reservoir to fluid production, an adequate description of the initial state of the system which prevailed prior to exploitation is necessary. In particular, good measurements are needed of the initial pressure and temperature distributions, natural heat flow at the surface and the sources and nature of any recharge to the system. Furthermore, information about the location and nature of the reservoir boundaries is useful in formulating a model of the reservoir.

As discussed by Pritchett, et al. [1978], a large quantity of data has been collected about the Wairakei system. Unfortunately, early measurements at Wairakei, i.e., those taken to measure pre-production conditions, are very sparse. Furthermore, the quality of this early data is questionable; this is particularly true of temperature measurements. Therefore, all our analyses are based, as are those of other investigators, on an incomplete data set.

Several resistivity surveys of the Wairakei region have been made in an attempt to delineate the boundaries of the reservoir system [see Pritchett, et al., 1978]. Figure 4.1 shows the spatial relationship among the various peripheral wells, the main bore field, and the resistivity boundary of the Wairakei/Tauhara field. It is generally believed that the resistivity boundary of the field can be taken as the region between the 10 and the 20 ohm-meter contours. Although the Wairakei field itself

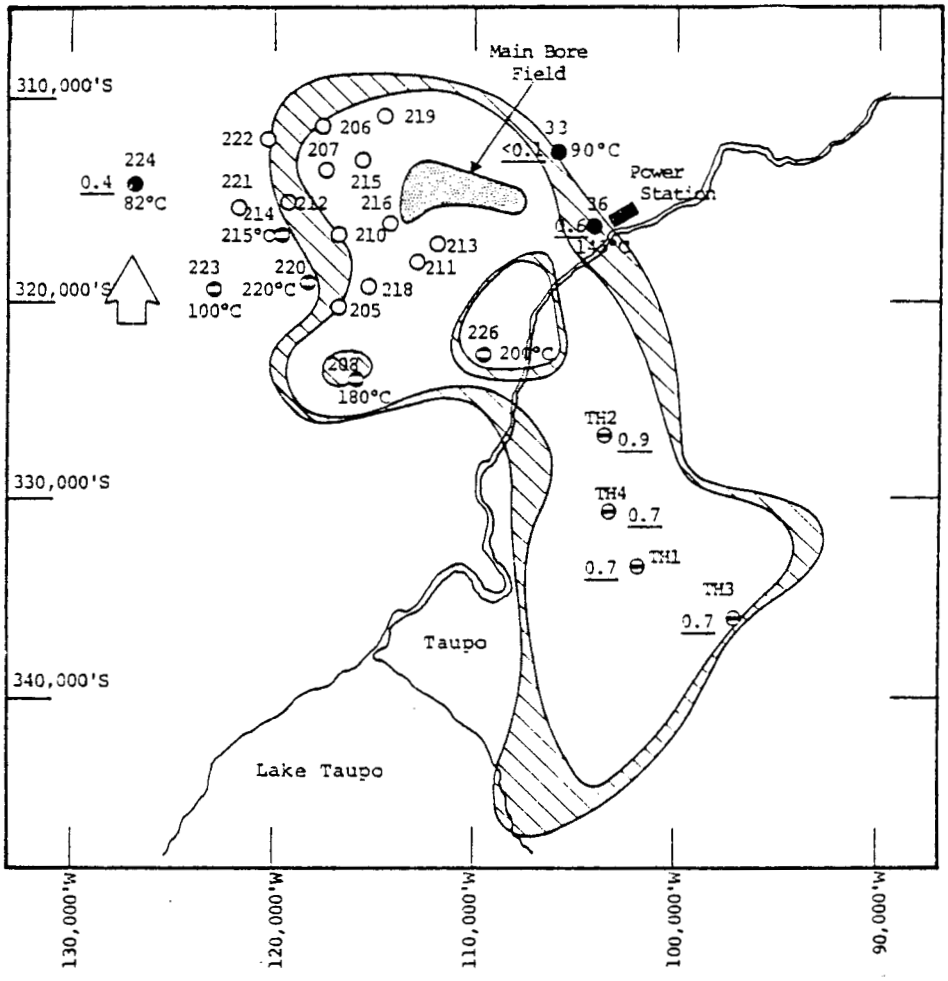

Coordinates are feet with respect to 1949 Maketu datum

"Resistivity boundary" of the field between 10 and 20 ohm-meters.

25 ○ Location and numbers of bores with maximum temperature > 225°C and with pressure histories matching main bore field.

0.6 36 ● 145°C Bore with maximum temperature < 225°C (i.e., 145°C) and with total pressure drop only a fraction (i.e., 0.6) of that of the main bore field as of mid-1968.

◒ 223 100°C Bore with low maximum temperature whose pressure history follows main bore field.

0.9 TH2 ◒ Bore with maximum temperature > 225°C with less pressure drop than main bore field.

Figure 4.1. Pressure and temperature distribution surrounding the main bore field.

covers only about fifteen square kilometers, the resistivity boundary certainly encloses a much larger region, since it suggests that Wairakei and Tauhara are connected. Downhole pressure measurements provide additional insight into the extent of the field. As discussed by Pritchett, et al. [1978], and as shown by inspection of Figure 4.1, the pressure response in the 200 series wells indicates that any impermeable boundary of the field must extend beyond the resistivity boundary to the west. The pressure response in the Tauhara wells to exploitation of the Wairakei main bore field leaves little doubt that the Tauhara and Wairakei systems are hydrologically connected. On the other hand, the lack of pressure response in Bore 33 suggests that the hydrological boundaries of the field coincide with the resistivity boundary to the northeast.

The Wairakei geothermal area was employed primarily for recreational purposes prior to its exploitation for the production of electrical power. Indeed, Wairakei and the neighborhood were popular tourist attractions, primarily due to the various geysers, hot pools and similar phenomena in the area. The most prominent such features were the geysers in Geyser Valley (just north of what became the main bore field at Wairakei), the thermal pools of the Waiora Valley (to the west), the Karapiti area (to the south) including the Karapiti Blowhole fumarole, and the geysers at the Spa Sights in the Tauhara region.

With the development of the Wairakei field, much of this natural activity has subsided. Activity in the Geyser Valley began to decline as early as 1954, and the

attraction was finally closed in 1972. The Waiora Valley, on the other hand, has continued to be active. The Karapiti Blowhole has ceased to discharge as have the geysers at the Spa Sights. As a general rule, surface manifestations such as geysers and hot springs have declined, whereas "steaming ground" has become more extensive. These observations are consistent, of course, with production-induced pressure drop in the reservoir and with an increase in the system volume occupied by steam (as opposed to liquid water).

Numerous assessments of the natural heat flow at the surface of the Wairakei region have been carried out since 1951. According to Fisher [1964] the estimates for total heat flow lie between 343 and 682 megawatts. Fisher concludes that the best estimate for heat flow (assuming a reference temperature of 285°K) is approximately 418 megawatts. Although no direct measurements of the natural mass discharge at the surface are available, estimates have been made from the heat flow data since it is assumed that the bulk of the natural heat flow is associated with the natural mass flux at the surface. Dawson and Dickinson [1970] present the partition of the heat loss due to several physical mechanisms. They estimated that less than three percent of the heat loss was due to convection. Therefore, using this assumption and assuming a mean enthalpy of 1025 joules/gram, Fisher obtained an estimate of the mass discharge of 440 kg/sec for the 1951-1952 period. The mass discharge at the surface is believed to have declined with time as the field has been developed.

Temperatures at Wairakei have been measured periodically throughout the life of the system. Grange [1937] presented a description of the thermal activity in New Zealand as part of a general geological survey. However, only with the interest in the development of the Wairakei system in the 1950's were regular temperature measurements made in the boreholes. The temperature measurements are all subject to considerable uncertainty (see Banwell [1955] and Pritchett, et al. [1978]) due to convective currents occurring in the borehole and because of the lack of equilibration time between drilling operations and some of the temperature runs. It is possible, however, to deduce general trends. Temperatures increase rapidly with depth down to the top of the Waiora formation where the temperature in the hotter region is about 200°C. In the Waiora aquifer, the temperature gradient is reduced, with maximum recorded temperatures near the bottom of the formation being about 250-260°C. Malcolm Grant (personal communication, 1979) believes that the early measured temperature and pressure readings in the original wells may reasonably be taken as representative of the pre-exploitation state of the system. He bases this belief on the fact that very little mass discharge occurred during the early 1950's. Pritchett, et al. [1978] present a suite of temperature profiles for the system. However, as they point out, the details of these profiles should be used with great caution. Indeed, the authors believe, as does Bolton [1970, 1977], that the reported temperature profiles within individual boreholes at best provide only an indication of the maximum temperature encountered by the well.

No direct reservoir pressure measurements were made at Wairakei during the early days. Instead, the wellhead pressures in wells standing shut and full of water were employed to calculate the pressures at depth. The temperature profiles measured in these shut-in wells together with the water level made it possible to calculate a density profile. Then, assuming hydrostatic equilibrium, the pressure profile within the bore was determined.

Inasmuch as the wellhead pressure declined very rapidly in some cases with production, a determination of the undisturbed pressure is uncertain. Using these techniques, however, it is estimated that the pre-exploitation pressure at RL-900 feet (i.e., 900 feet below sea level) lies between 880 and 900 psi. Since within shut-in bores the pressure distribution is essentially hydrostatic, a single datum such as the RL-900 feet levels can be used to approximate the entire pressure profile.

V. ONE-DIMENSIONAL SIMULATION

A series of one-dimensional calculations was first undertaken in order to gain understanding of the gross behavior of the reservoir system. The one-dimensional vertical mode of simulation was chosen for these preliminary calculations because of the apparent horizontal uniformity of behavior of the system, particularly the nearly uniform pressure drop across the main part of the reservoir with time.

The grid configuration used for these one-dimensional calculations is shown in Figure 5.1. This geometry approximates the average lithologic sequence underlying the main borefield. The grid consists of a vertical column of 22 grid blocks as shown in the figure, with block number 1 being the deepest and block number 22 lying just below the ground surface. The assumed stratigraphic sequence is as follows: 100 meters of breccia, then 100 meters of Huka Falls formation, then 675 meters of Waiora aquifer, with ignimbrites below. The rock properties used for this calculation are presented in Table 5-1. Throughout the series of one-dimensional calculations which were performed, several different relative permeability curves were used.

The steam phase must be sufficiently mobile at low steam saturations to give the observed increase in the enthalpy of the produced fluid at early times, and also to prevent buildup of steam phase in the production horizon at late times. Considerable numerical experimentation was required to deduce the appropriate relative permeability

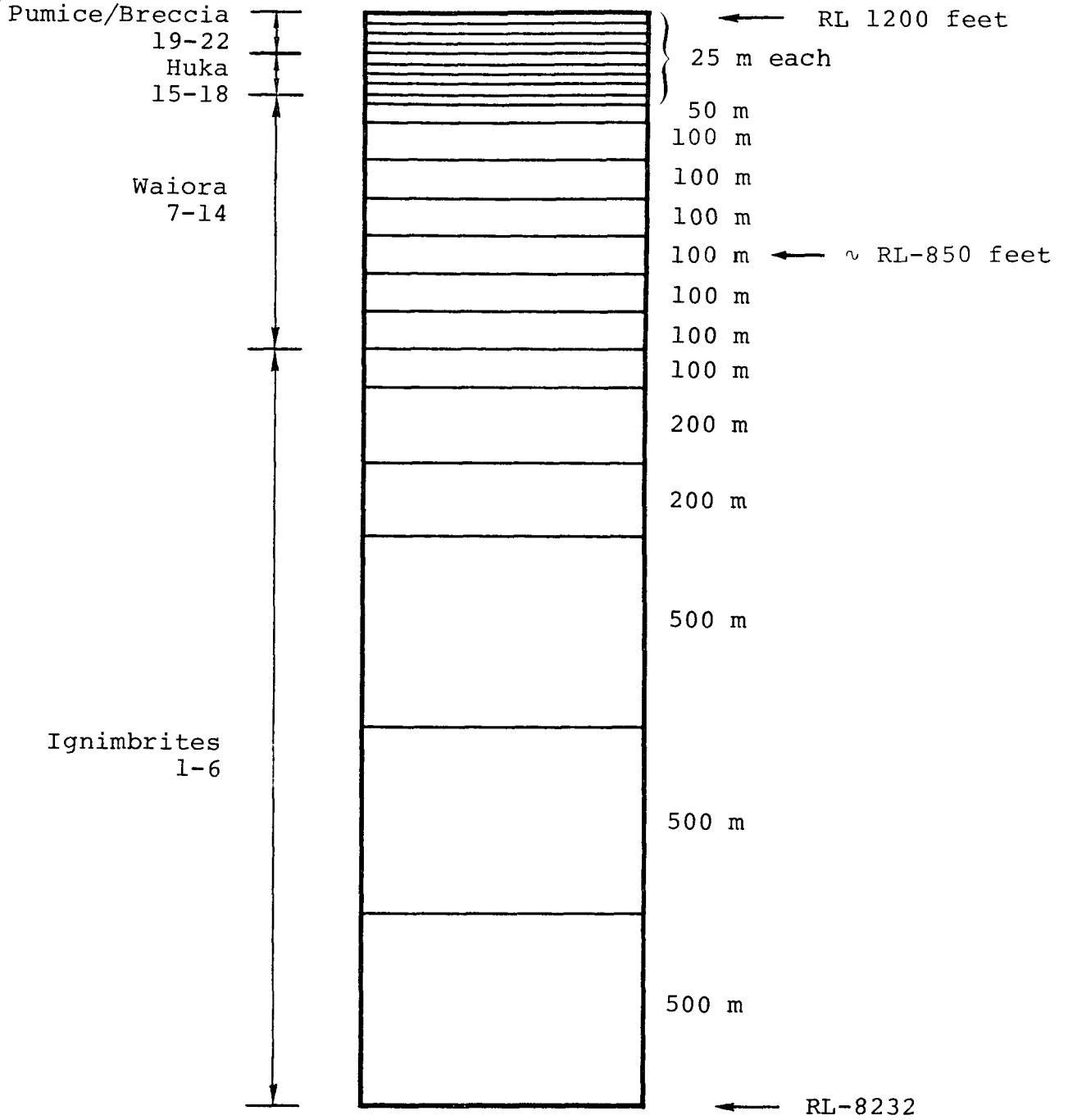

Figure 5.1. Grid Used for One-Dimensional Calculations.

TABLE 5-1

ROCK PROPERTIES USED IN ONE-DIMENSIONAL SIMULATION

ROCK TYPE	POROSITY	DENSITY (g/cc)	THERMAL CONDUCTIVITY (ergs/sec-cm°C)	HEAT CAPACITY (ergs/gram-°C)	VERTICAL PERMEABILITY (md)	UNIAXIAL MODULUS ($dyne/cm^2$)
Pumice/Breccia	.244	2.15	5×10^5	9.390×10^6	100	1.7×10^9
Huka	.199	2.26	5×10^5	8.757×10^6	1	5.0×10^9
Waiora	.194	2.27	5×10^5	8.475×10^6	50	5.0×10^9
Ignimbrites	.072	2.54	5×10^5	7.666×10^6	20	5.0×10^{10}

curves. Corey relative permeability relations were found to give unacceptably large variations in the enthalpy of the produced fluid. Those relative permeability curves which produced the best results in matching the production pressure and enthalpy histories are illustrated in Figure 5.2.

For the one-dimensional case, the initial temperature distribution was estimated based on the (admittedly very sparse) early temperature measurements. From the ground surface to a depth of 150 meters, temperature was taken as approximately linear with depth, with a surface temperature of 20°C and a temperature gradient of about 1°C/meter. Below 150 meters, the temperature gradient begins to decline with increasing depth; the assumed initial temperature profile reaches 256°C at a depth of 525 meters. Below 525 meters, temperature was taken as constant (256°C). In reality, temperature probably should continue to rise slowly with depth below 525 meters, but available measurements are inadequate to determine the deep temperature gradient. The computed response, in any event, should be relatively insensitive to the temperature gradient assumed at great depth.

The initial pressure distribution was then computed by assuming a pressure of one bar at the ground surface and then calculating a hydrostatic distribution of pressure with depth, subject to the initial temperature distribution, for zones 15-22 (depth from zero to 200 meters). For zone 14, which is the top layer of the Waiora formation, the initial pressure (20.36 bars) was taken equal to the saturation pressure corresponding to the initial temperature for that zone (213°C). Below zone

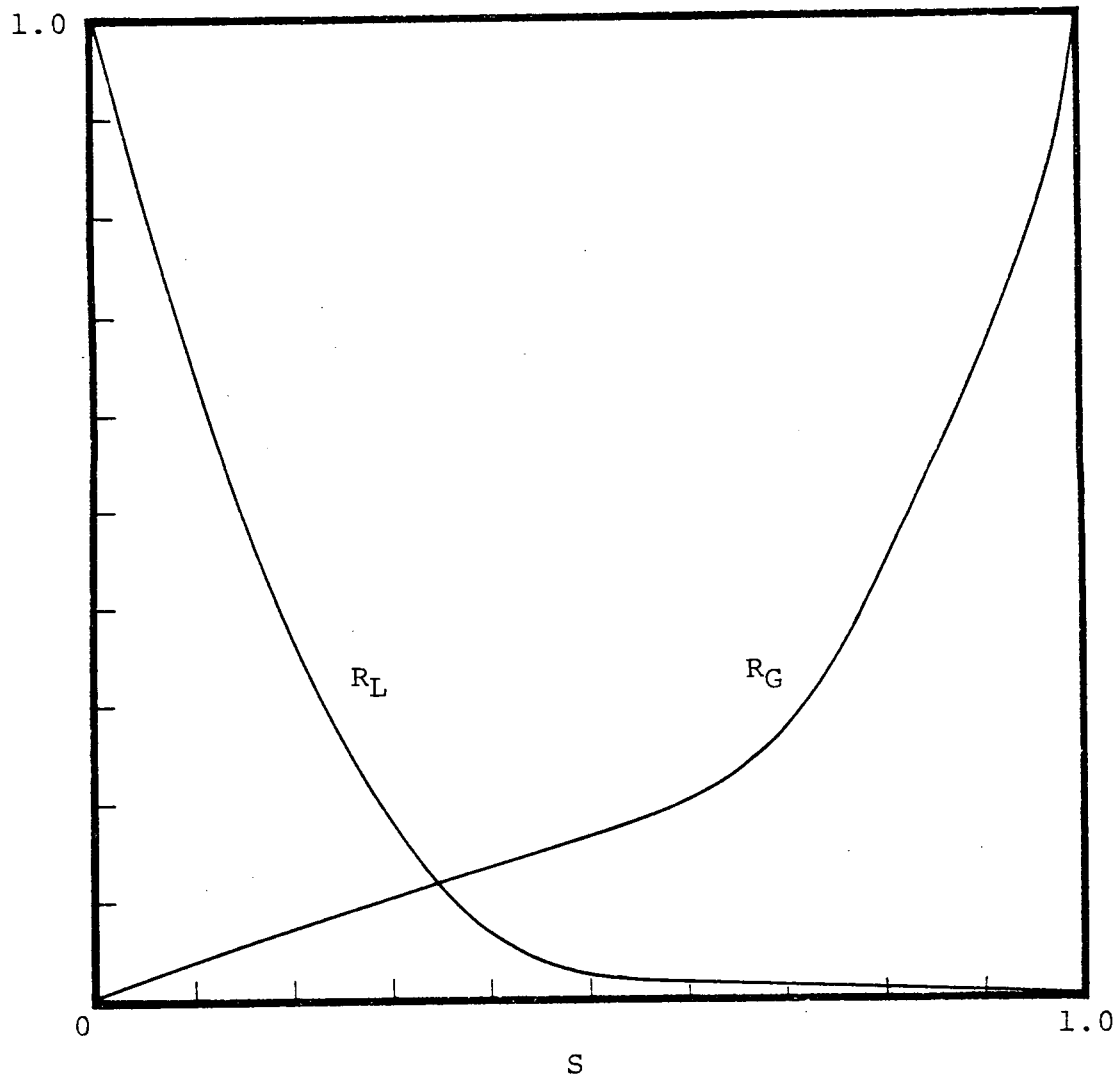

Figure 5.2. Relative Permeability Curves used for One-Dimensional Simulation.

14, the pressure distribution was again assumed to be hydrostatic. The initial distributions of temperature, pressure and vapor saturation are summarized in Table 5-2.

It should be noted that the initial conditions assumed, as shown in Table 5-2, imply that a two-phase region existed prior to production at Wairakei, near the top of the Waiora aquifer. Early analyses of the field by other investigators (Mercer, et al. [1975]) have assumed that Wairakei was initially single-phase liquid, and that two-phase behavior began only after substantial fluid production had taken place. Recent studies of the Wairakei data clearly indicate, however, that Wairakei must have contained a "steam cap" (a region in which liquid water and steam coexist) prior to production. First, as pointed out by Pritchett, et al. [1978], the effective compressibility of the reservoir fluid, as deduced from the initial relation between reservoir pressure drop and cumulative production, is far too great for an all-liquid system; some indeterminate quantity of high-compressibility steam must have been present at the outset. Also, Pritchett [1979] recently analyzed very early discharge enthalpy data from a few early wells located within the boundaries of the present main bore-field. A number of these wells, completed in the upper part of the Waiora aquifer, were characterized by anomolously high discharge enthalpies from the very beginning. These high discharge enthalpies can only be explained by the presence of a steam cap.

Together with the initial conditions (discussed above), we imposed boundary conditions in a straight-forward way; the pressure and temperature at the top (D=0,

TABLE 5-2

INITIAL CONDITIONS FOR ONE-DIMENSIONAL SIMULATION

LAYER NUMBER	PRESSURE (bars)	TEMPERATURE (°C)	INITIAL STEAM SATURATION (%)
Top Boundary Condition =	1.00	20	
22	2.22	30	
21	4.61	55	
20	6.98	80	
19	9.32	105	
18	11.64	130	
17	13.93	155	
16	16.16	175	
15	18.32	200	
14	20.36	213	56
13	23.45	220	
12	29.51	232	
11	37.40	246	
10	45.14	256	
9	52.90	256	
8	60.66	256	
7	68.42	256	
6	76.20	256	
5	87.88	256	
4	103.49	256	
3	130.90	256	
2	170.25	256	
1	209.79	256	
Bottom Boundary Condition =	229.66	256	

P=1 bar, T=20°C) and at the bottom (D=2875 meters, P=229.7 bars, T=256°C) were maintained constant throughout the production calculation. This permits recharge to take place both from surface groundwater and from below the geothermal reservoir.

A major product of the earlier data collection effort (Pritchett, et al. [1978]) was a magnetic tape containing, among other data, locations, depths of open intervals, and monthly production totals for each well at Wairakei. The monthly production data (summed over all wells) is shown in Figure 5.3. The production data stored on this magnetic tape was used to drive the one-dimensional simulation, as follows. First, the total production data for all wells was averaged on an annual basis, so that average total production rates for each year were obtained as shown in Figure 5.4. The next task was to allocate the production vertically. For each year of production, the open intervals in each well which actually produced fluid during the year were projected onto the grid. For each year, the composite of all such projections determined the list of grid blocks from which fluid would be withdrawn. For the entire history, this procedure yielded production only from blocks 7-14 (the Waiora aquifer); in any particular year, not all of these zones were necessarily productive.

With the productive layers identified for each year, the total annual fluid production was allocated among the various layers using kinematic mobility weighting. Let us consider a well of radius r_w producing from a layer of thickness h_i. The liquid (steam) mass flow to the well is given by

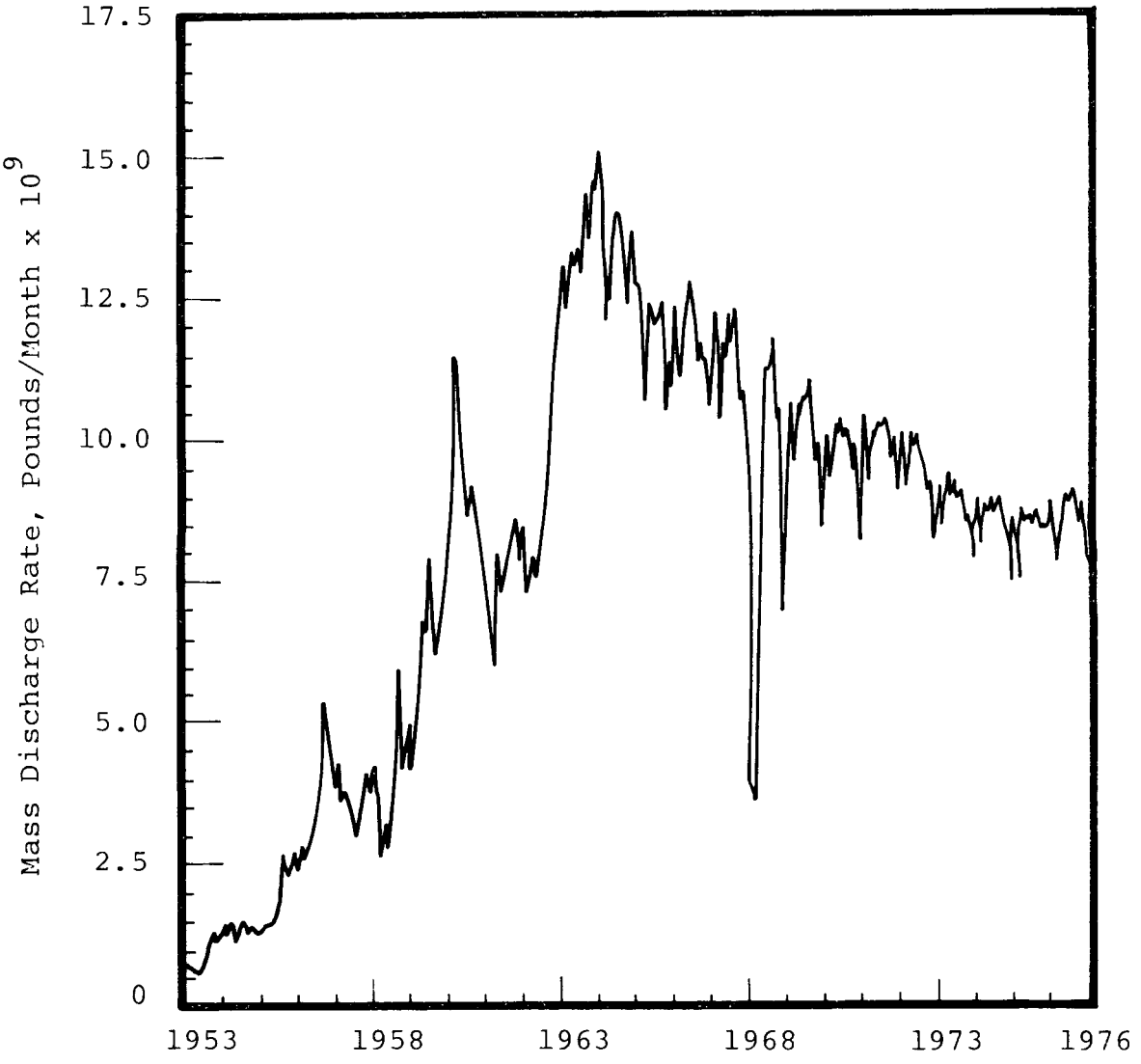

Figure 5.3. Mass discharge rate (all bores) as a function of time.

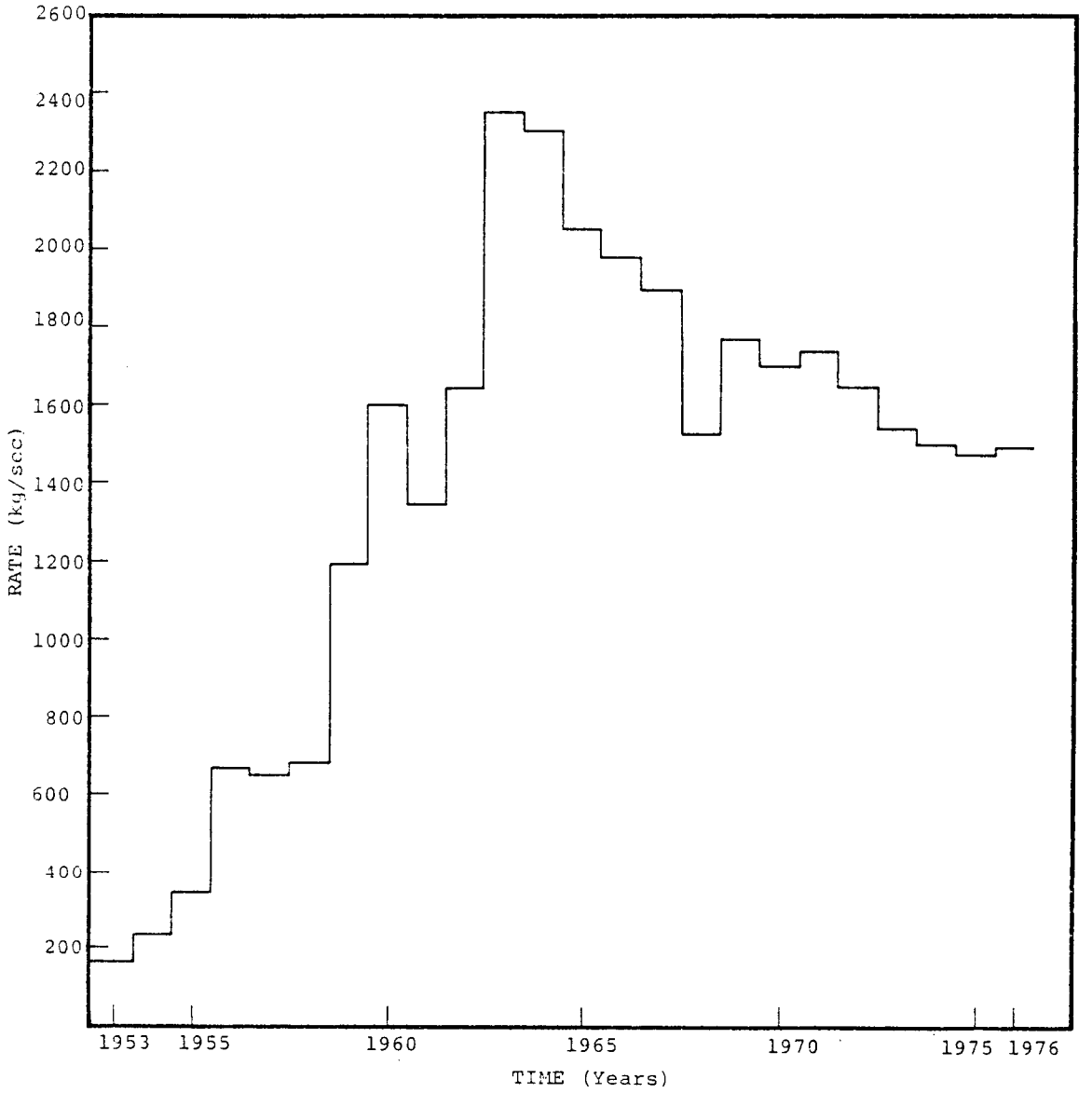

Figure 5.4. Discharge Rate from Wells (yearly averages).

$$\dot{m}_{\ell,g} = 2\pi\, r_w\, h_i\, \rho_{\ell,g}\, v_{\ell,g} \qquad (5\text{-}1)$$

where

$\rho_\ell (\rho_g)$ = liquid (steam) phase density
$v_\ell (v_g)$ = liquid (steam) phase volume flux.

Recalling Darcy's law

$$v_{\ell,g} = \frac{-k\, R_{\ell,g}}{\mu_{\ell,g}} \frac{\partial p}{\partial r} \qquad (5\text{-}2)$$

where

$R_\ell\ (R_g)$ = liquid (steam) phase relative permeability
$\mu_\ell\ (\mu_g)$ = liquid (steam) phase viscosity,

Equation (5-1) can be rewritten as

$$\dot{m}_{\ell,g} = -2\pi\, r_w\, h_i \left(\frac{k\, R_{\ell,g}}{\nu_{\ell,g}} \right) \frac{\partial p}{\partial r} \qquad (5\text{-}3)$$

where

$$\nu_{\ell,g} = \frac{\mu_{\ell,g}}{\rho_{\ell,g}} = \text{kinematic viscosity.}$$

The fraction of liquid (steam) flow is, therefore, given by:

$$\frac{\dot{m}_{\ell,g}}{\dot{m}_\ell + \dot{m}_g} = \frac{h_i\, (k/\nu)_{\ell,g}}{h_i\, (k/\nu)_T} \qquad (5\text{-}4)$$

where

$(k/\nu)_{\ell,g}$ = kinematic mobility for liquid (steam) phase $(= kR_{\ell,g}/\nu_{\ell,g})$,

$(k/\nu)_T$ = $(k/\nu)_\ell + (k/\nu)_g$ = total kinematic mobility.

The generalization of Equation (5-4) for N layers (i = 1, 2, ... N) is given by:

$$\frac{\left(\dot{m}_{\ell,g}\right)_i}{\dot{m}} = \frac{h_i \left[(k/\nu)_{\ell,g}\right]_i}{\sum h_i \left[(k/\nu)_T\right]_i} \qquad (5\text{-}5)$$

where

$$\dot{m} = \sum_{i=1}^{N} (\dot{m}_\ell + \dot{m}_g)_i \quad .$$

The MUSHRM reservoir simulator employs the above scheme to calculate the mass sinks at each time step as an integral part of the calculational procedure; however, no external printouts of the individual mass sinks are produced.

Finally, the surface area of the system must be determined. Initially, we treated the effective area as constant. Clearly, however, as time goes on the effective area should increase somewhat with time, reflecting the effects of lateral recharge. Somewhat arbitrarily, therefore, we used an effective reservoir area of seven square kilometers for the first ten years of production, then increased the area to 8.5 square kilometers thereafter.

Results of the final one-dimensional simulation are shown in Figures 5.5, 5.6, 5.7 and 5.8. Figure 5.5 shows that, as time goes on, the two-phase region increase markedly in size. This occurs, of course, because production-induced pressure drop causes more and more of the fluid in the reservoir to reach saturation conditions. Figures 5.6 and 5.7 show that both the pressure response and average discharge enthalpy histories for the field are reasonably well matched by this calculation. As the field data shows (see Pritchett, et al. [1978]), at depths exceeding 500 meters or so the pressure drop as a functon of time was remarkably uniform at Wairakei throughout the vicinity of the main borefield; the scatter band of measurements of this type is indicated in Figure 5.6 along with the calculated deep pressure drop history produced by the one-dimensional simulation. The discharge enthalpy histories for individual wells vary substantially from well to well, due to differences in location and completion depth, but the average discharge enthalpy for the field as a whole shows the general trend indicated in the scatter band of Figure 5.7, consisting of a general rise in overall discharge enthalpy until the mid-1960's, followed by a gradual decline. Qualitatively, the same general trend is evident in the results of the present one-dimensional simulation, although early discharge enthalpies are somewhat lower than measured values and the enthalpy maximum is delayed slightly, to about 1970.

Figure 5.8 shows the recharge to the Waiora formation from the top (i.e., Huka Falls) and the bottom (i.e., Wairakei Ignimbrites) boundaries. As can be seen,

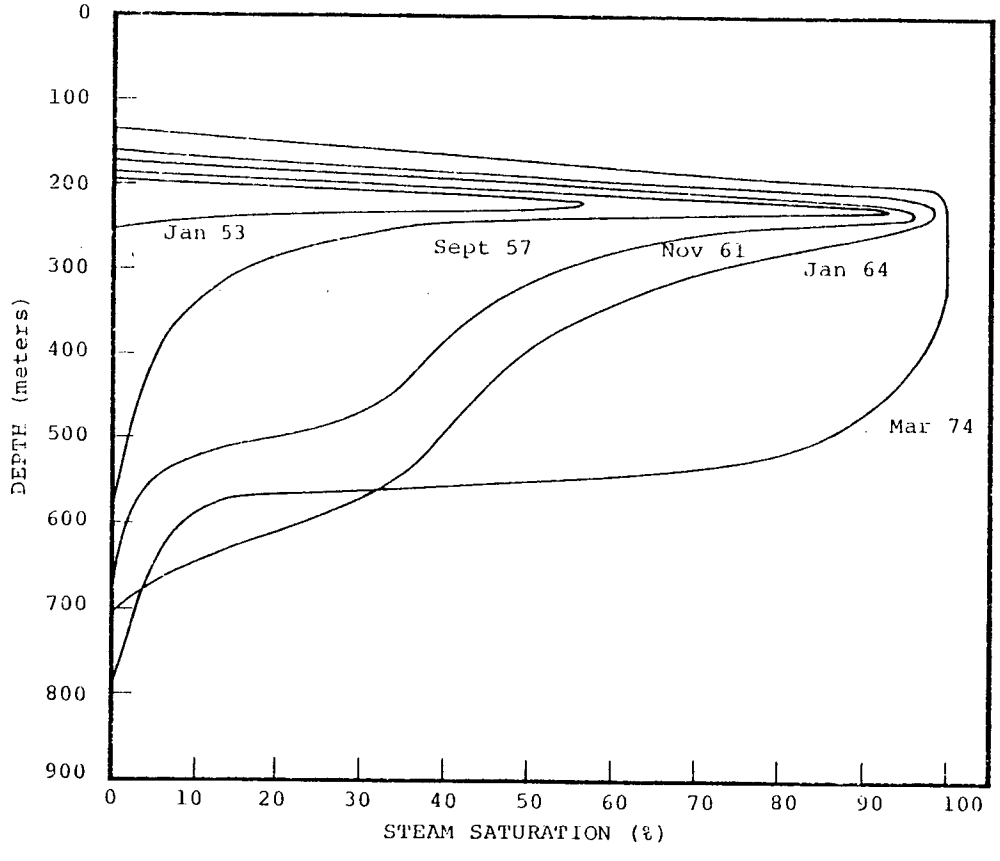

Figure 5.5. Steam Saturation Distribution for One-Dimensional Simulation at Various Times.

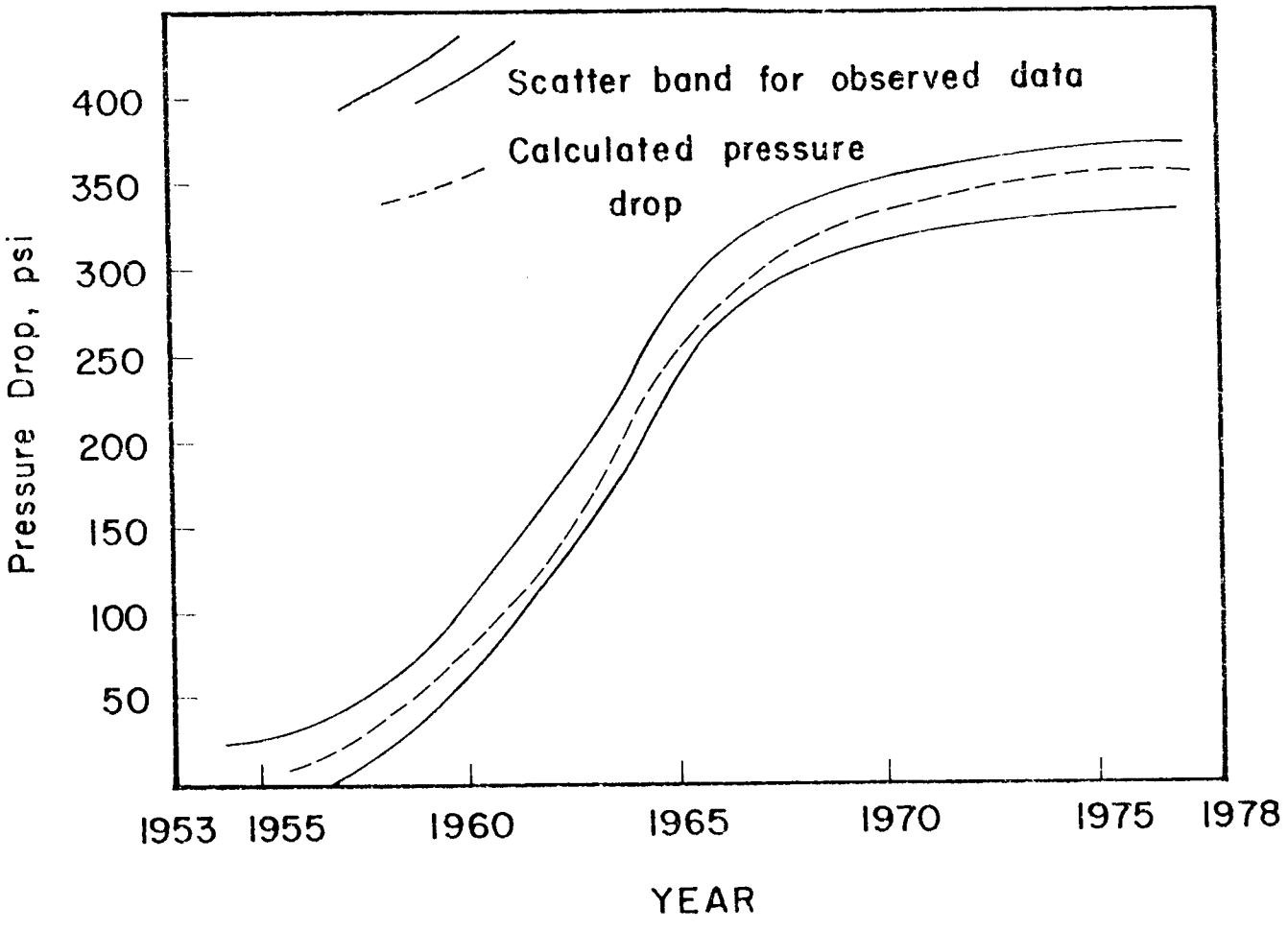

Figure 5.6. Calculated Pressure Drop at about RL - 900 feet: One-Dimensional Case.

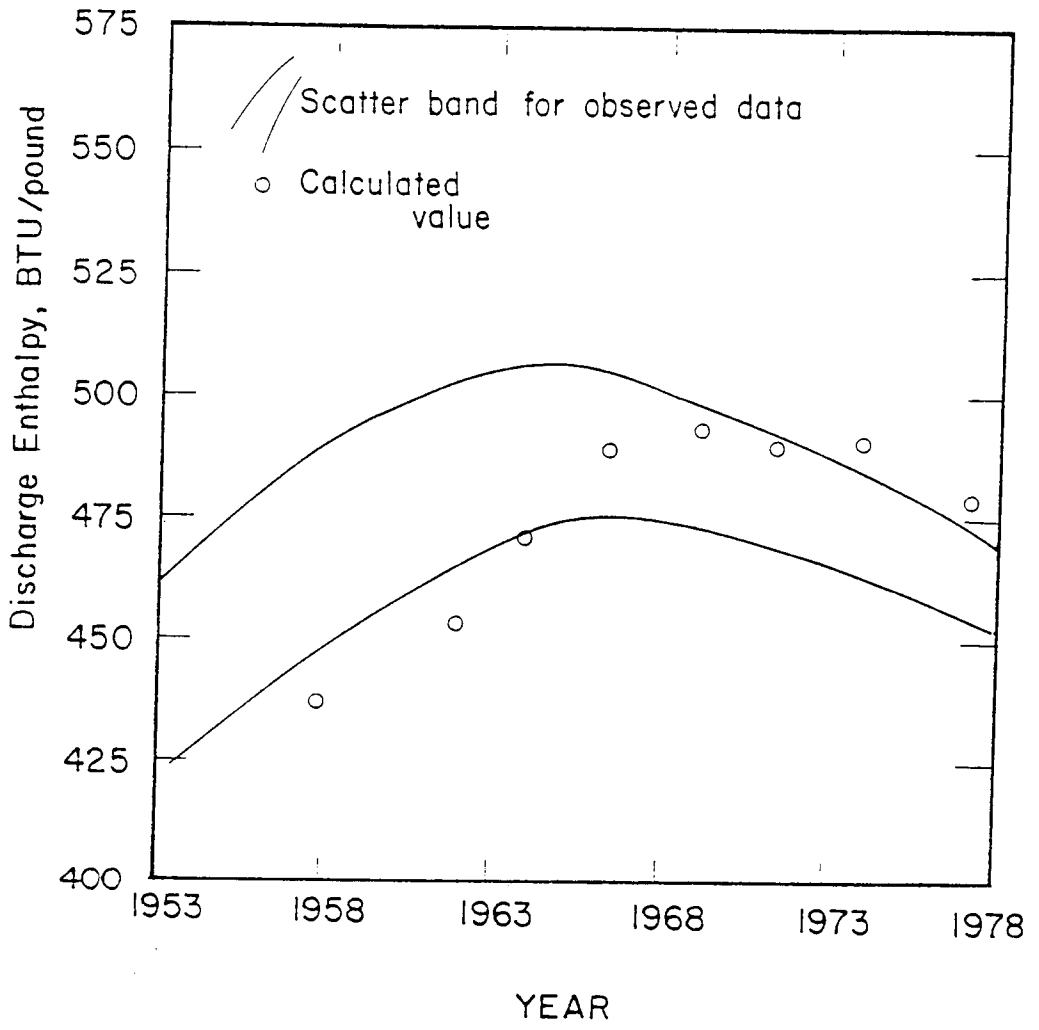

Figure 5.7 Calculated Enthalpy: One-Dimensional Case.

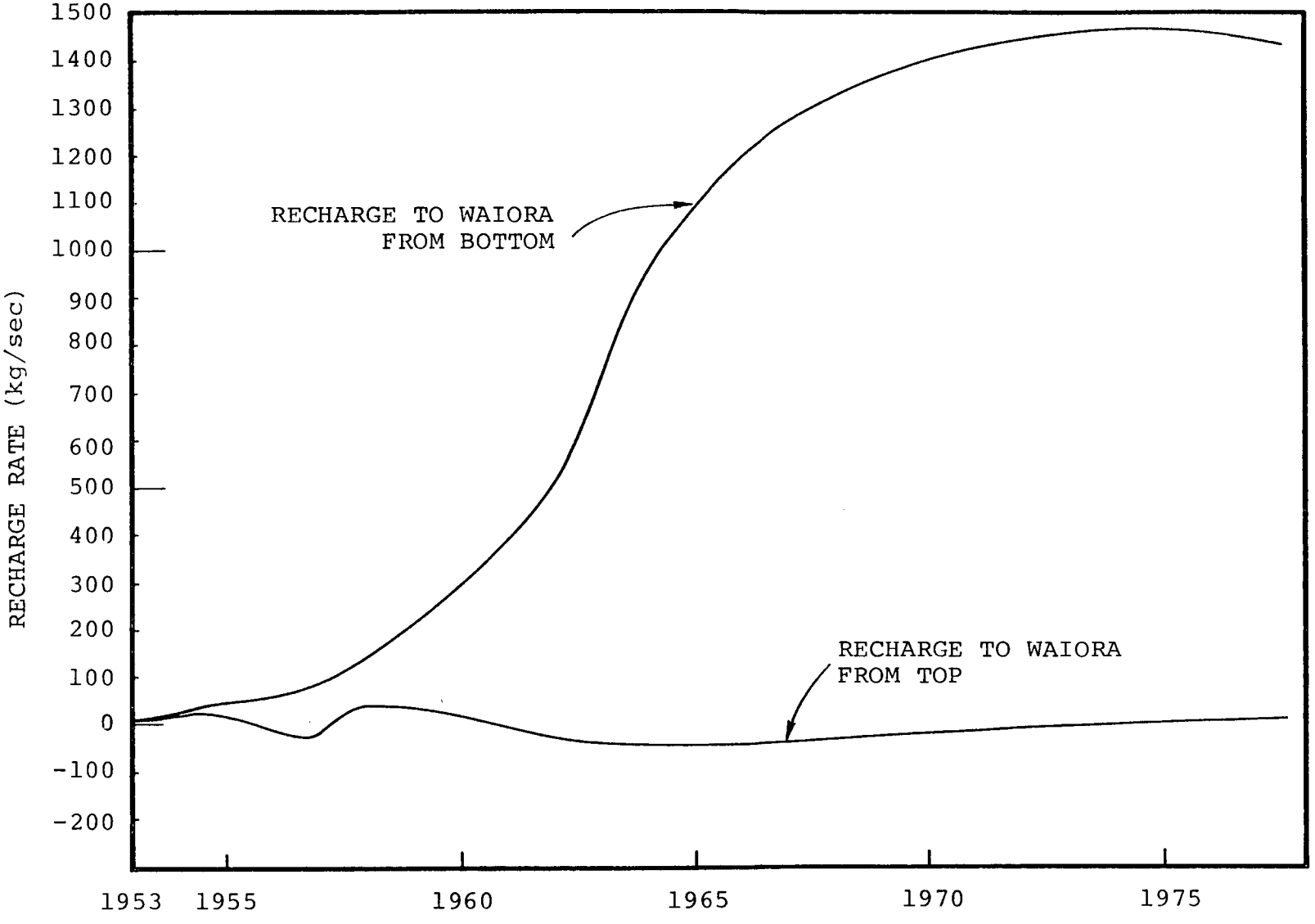

Figure 5.8. Recharge to Waiora Formation From Top (i.e., Huke Falls Formation) and Bottom (i.e., Ignimbrites).

the major portion of the recharge occurs through the Ignimbrites; the fluid influx from the bottom boundary gradually increases to a maximum of approximately 1470 kg/sec around 1974 and then slowly declines. For most of the calculation, a small discharge takes place through the Huka formation; the calculated discharge through the Huka formation is, however, significantly less than the natural mass discharge from the Wairakei geothermal system. As a matter of fact, no attempt was made in these one-dimensional simulations to match the surface heat and mass discharges since the one-dimensional geometry does not allow for convenient representation of simultaneous mass recharge and discharge at different spatial points on the surface. Surface heat and mass discharges are best matched with multi-dimensional (2-D and 3-D) simulations. The results of the present simulation do, however, provide an estimate of the total recharge to the Waiora formation required to match the observed pressure history.

It is doubtless true that pressure and enthalpy measurements could be matched even better by pursuing the one-dimensional case further, but the limitations inherent in the one-dimensional approach suggest that further work along these lines would probably provide few new insights. It should be pointed out that the final one-dimensional simulation presented here represents the culmination of a series of approximately sixty calculations in which the parameters describing the problem were varied in various ways. Generally speaking, results were most sensitive to (1) the initial temperature distribution assumed in the Waiora formation, (2) the forms of the relative permeability functions employed, and (3) the vertical permeability assumed for the Huka Falls

formation. Initial temperatures are important since the temperature at a particular depth determines the pressure drop required before two-phase behavior begins at that level, and therefore initial temperatures profoundly influence both pressure response and discharge enthalpy. Relative permeabilities are important since, for two-phase flow, the relative permeability curves determine both net flow resistance (which influences pressure response) and the ratio of water to steam in the discharge (which determines discharge enthalpy). Of course, numerous sets of curves may be used to obtain reasonable matches; in fact, as will be seen, a different set was used in the 2-D calculations presented in Section VI. On the other hand, certain curves are clearly inadequate; for example, the classical Corey relations are inappropriate since they cause much too wide a variation in discharge enthalpies irrespective of the other problem parameters. Finally, the Huka Falls permeability was found to be a key parameter. If the Huka permeability is too low, excessive pressure drop will result since surface recharge will be inhibited. If the Huka permeability is too large, cold-water recharge from the surface will be excessive; this cold water will overcool the system, causing discharge enthalpies to drop precipitously and also causing low pressure drops due to loss of two-phase flow resistance.

Although certain aspects of the final one-dimensional simulation are somewhat less than satisfying, this series of calculations proved valuable in several respects. As mentioned above, the calculations showed clearly that it is necessary to represent the effects of lateral recharge to the reservoir to obtain a good match

with measurements. The relative ease with which one-dimensional calculations may be carried out permitted an enormous number of parameters to be varied efficiently, so that key parameters could be identified and appropriate ranges of values established. The background provided by our experience with the one-dimensional model proved very useful in the subsequent multi-dimensional simulation work which permitted lateral variations to be taken into account.

VI. TWO-DIMENSIONAL SIMULATION

To represent the effects of lateral variations, realistic geological structure and horizontal flow, we next considered the two-dimensional case. A vertical cross-section of the reservoir was chosen which extends from west to east across the main bore field and which extends toward the Tauhara region. In the transverse (north-south) direction, a width of three kilometers was employed. Figure 6.1 shows the location of the vertical section AA'. We used S^3's MUSHRM numerical simulator to model both the pre-production and the production behavior of the Wairakei system as represented by this vertical cross-section AA'. Since the response to production at Wairakei is remarkably uniform areally (i.e., in the horizontal plane), the choice of a particular vertical cross-section is not extremely critical. The vertical section approach, however, as contrasted with the areal models of Mercer, et al. [1975] and Mercer and Faust [1979], allows an accurate representation of two-phase effects (e.g., vertical segregation of the steam phase), and recharge from both the top and bottom boundaries, as well as from the sides.

Figure 6.2 provides an areal view of the Wairakei geothermal field and gives approximate elevation of the ground surface. The main borefield at Wairakei lies in a shallow valley; the ground rises to the west and, to a lesser degree, to the north and south. This uneven topography must somehow or other be represented in the numerical model. If one assumes that the water table coincides with the surface, then the top layer of the numerical grid can be configured to follow the topography,

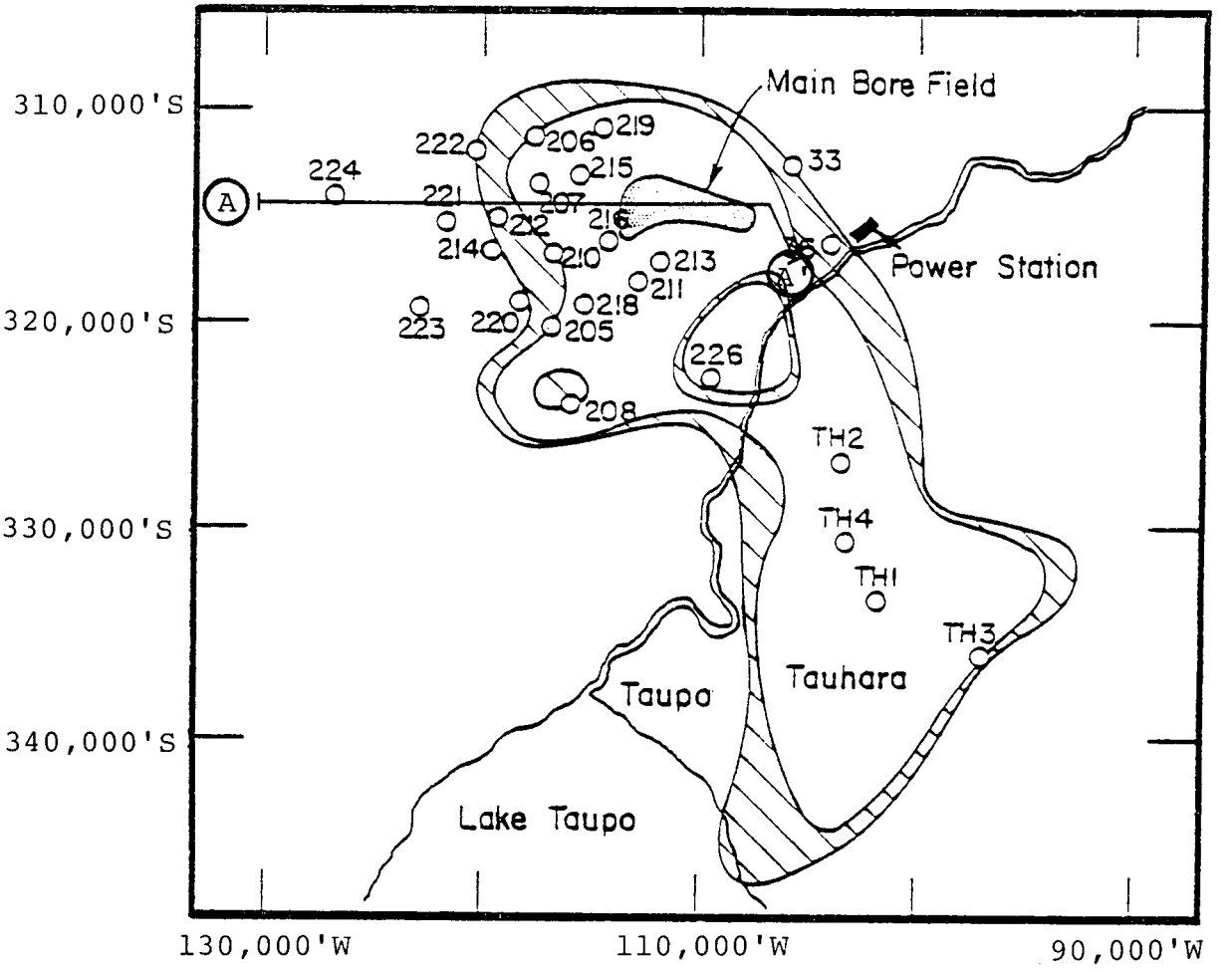

Figure 6.1. Location of Vertical Section AA'.

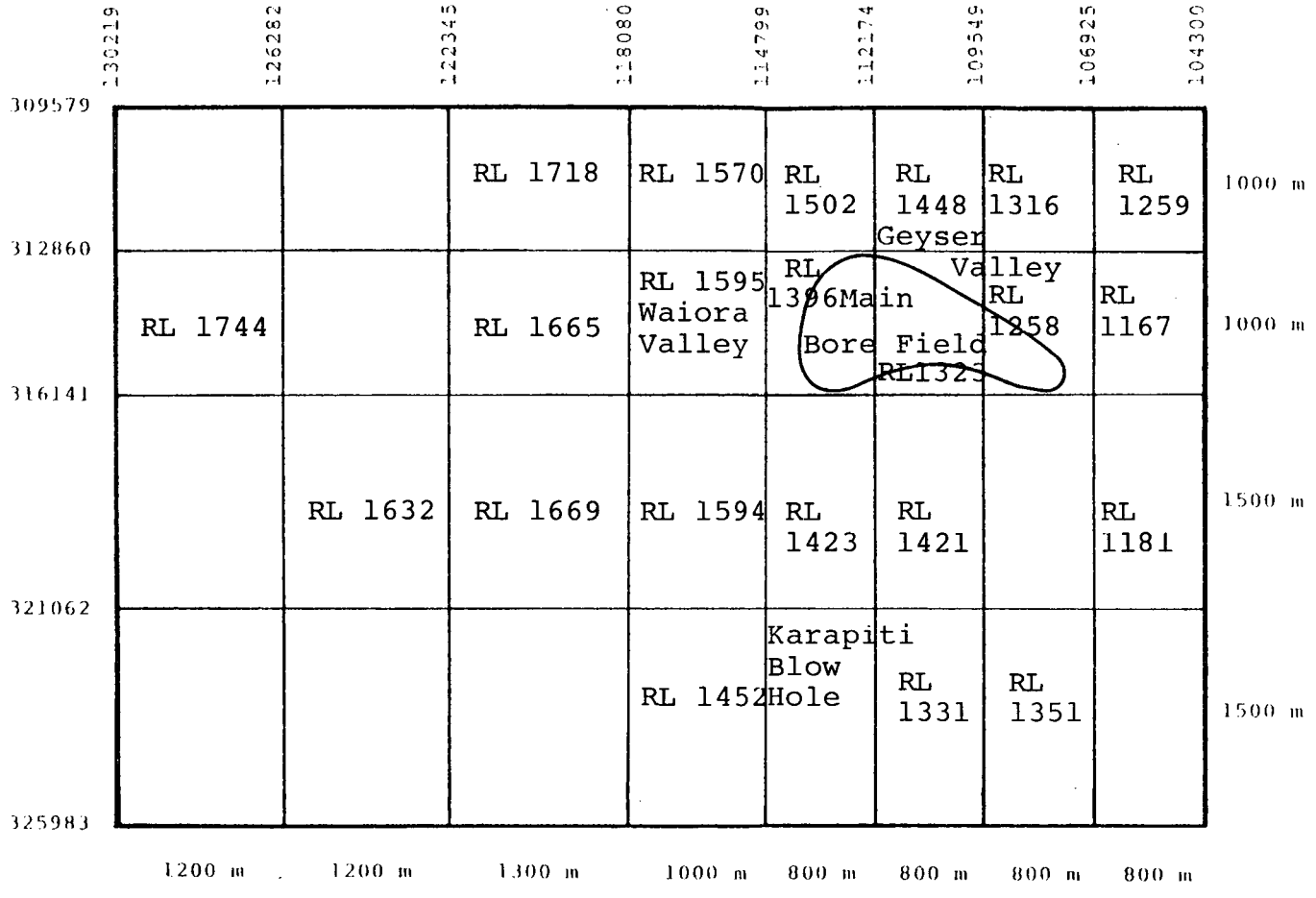

Figure 6.2. Areal View of Wairakei Geothermal Field Showing Elevation of the Ground Surface. The Cross - Section AA' Passes Through the Second Layer (from the top of the page).

and a one-bar pressure imposed along the surface. Evidence exists, however, that this treatment may not be entirely appropriate. Considering the differences in elevation of the surface at the eastern and western edges of cross-section AA', assuming that the water table coincides with the surface implies that an east-west pressure gradient averaging about 2.5 bars/kilometer should be present across the grid. Early pressure data based on downhole measurements, on the other hand, indicate a substantially weaker east-west gradient - approximately one bar per kilometer. Thus, these measurements suggest that the water table in the west may lie well below the surface. Since, however, no direct measurements of water table elevations are available, the early subsurface pressure measurements must be relied upon to prescribe the boundary conditions at the top of the grid. In the following, we will assume that the water table in the west is at an elevation of 92 m above that in the east (see Figure 6.3); this amounts to imposing an average east-west pressure gradient of approximately 1.1 bars/kilometer.

As Figure 6.1 shows, the cross-section chosen passes through the main borefield from which most of the fluid production from Wairakei has taken place. Furthermore, owing to the large number of wells located on or near section AA', the subsurface geological structure is reasonably well defined. Well log data was employed to generate the computational grid shown in Figure 6.3, and to define the rock types believed to be present in each zone, as indicated. It should be noted that the deepest layer shown in Figure 6.3 is a fictitious layer of

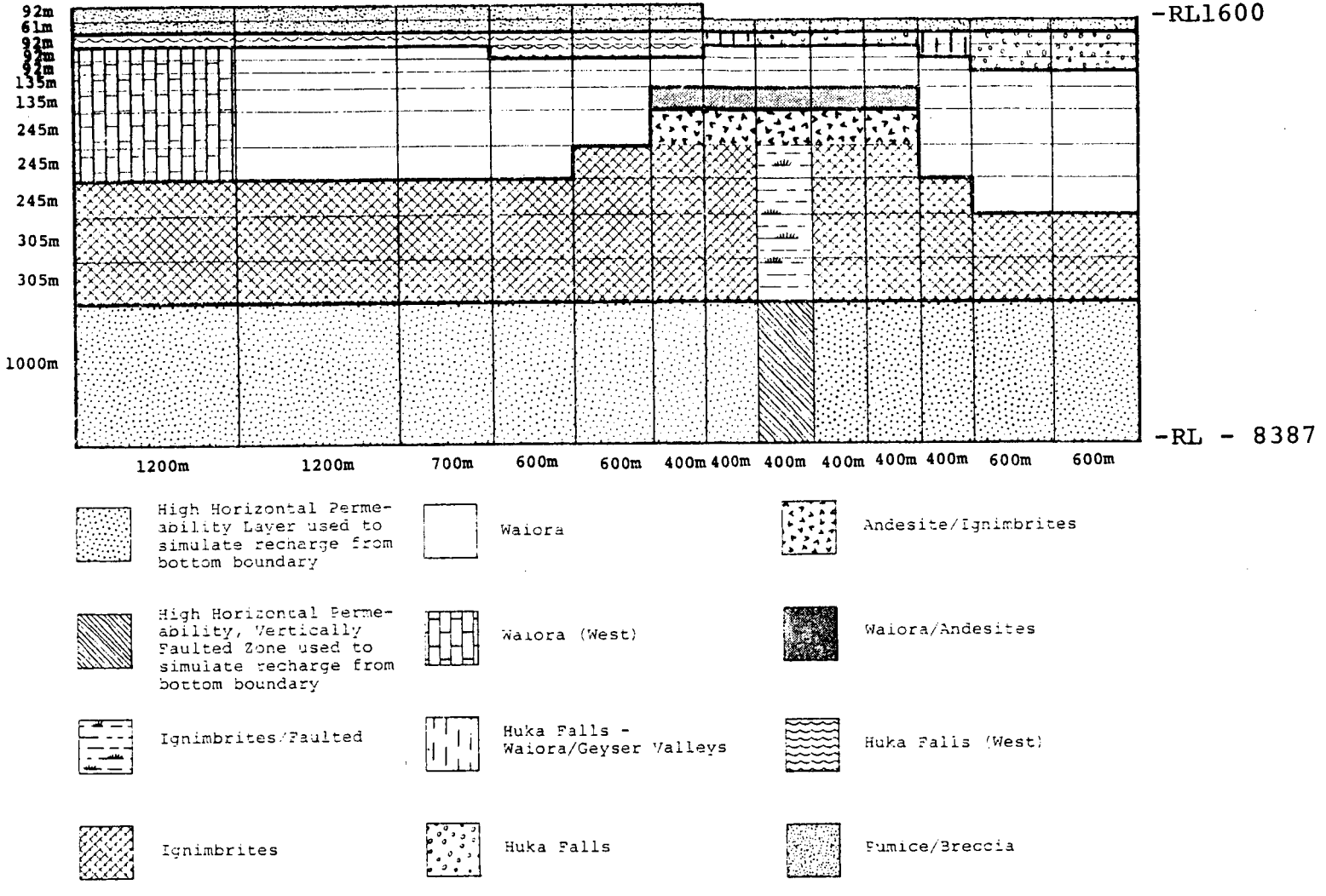

Figure 6.3. Vertical Cross-Section AA'

high horizontal permeability (1000 md) which acts as a manifold to distribute deep recharge according to the local pressure drop.

The rock properties of primary interest for use in this simulation effort are the porosity, permeability, density, thermal conductivity and heat capacity of each of the geologic formations. As discussed by Pritchett, et al. [1978], laboratory measured values for these parameters are often considerably different from the values needed to explain the behavior of the reservoir. In particular, measured porosities are higher and permeabilities are much lower than those which are reflected by the performance of the system. This discrepancy leads one to believe that the effective permeability of the system is largely controlled by the fracture network which is present throughout the region. Effective permeabilities on the order of 100 millidarcies and effective porosities of about 20 percent for the Waiora aquifer have been used in several analyses (see Mercer, et al. [1975] and Pritchett, et al. [1976]) which have yielded fairly good agreement between observed field response and calculated values. A summary of the rock properties used in the present two-dimensional calculations is given in Table 6-1.

No direct measurements from which relative permeabilities may be deduced are available for Wairakei (see, for example, Pritchett, et al. [1978]). The curves previously used for the one-dimensional simulation described in the preceeding section produced unsatisfactory results; hence, a trial-and-error procedure was

TABLE 6-1

ROCK PROPERTIES USED IN TWO-DIMENSIONAL VERTICAL CROSS-SECTION SIMULATION

ROCK TYPE	POROSITY	DENSITY (g/cc)	THERMAL CONDUCTIVITY (ergs/sec-cm°C)	HEAT CAPACITY (ergs/gram-°C)	HORIZONTAL PERMEABILITY (md)	VERTICAL PERMEABILITY (md)	UNIAXIAL MODULUS ($dyne/cm^2$)
Pumice/Breccia	.25	2.15	5×10^5	9.39×10^6	100.0	100.0	1×10^9
Huka Falls - Waiora - Geyser Valleys	.20	2.26	5×10^5	8.757×10^6	2.0	10.0	1×10^9
Huka Falls - West	.20	2.26	5×10^5	8.757×10^6	.5	.1	1×10^9
Huka Falls	.20	2.26	5×10^5	8.757×10^6	1.0	1.0	1×10^9
Waiora - West	.20	2.27	5×10^5	8.475×10^6	50.0	25.0	5×10^9
Wairoa/Andesites	.20	2.27	5×10^5	8.475×10^6	300.0	25.0	5×10^9
Waiora	.20	2.27	5×10^5	8.475×10^6	300.0	25.0	5×10^9
Ignimbrites/Andesites	.10	2.54	5×10^5	7.666×10^6	300.0	25.0	5×10^{10}
Ignimbrites/Faulted	.10	2.54	5×10^5	7.666×10^6	3.0	30.0	5×10^{10}
Ignimbrites	.10	2.54	5×10^5	7.666×10^6	3.0	3.0	5×10^{10}
Bottom Layer - High Horizontal Permeability	.10	2.54	5×10^5	7.666×10^6	1000.0	3.0	5×10^{10}
Bottom Layer - High Horizontal Permeability/ Faulted	.10	2.54	5×10^5	7.666×10^6	1000.0	30.0	5×10^{10}

employed to establish various sets of relative permeability functions which produced computed results consistent with the known data. Several different sets of relative permeability curves were found which all produced a satisfactory pre-production state of the system. However, once the simulator was used to model the production behavior of the field, it soon became apparent that some curves were inadequate.

Grant [1977] presents a relationship between the liquid and vapor relative permeability curves which was inferred from bore histories at Wairakei. This relationship is shown in Figure 6.4. He found that this relationship appears to apply on a large scale and therefore believes it may comprise an effective average for the fracture/matrix system. For purposes of these two-dimensional analyses we used the following functional form for liquid relative permeability:

$$
\begin{aligned}
R_L &= (1-2S)^4 && \text{for} \quad 0 \leq S < 0.25 \\
&= (1-2S)/8 && \text{for} \quad 0.25 \leq S < 0.5 \\
&= 0 && \text{for} \quad S \geq 0.5
\end{aligned}
$$

where

S = steam saturation

The vapor relative permeability was then derived from Grant's curve (Figure 6.4). The resulting relative permeability curves (R_L, R_G) used for these calculations are shown in Figure 6.5.

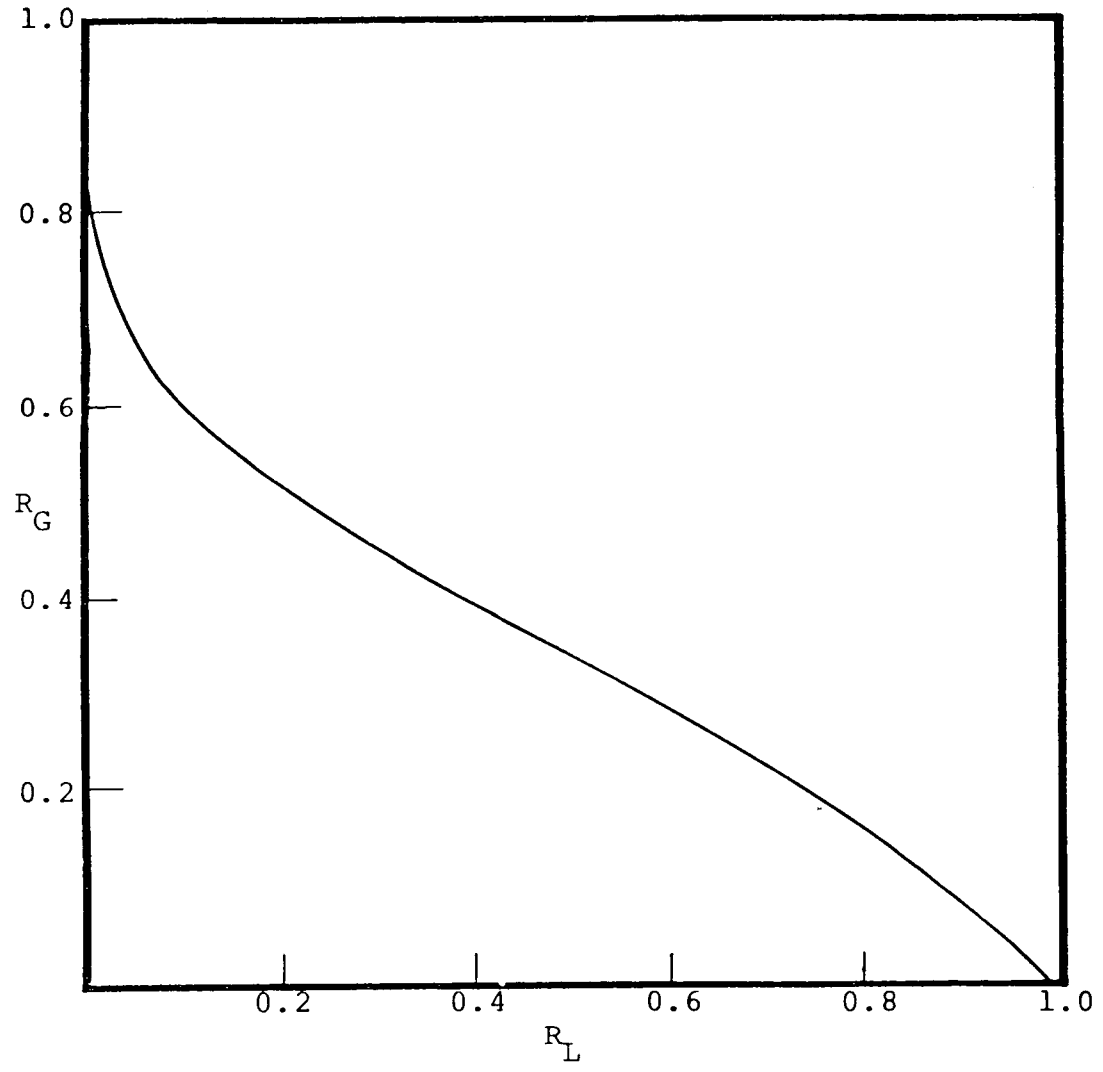

Figure 6.4. Empirical relation between liquid and steam relative permeabilities (reproduced from Grant [1977]).

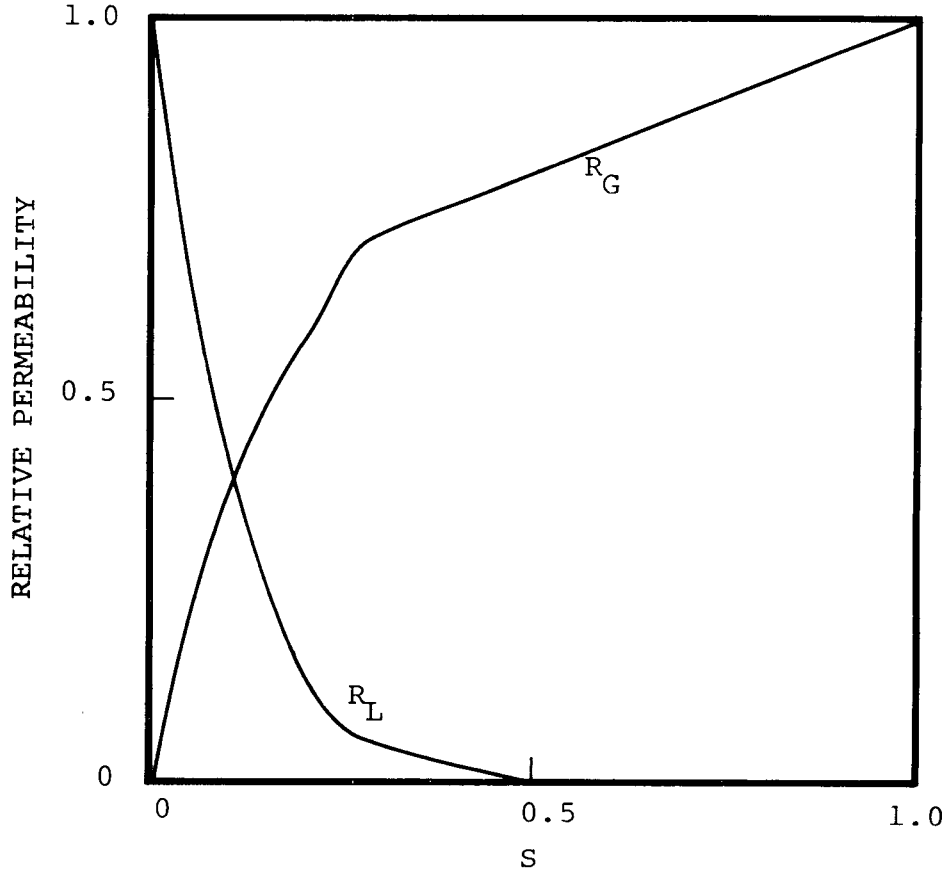

Figure 6.5. Relative permeability curves for simulation studies.

For modeling purposes, we have assumed that the Huka Falls formation transmits both heat and mass vertically from the Waiora aquifer. Mass leakage is also allowed through the ignimbrite formation, primarily through the faulted regions which intersect the formation. Our conceptual model of the reservoir further permits recharge to the system from both side boundaries, with the recharge from the right (east) boundary implicitly used to simulate the connection between the Wairakei and Tauhara regions.

Mass (and hence convective heat) discharge at Wairakei takes place through narrow vents; it is not directly possible to represent these vents in a large-scale continuum model. While the temperature of the fluid exiting through the vents is quite high, the average temperature of the surface water table is close to 20°C. A convenient way to simulate surface heat/mass discharge is through the use of a convective - radiative boundary condition. A 1 bar, 20°C boundary condition was imposed at the top of the grid to allow mass recharge/discharge at the surface. If the mass flux is out of the system at that boundary, the temperature of the fluid crossing the interface is the temperature associated with the grid block from which it comes. If the flux is into the system, it enters at a temperature of 20°C. Heat discharge at the surface is simulated by adding an energy sink $\dot{e}$ to the top layer of the grid,

$$\dot{e} = - 1.66666 \times 10^4 \ (T-T_o) \ \text{ergs/cm}^2$$

where

$\dot{e}$ = energy discharge per unit area of the surface

T_o = A reference temperature (= 20°C)

T = Temperature in the grid block.

The numerical coefficient in the expression for $\dot{e}$ was obtained by matching the calculated pre-production heat discharge with the measurements.

For purposes of calculating a pre-production state of the system, the bottom and the side boundaries were assumed to be impermeable and insulated. The pre-production mass flux through the bottom boundary was represented by adding a constant mass source to the bottom row of the grid. Assumption of impermeable side boundaries is tantamount to neglecting any west to east flow; this assumption should not introduce any great error since the effects of such pre-production flow will be quickly swamped by perturbations induced by the production of the field. The calculated steady-state pre-production state was found to be independent of the starting state (i.e., initial conditions) for the computations.

In order to match the pre-production conditions (temperatures, pressures, and mass and heat discharges at the surface), we varied (1) the permeability of the Huka Falls formation and (2) the mass flux through the base of the ignimbrites, i.e., into the bottom layer of the grid. The values for Huka permeability listed in Table 6-1 produced the best of several initial states of the system. The best estimate for the pre-production recharge through the base of the ignimbrites is 330 kg/sec at 285°C. The total heat and mass discharges at the surface

were calculated to be 360 megawatts and 400 kg/sec, respectively. These calculated values are approximately 10 percent smaller than those estimated by Fisher [1964]. The calculated mass discharge is, however, in fairly good agreement with that employed by Sorey [1978] to model the Wairakei system. The calculated pressure at RL-900 feet of 875 psi (60.33 bars) is in good agreement with early pressure data. The model also predicted initial two-phase conditions in upper sections of the reservoir prior to exploitation of the field.

Figure 6.6 shows the initial temperature distribution throughout the grid. Note that at the depth of main production from the reservoir, i.e., approximately RL-900, the temperature underlying the main bore field is in the 265-275°C range (Figures 6.7 and 6.8 show the computed temperature distribution at January, 1965 and June, 1977, respectively). Figure 6.9 shows the initial vapor phase saturation distribution throughout the grid system (Figures 6.10 and 6.11 are vapor saturations in January, 1965 and June, 1977 respectively). Figure 6.12 shows the initial pressure distribution throughout the grid (Figures 6.13 and 6.14 are for later times). Note that the pressure of 875 psi (60.33 bars) at RL-900 feet is an interpolated value using the value of pressure calculated by the code at RL-1095 feet and correcting to the RL-900 level by subtracting ρgh where h is 195 feet.

The pre-production model of the system described above was used as the initial state for the production calculations to match the historical performance of the reservoir system. For this purpose, it was necessary to allocate production from the wells to the appropriate grid

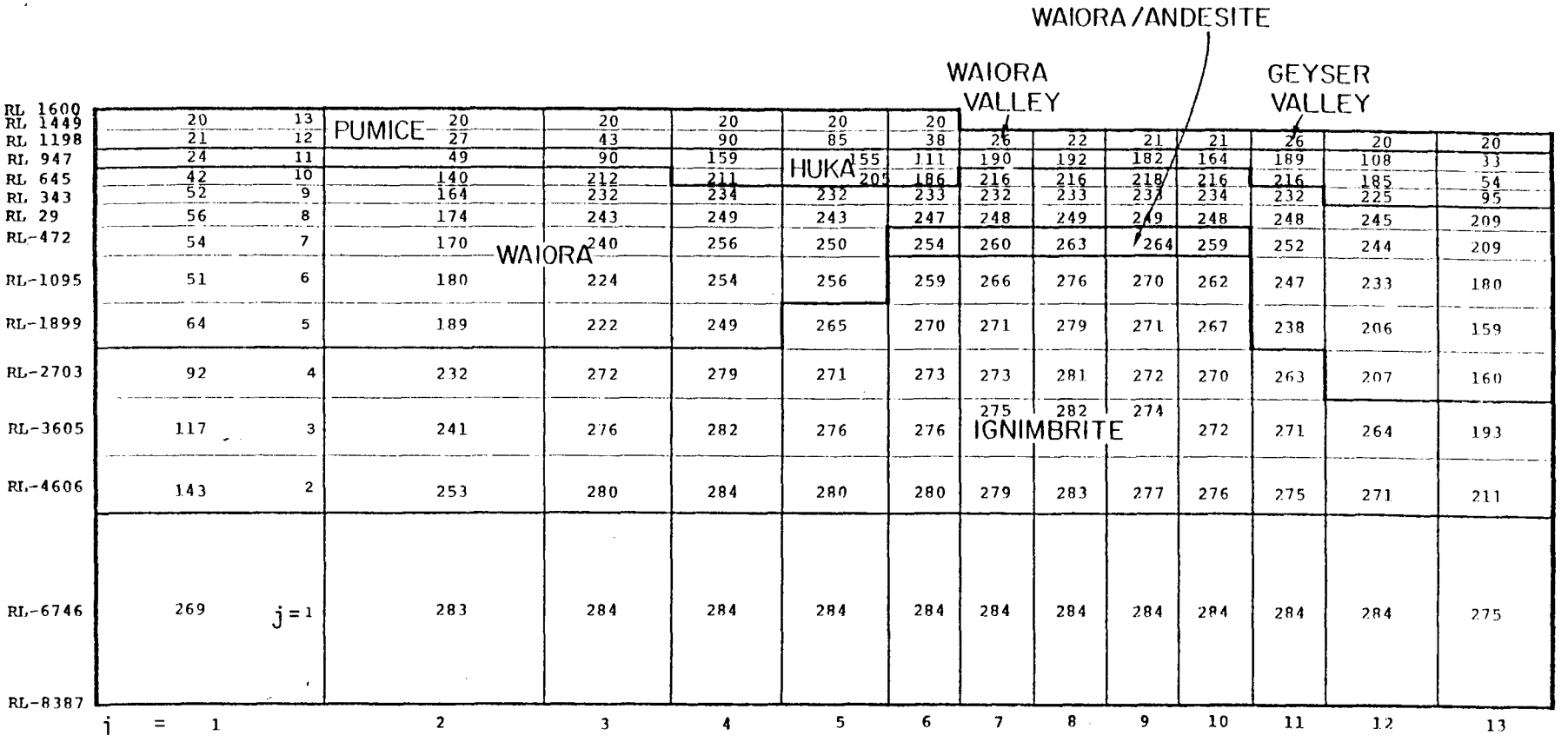

Figure 6.6. Initial Temperature Distribution (°C)

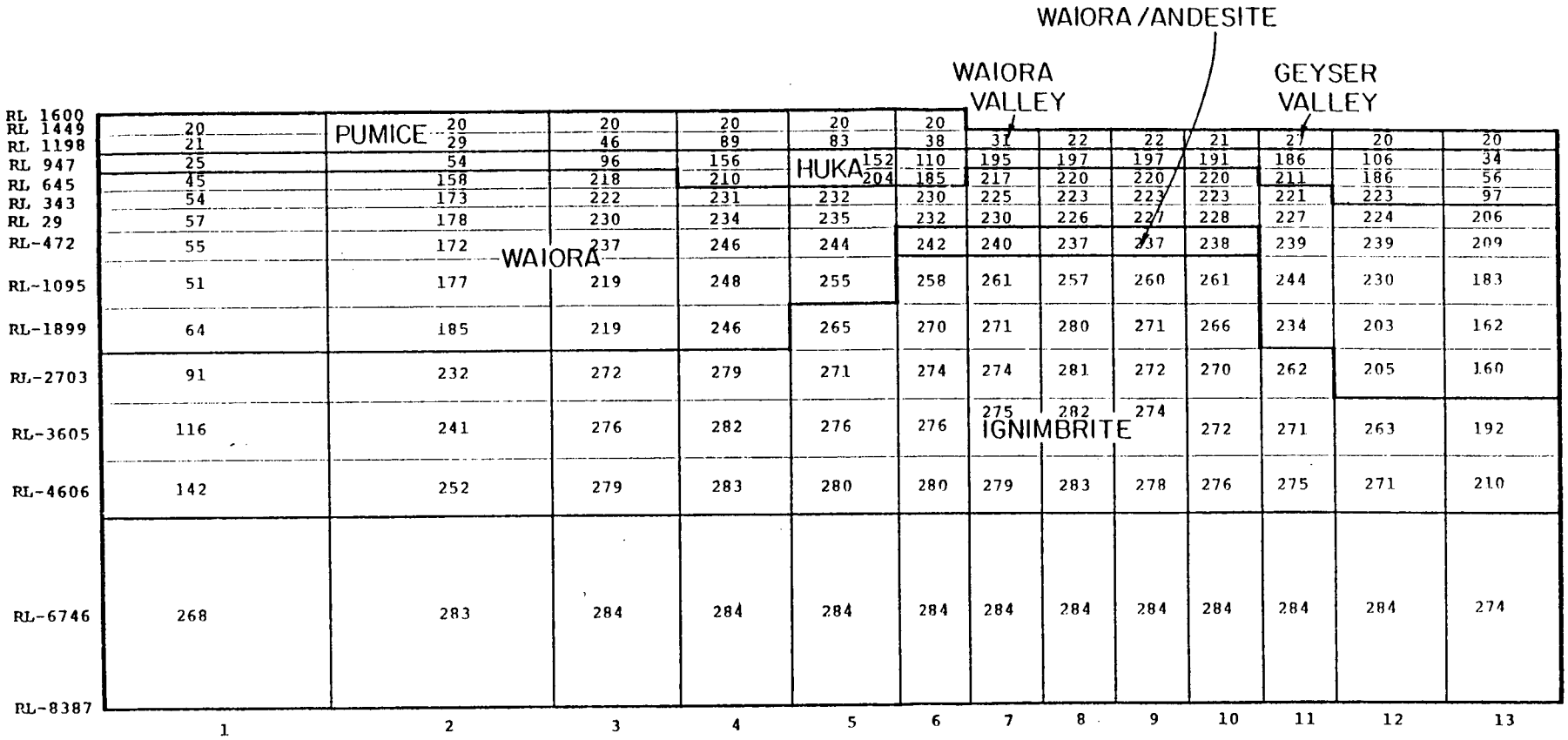

Figure 6.7. Temperature Distribution: January, 1965 (°C)

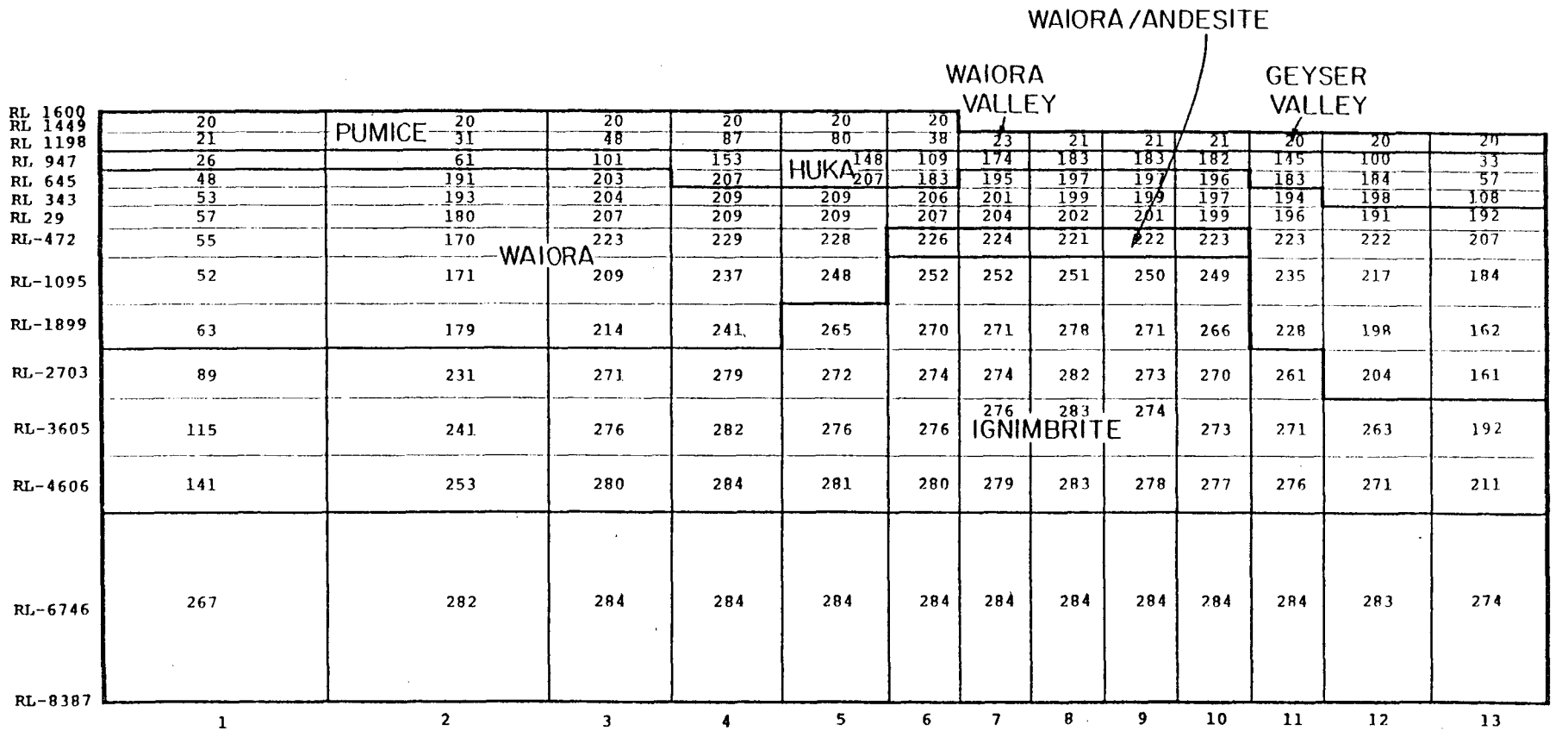

Figure 6.8. Temperature Distribution: June, 1977 (°C)

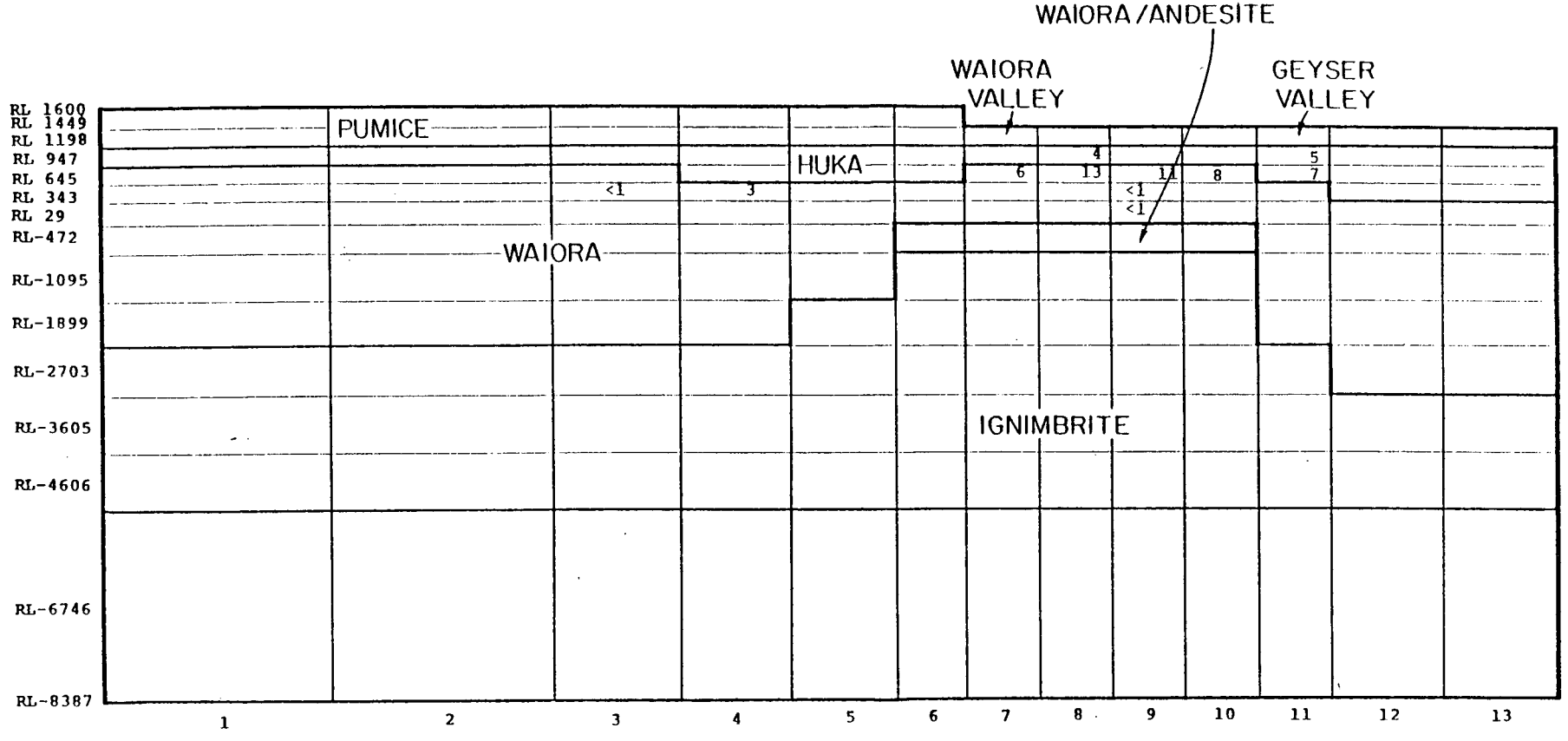

Figure 6.9. Initial Steam Saturation (%)
(Blanks are zero)

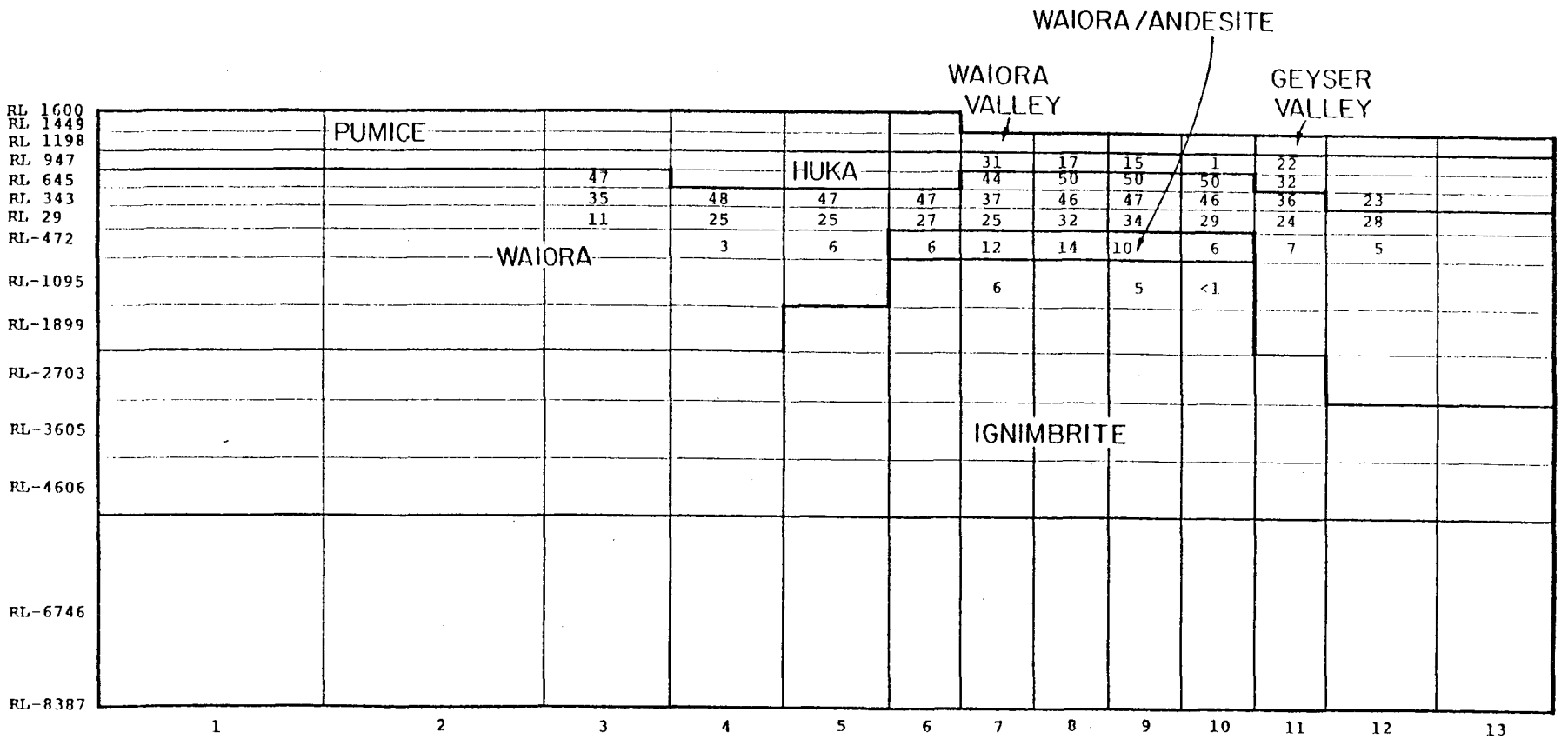

Figure 6.10. Steam Saturation (%): January, 1965
(Blanks are zero)

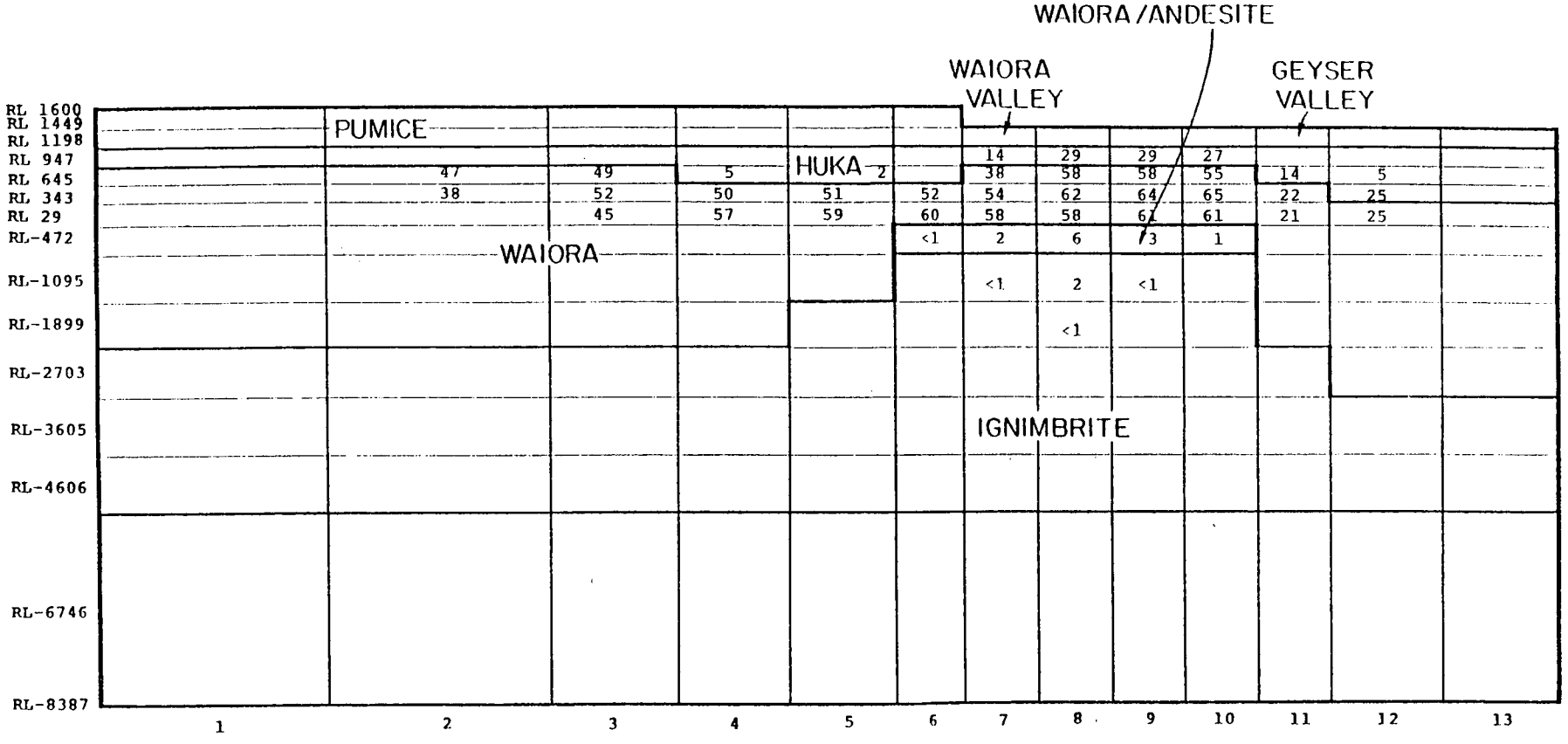

Figure 6.11. Steam Saturation (%): June, 1977
(Blanks are zero)

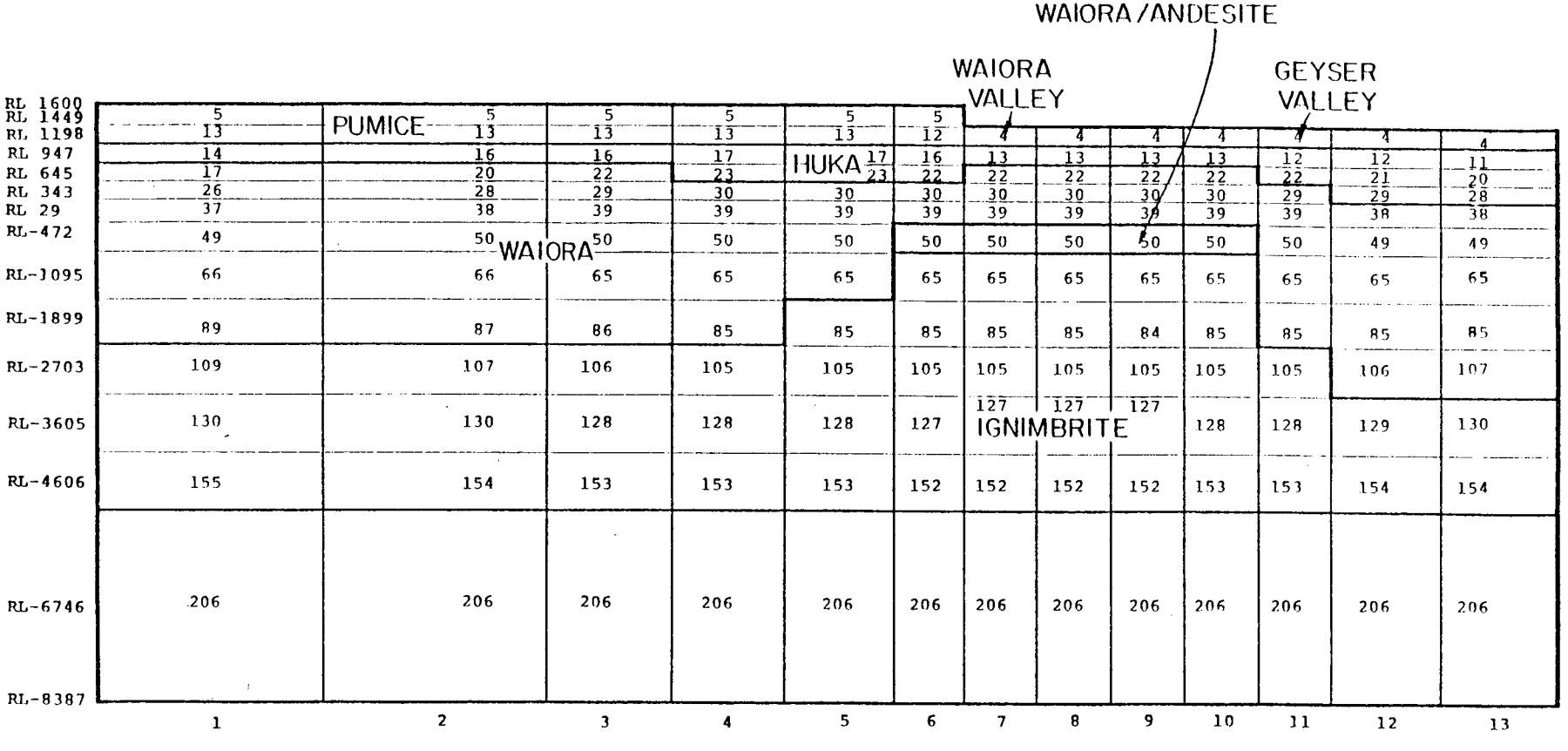

Figure 6.12. Initial Pressure Distribution (bars)

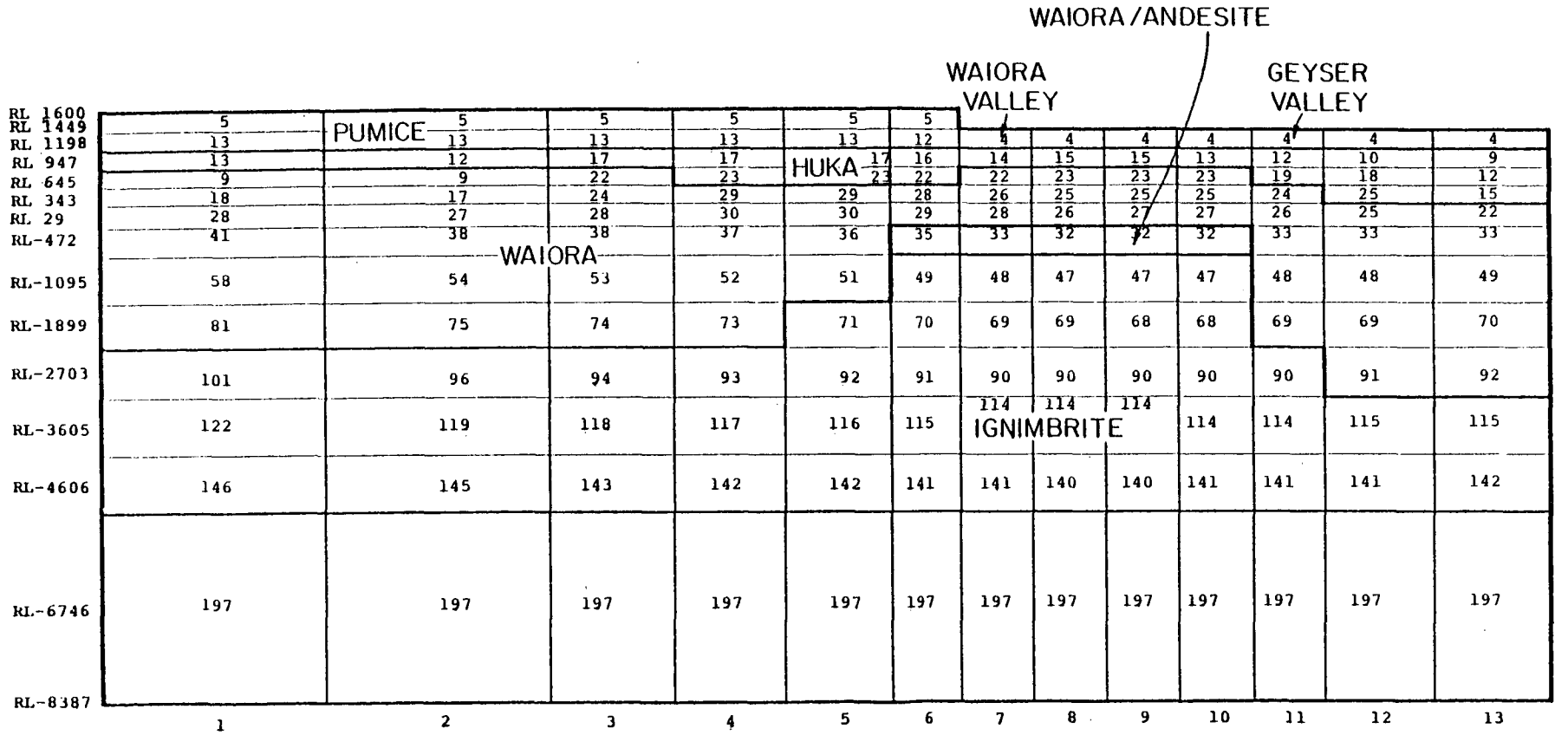

Figure 6.13. Pressure Distribution: January, 1965 (bars)

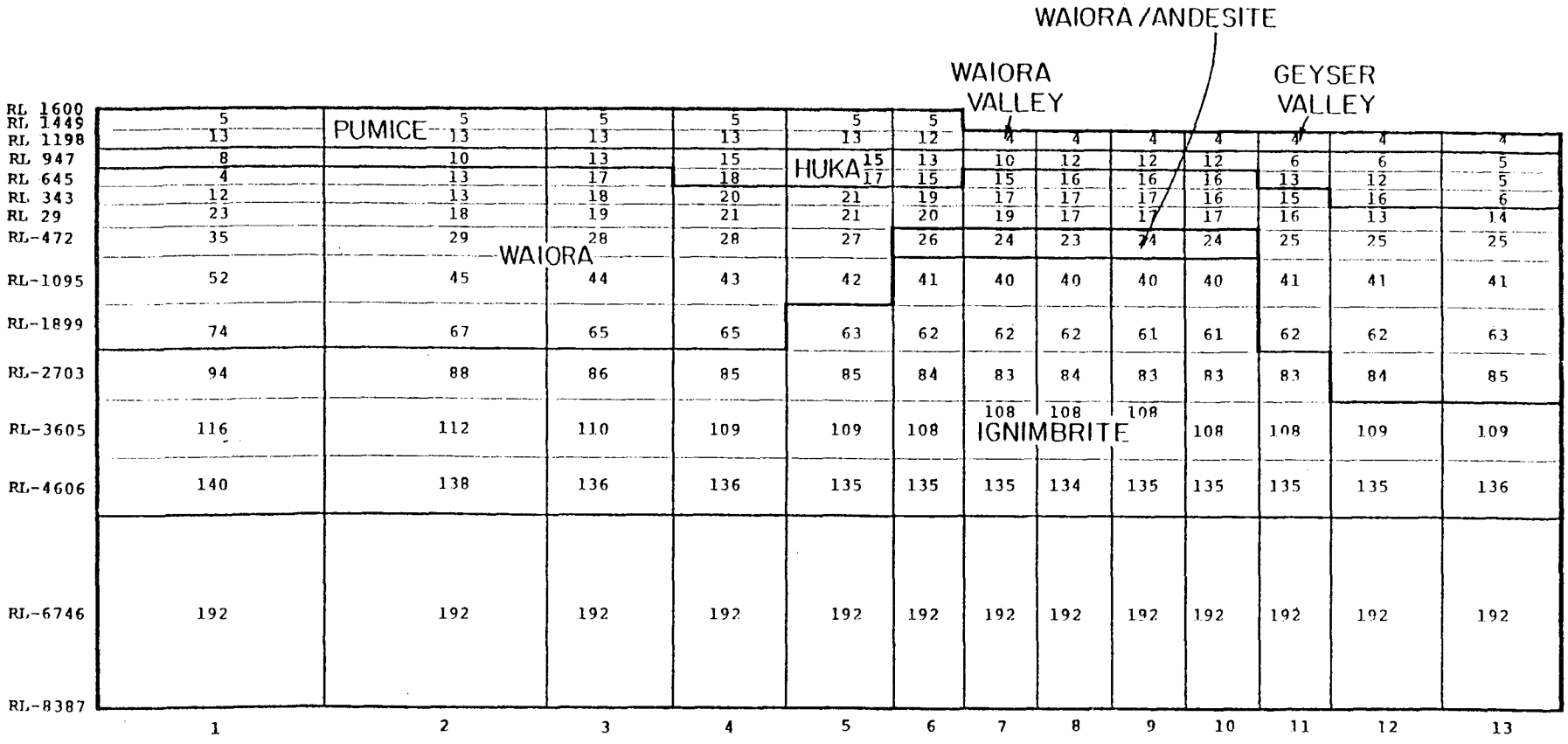

Figure 6.14. Pressure Distribution: June, 1977 (bars)

blocks in the numerical grid system. Each well was projected onto the cross-section, taking particular note of the projection on the grid of the intervals open to flow in the well. The production rate for a given well was then allocated to the grid blocks which intersected the projection of the open flow intervals (see Table 6-2 for the list of grid blocks intersected by each well). The allocation of the total rate for the well among these grid blocks was based on the total instantaneous kinematic mobility of the blocks intersected (Garg [1978]). For purposes of these calculations, yearly averages of production data for each well were used as reported by Pritchett, et al. [1978].

As production from the field occurs, the fluid reduction in the system causes the pressure to decline which in turn causes fluid influx to the system from the boundaries. For the numerical simulation, the fluid flux through the vertical boundaries was taken to be locally proportional to the pressure drop in the grid block adjoining the boundary, in particular:

$$(M_{influx})_{\text{vertical boundaries}} = \alpha_{ij}\Delta P_{ij}$$

where ij denotes a particular grid block and ΔP_{ij} is the pressure drop in dynes/cm^2. The multipliers α_{ij} (constant in time, but varying from block to block) were adjusted so as to obtain the observed pressure drops near the vertical boundaries. Table 6-3 lists the $(\alpha/v)_{ij}$'s employed in the numerical simulation, where v_{ij} is the volume of grid block ij. Field data indicates that the pressure drop at the eastern end of the field is approximately the same as that in the main borefield

TABLE 6-2

SPATIAL LOCATION OF THE PRODUCTIVE INTERVAL OF VARIOUS WELLS

Well No.	I	J
4	12	8-9
4/1	12	7-9
4/2	12	8-9
8A	10	10
9	11	10-11
11	8	10
12	8	8-10
13	9	8-10
14	10	10-11
15	9	10-11
16, 16/1	10	9-10
17	9	9-10
18	9	5-8
19	10	5-6
20	9	7-8
21	9	9-10
22	8	7-8
23	12	8-10
24	8	6-9
25	8	6-10
26, 26A	8	7-8
26B	8	6-8
28	8	7-8
29,30	8	6-8
31	9	7-9
37	11	7-8
38	12	7-9
39	12	6-8
40	12	7-9
41, 42, 43	12	8-9
44	8	6-7
45	10	6-7
46	8	6-7
47	8	6
48	8	4-7
49	8	7, 10-11
50	8	6-8
52	10	6-8
53	12	7-9
55	9	6-7
56	7	6-8
57	8	6-8
58	12	7-8
59	11	6-8

Well No.	I	J
60	11	5-8
61, 62	11	6-9
63	11	7-9
65	9	10-11
66	9	6-7
67, 68	9	6-8
70	8	7-8
71	8	6-8
72	8	7-8
73	10	9-10
74	8	6-8
75	9	6-8
76	8	7-8
78	9	6-8
80	8	6-10
81	9	7
82, 83	8	7-9
86, 88, 92	8	6-8
96	7	6-8
101	8	6-8
103	8	6-9
105	7	6-10
107, 108, 109	8	6-9
110, 116	7	7-9
118, 119	7	6-10
203	6	9-10
204	5	9-12
205	5	6-11
206	5	6-8
207	5	5-8
210	5	6-9
211	8	8-10
212	4	4-7
214	4	6-9
215	6	6-9
216	7	6-9
217	6	6-9
218	6	5-7
219	7	4-8
220	4	6-10
221	3	5-8
222	3	6-8

TABLE 6-3

NUMERICAL VALUES OF $(\alpha/v)_{ij}$ EMPLOYED IN THE NUMERICAL SIMULATION

I	J	$(\alpha/v)_{ij}$ (gms/sec-cm-dynes)
Left Boundary		
1	5	0.44445×10^{-17}
1	6	0.44445×10^{-17}
1	7	0.44445×10^{-17}
1	8	0.44445×10^{-17}
1	9	0.66667×10^{-17}
1	10	0.88887×10^{-17}
1	11	0.22223×10^{-19}
Right Boundary		
13	4	0.8750×10^{-17}
13	5	0.8750×10^{-17}
13	6	0.8750×10^{-17}
13	7	0.8750×10^{-17}
13	8	0.8750×10^{-17}
13	9	0.4375×10^{-19}
13	10	0.4375×10^{-19}
13	11	0.4375×10^{-19}

whereas the pressure drop at the western end is about 40 percent that of the main borefield. Recharge along the vertical boundaries was allowed to enter the grid into all formations except the ignimbrites and the Pumice/Breccia.

The total mass influx through the base of the ignimbrites, i.e., influx to the system via the high permeability recharge source zones along the base of the grid, is given by

$$(M_{influx})_{bottom} = M_0 + \beta \Delta \overline{P}$$

where M_0 denotes the total pre-production mass influx of 330 kg/sec and $\Delta\overline{P}$ denotes the spatially-averaged instantaneous pressure drop (in bars) at the bottom boundary. The constant coefficient β ($\approx$ 33.5995 kg/sec-bar) was adjusted so as to obtain the best agreement between the calculated and observed pressure response of the system. Recharge (or discharge) at the surface was not prescribed, but was calculated by the simulator based upon the surface boundary condition (1 bar) imposed. The computed total natural mass discharge and recharge to the model are shown as functions of time in Figure 6.15. The mass recharge increases and the total mass discharge declines with time. At the end of the calculation (end of 1976), the calculated recharge to the system slightly exceeds fluid production from the reservoir.

The calculated pressure drop at approximately RL-900 feet is shown as a function of time in Figure 6.16. Figure 6.16 also shows the scatter band for the observed pressure drop. The agreement between the calculated and observed values is very good. Everywhere on the graph the calculated values lie within the scatter of the observed data.

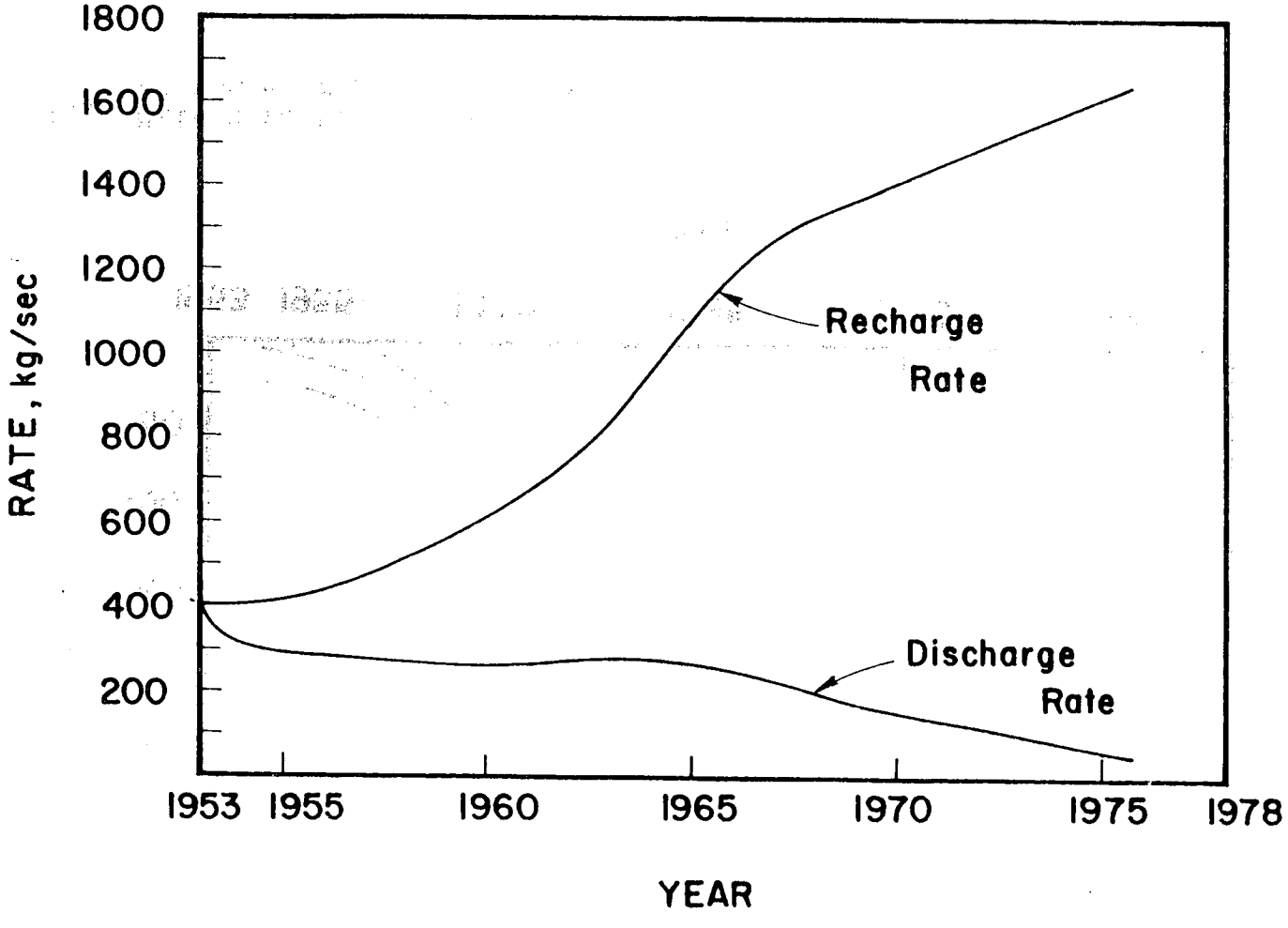

Figure 6.15. Natural Mass Recharge and Discharge Rates

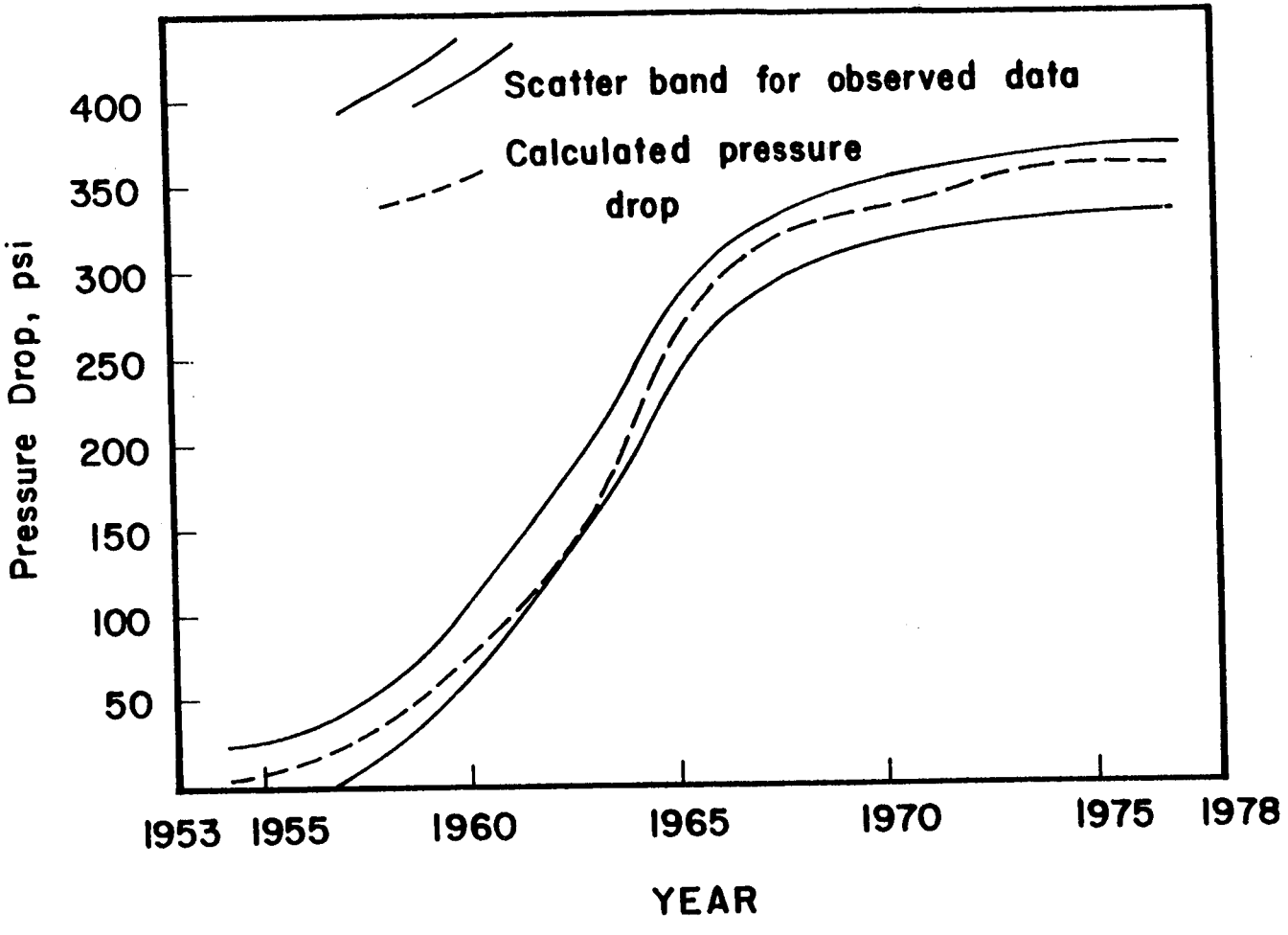

Figure 6.16. Main Bore Field Pressure Drop as a Function of Time. Calculated pressure drop is at about RL-900 feet.

Figure 6.17 shows the pressure distribution across the cross-section at RL-900 feet for several discrete times. This figure demonstrates the horizontal unifomity of the pressure response. Bolton [1970] presents some east-west pressure profiles (see Figure 6.18) for a somewhat different cross-section (particularly in the east) from the one employed in the present work. The calculated values are compared with Bolton's data in Figure 6.19; the agreement between the two is good provided allowance is made for different cross-sections and the precision of pressure measurements.

For the modeling effort to be completely successful, not only must the calulated pressure response agree with observed data, but also the calculated enthalpy of the produced fluid must agree with measured values. Figure 6.20 displays the calculated enthalpies and the scatter band for the observed data. The calculated values generally lie within the scatter of the data except for the years 1964-1969, where they exceed observed values by up to 10 percent. We speculate that this divergence is due to three-dimensional effects which were not accounted for in this simulation. In particular, this vertical two-dimensional model does not allow for north-south temperature variations. If, for example, deep temperatures to the north and/or south of the main borefield were lower than those directly below the production area, at late times fluid withdrawal would be expected to cause this cooler fluid to enter the borefield, reducing late-time discharge enthalpies. Effects of this sort may be incorporated into a three-dimensional simulation.

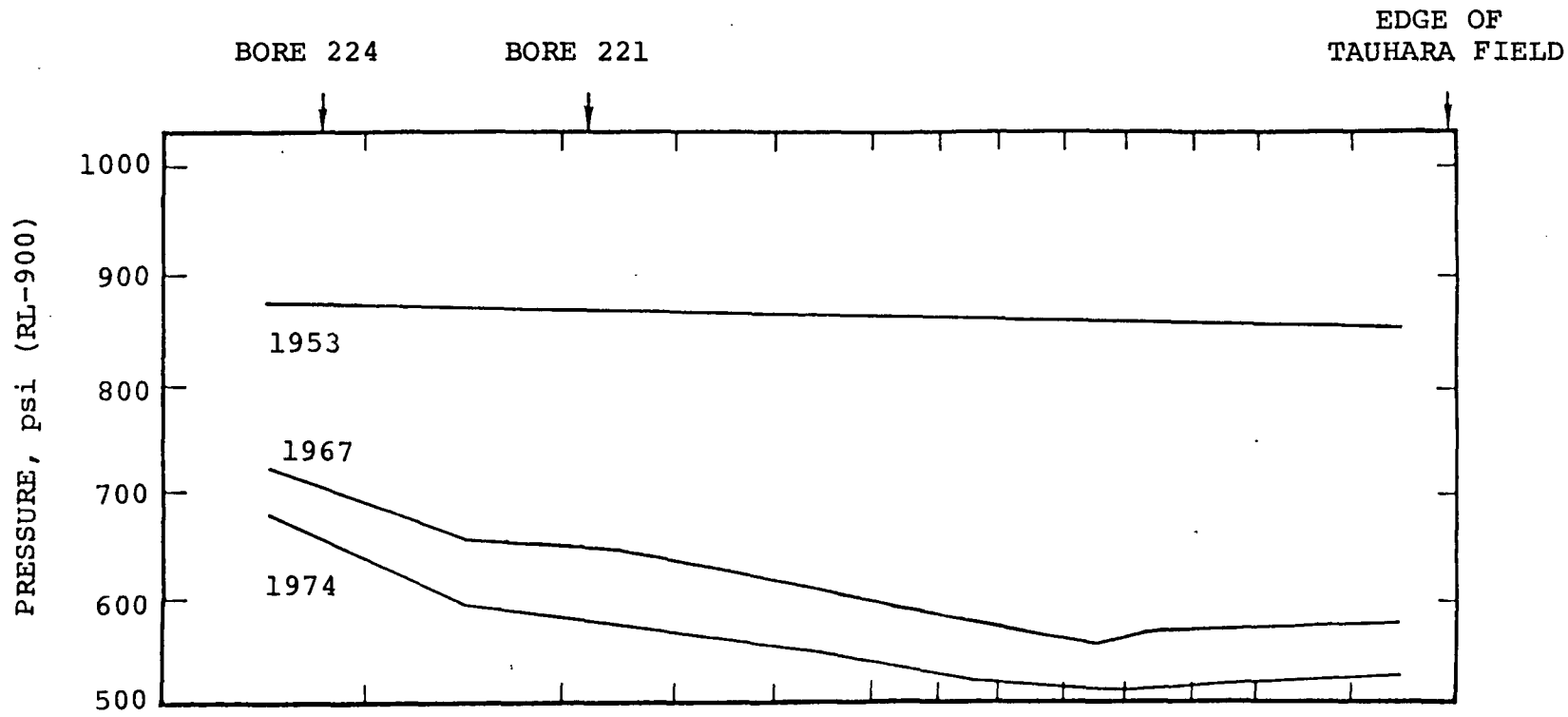

Figure 6.17. Pressure Distribution across the Cross-Section at RL-900 feet for years 1953, 1967 and 1974.

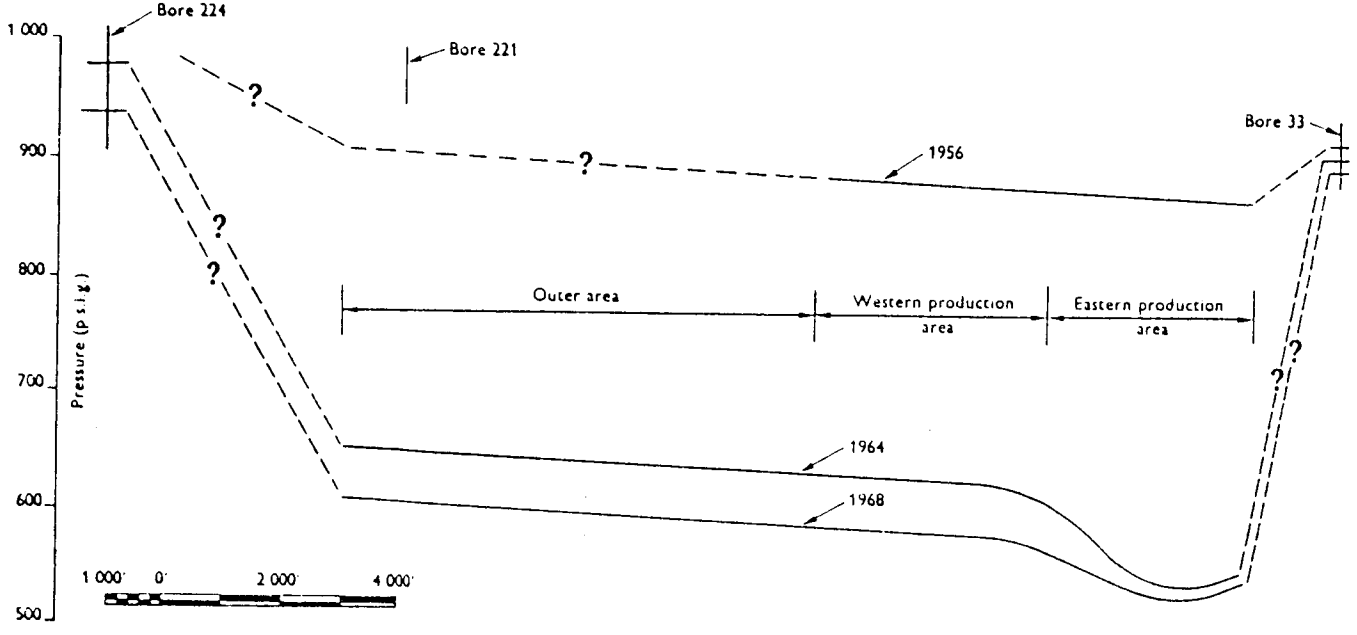

Figure 6.18. East-west pressure distribution at Wairakei at RL-900 for 1956, 1964 and 1968 [after Bolton, 1970].

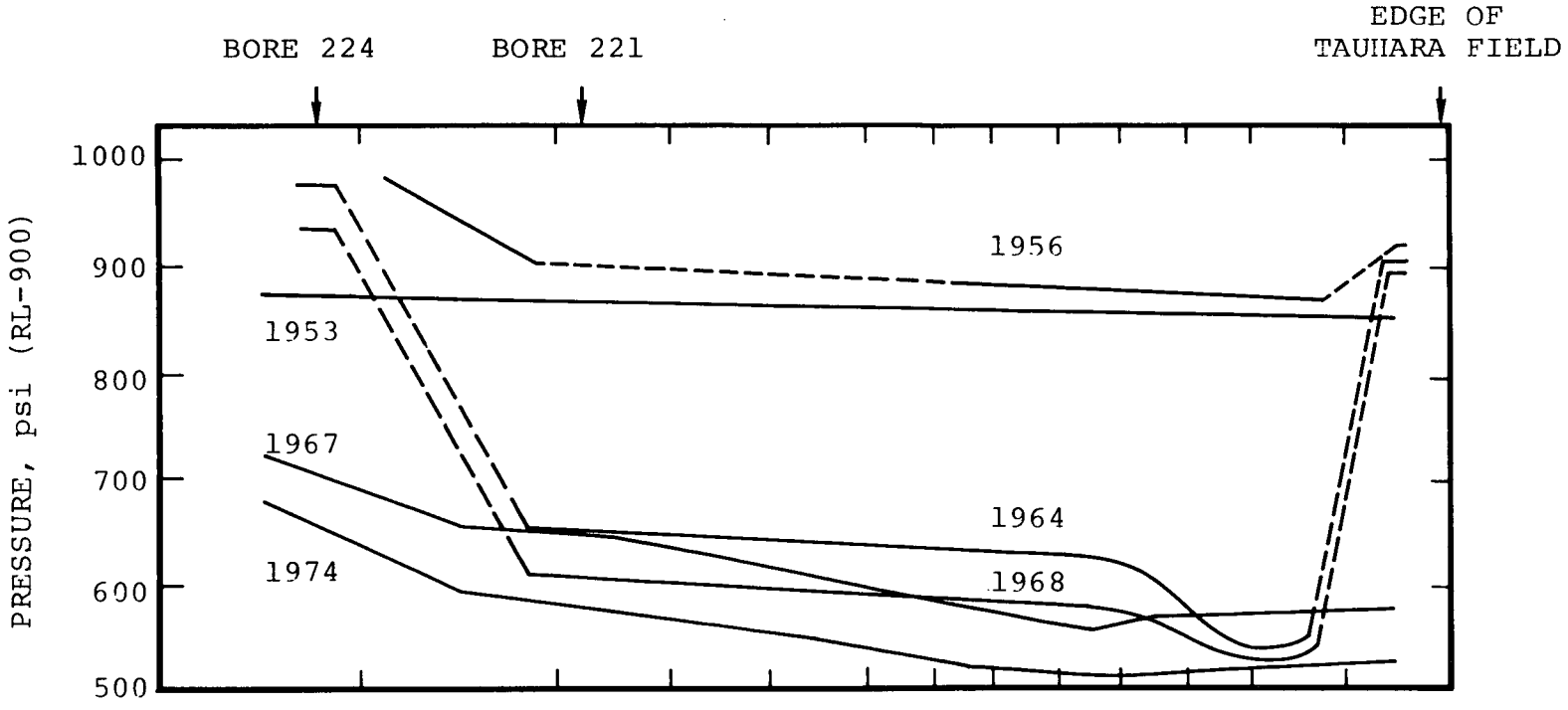

Figure 6.19. Comparison of calculated east-west pressure distribution at RL-900 feet with Bolton's (1970) data. Curves labeled 1953, 1967, and 1974 ∿ calculations; curves labeled 1956, 1964, and 1968 ∿ Bolton's data.

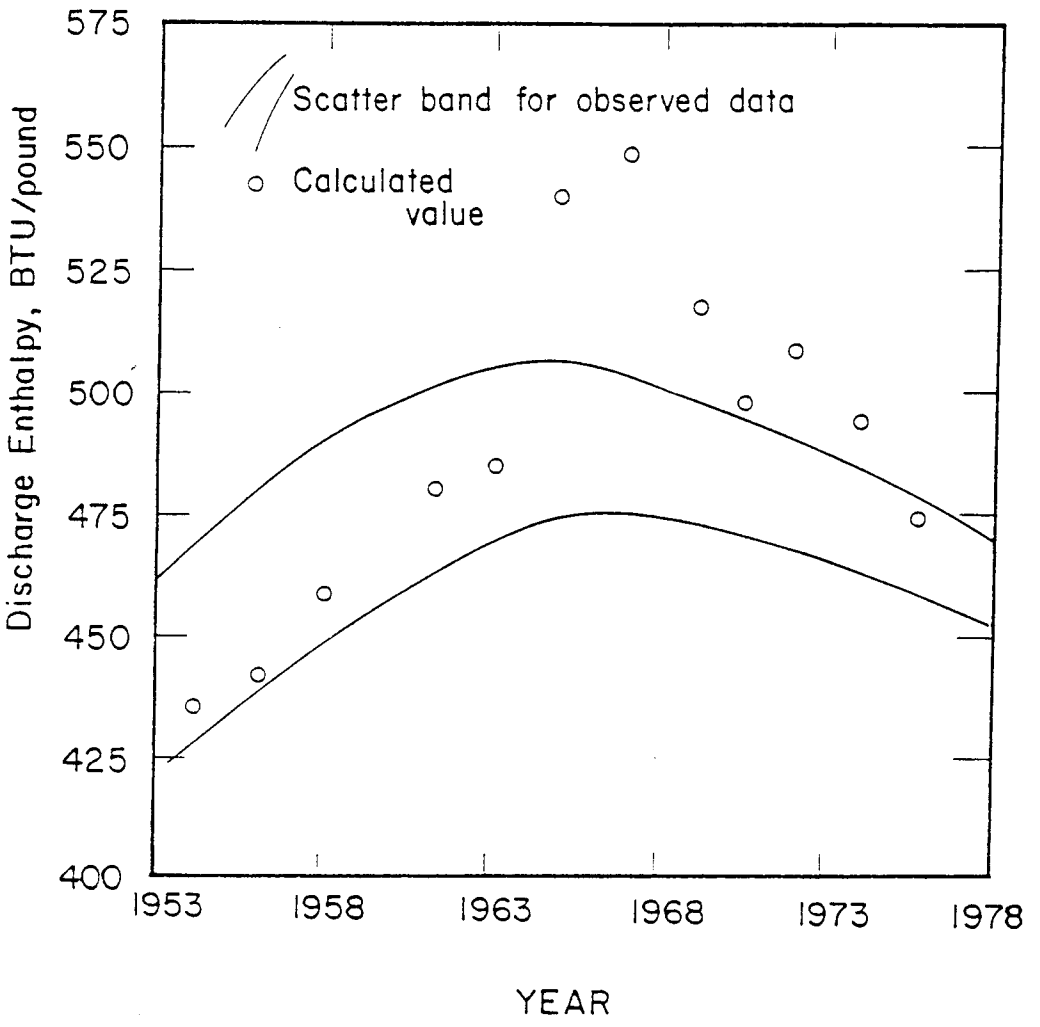

Figure 6.20. Field Discharge Enthalpy

Prediction of Future Performance

A single prediction of future performance of the reservoir, i.e., after 1976, was performed. The calculation was merely an extension of the matched performance up through 1976. The computer code was restarted at the end of 1976 and allowed to run for an additional 16 years. Production rates were held constant at the value used for 1976. Figure 6.21 shows the predicted pressure performance of the system. Figure 6.22 shows the predicted enthalpy of the produced fluid. There appears to be some cooling of the system as evidenced by the declining enthalpy, but the pressure seems to be holding fairly constant with a slight rise in pressure at the end of the simulated period.

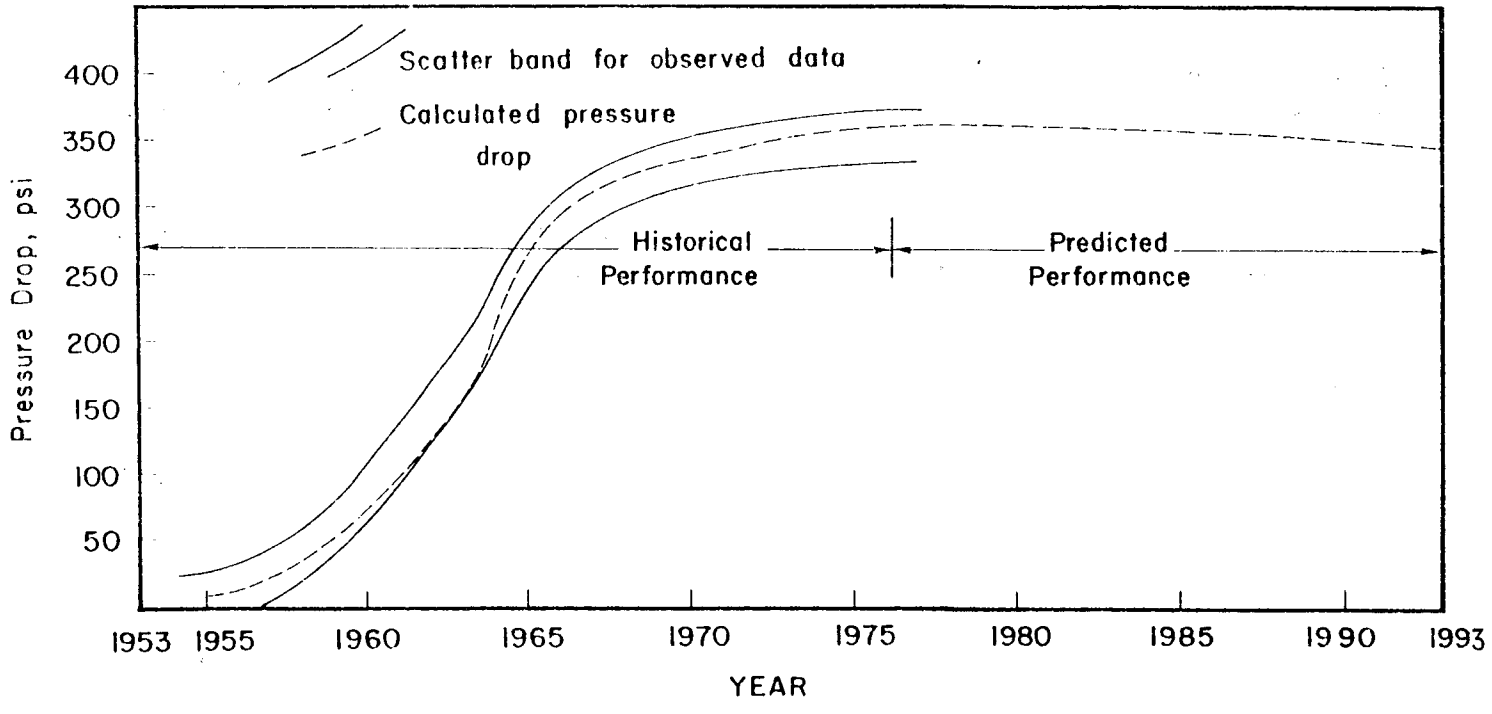

Figure 6.21. Predicted Reservoir Pressure Drop 1976 - 1993. Calculated Pressure Drop is at About RL-900 feet.

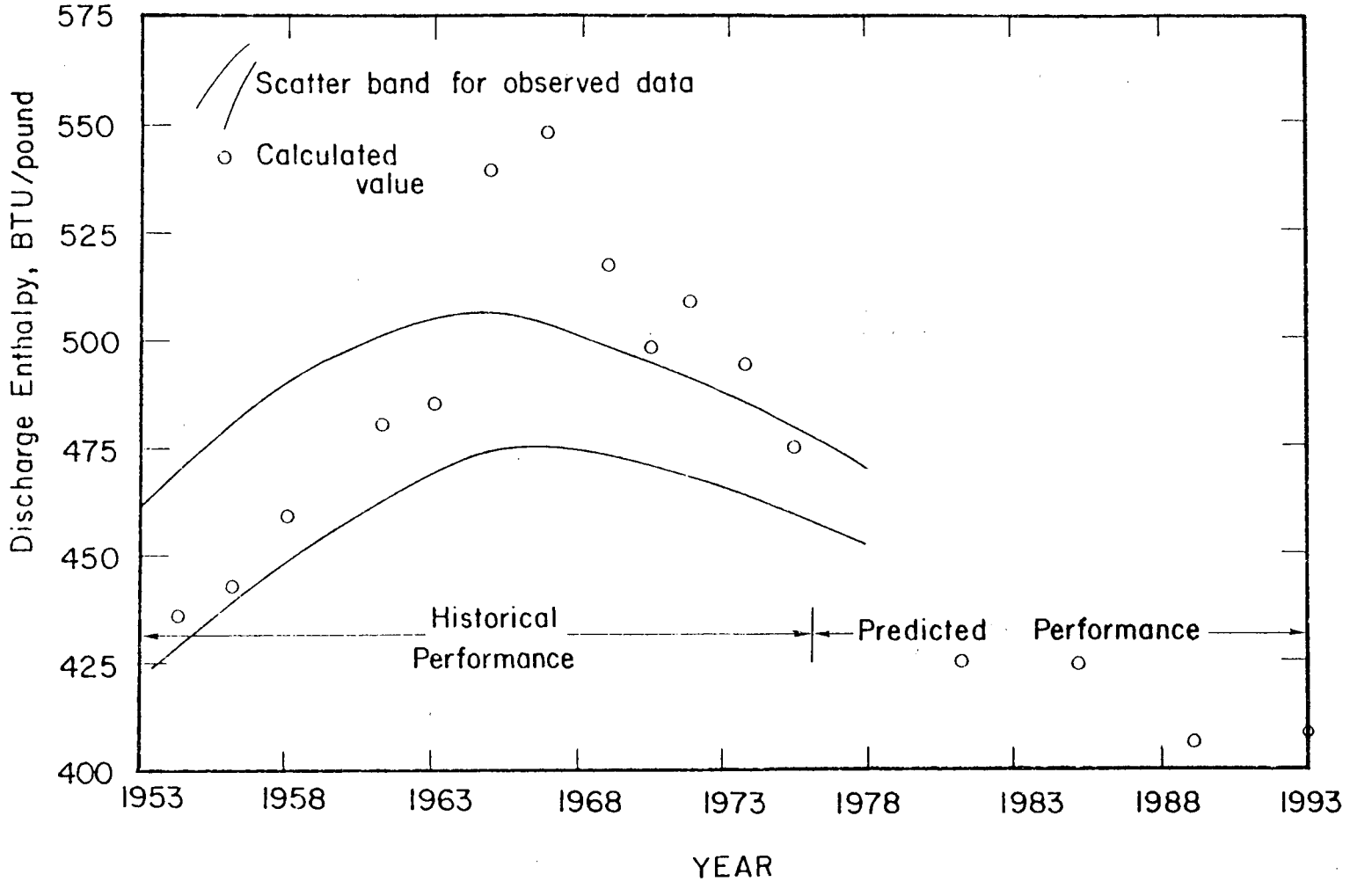

Figure 6.22. Predicted Discharge Enthalpy 1976-1993.

VII. LAND SUBSIDENCE AT WAIRAKEI

Ground subsidence at Wairakei was first measured in 1956 when benchmark levels were compared with those established in 1950 (Hatton [1970]). A subsidence network was then established, first on the steam main supports and then outward in the field. Periodic measurements have indicated that the area affected by subsidence exceeds 11.5 square miles (Bixley [1977]). The area of maximum subsidence (subsidence $\geq$ 0.5 m), however, lies outside the main production region. Maximum subsidence at Wairakei is of the order of 15 feet (4.5 m); this has been accompanied by horizontal movements of the order of 1.5 feet (0.5 m). Pritchett, et al. [1978] describe in detail the vertical and horizontal controls along with the measurements of ground deformation at Wairakei.

Land subsidence at Wairakei is believed to be due to the withdrawal of fluids from the Waiora aquifer. Fluid production has resulted in a pore pressure drop (in the deeper liquid regions of the Waiora aquifer) of approximately 350 psi. (It should, however, be noted here that the pressure drop is not uniform with depth. At the top of the Waiora aquifer, the observed pressure drop is only of the order of 150 psi.) One of the principal effects of a reduction in pore pressure (and possibly temperature) is a corresponding reduction in porosity ϕ. (Changes in pore pressure can also trigger other geological phenomena such as slippage along pre-existing faults etc.) For small deformations, changes in porosity are governed by the relation (Brownell, et al. [1977]):

$$\Delta\phi = \left[\frac{1}{K_s} - \frac{1-\phi}{K}\right] \Delta(P_c - P_f) + 3(1 - \phi)(\eta - \eta_s)\Delta T \qquad (7\text{-}1)$$

where

$K(K_s)$ = Bulk modulus of porous rock (rock grain)
$\eta(\eta_s)$ = Coefficient of linear thermal expansion of porous rock (rock grain)
P_c = Total or Confining Pressure
P_f = Fluid Pressure
ΔT = Change in fluid/rock temperature.

At Wairakei, the temperature change is relatively small (< 20°C), and we can, therefore, in a first order theory ignore the second term in the relation for $\Delta\phi$.

A general approach to modeling pore collapse/crack closure (and associated surface deformation) consists in solving the fluid flow and the stress-deformation equations in a coupled manner (Brownell, et al. [1977]). The stress-deformation field is, in general, three-dimensional. Since available data on subsidence and material properties at Wairakei are rather limited, the above mentioned approach appears to be unwarranted at this time. We will instead, following the previous work of Pritchett, et al. [1976] and of Narasimhan and Goyal [1979], utilize the simpler one-dimensional consolidation theory to study compaction at Wairakei.

One-dimensional consolidation theory can be obtained as a special case from the general three-dimensional coupled stress-deformation/fluid flow equations (Brownell,

et al. [1977]). In deriving the one-dimensional consolidation theory, it is necessary to assume the following conditions:

1. The reservoir undergoes primarily vertical compaction, and horizontal deformations are negligible. (This condition is, strictly speaking, not met at Wairakei. Maximum horizontal deformation is over 10 percent of the maximum vertical movement.)

2. The mass of fluid withdrawn is small so that the overburden remains essentially constant. (At Wairakei, recharge at the reservoir boundaries replaces most of the fluid produced from the reservoir such that the net fluid withdrawn is indeed small.)

3. The bulk modulus of the rock grain is much greater than the bulk modulus of the porous rock ($K_s >> K$).

Assumptions (1) and (2) imply that stress equilibrium is satisfied trivially. In this case, it is not necessary to explicitly solve the coupled stress-fluid flow equations; the vertical strain-rate is given by the relation:

$$\frac{\partial \varepsilon_z}{\partial t} = \frac{1}{h} \frac{\partial h}{\partial t} = C_m \frac{\partial P_f}{\partial t} \qquad (7\text{-}2)$$

where

h = formation thickness

C_m = $1/(K + 4/3\,\mu)$ = formation compressibility

μ = shear modulus of porous rock

ε_z = vertical strain

Furthermore, the porosity relationship becomes:

$$\frac{\partial \phi}{\partial t} = (1-\phi)\, C_m \frac{\partial P_f}{\partial t} \qquad (7\text{-}3)$$

To utilize the above strain-rate expression to predict land subsidence, we require (1) compressibility data for the various reservoir rocks, and (2) fluid pressure drop rate for the various formations. The fluid pressure drop rates can be obtained from the reservoir engineering calculations reported in the preceding chapters. Figure 7.1 shows the pressure drop distribution at the beginning of 1974 given by the two-dimensional cross-sectional model discussed in Chapter VI. The area of maximum subsidence lies close to the eastern end of the two-dimensional grid of Figure 7.1. The pressure drop is remarkably uniform (in the horizontal direction) in the eastern part of the field. In the area of maximum subsidence, the pressure drop (as of the end of 1973) averaged through thickness is approximately 23.5 bars ($\sim$ 340 psi) in the Waiora formation, and 8.7 bars ($\sim$ 125 psi) in the Huka formation. Note that the average pressure drop in the Huka mudstones is only a fraction ($\sim$ 1/3) of that in the Waiora formation; furthermore, little or no pressure drop occurs in the Pumice/Breccia formations overlying the Huka mudstones. For all practical purposes, the pressure drop history in the Waiora formation underlying the area of maximum subsidence can be

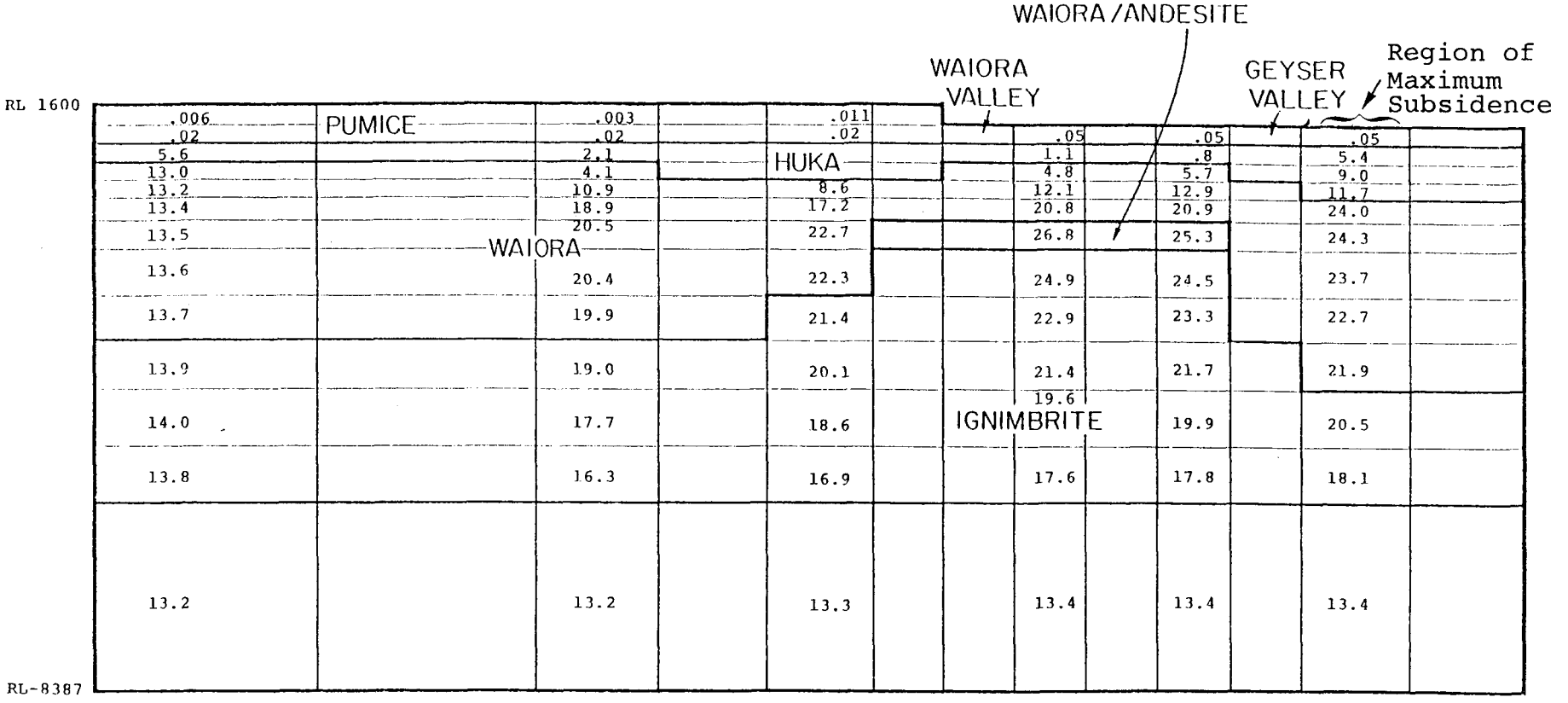

Figure 7.1. Spatial distribution of calculated pressure drop (in bars) at the beginning of 1974.

SSS-R-80-4313

taken to be identical with the field average. Also, for present purposes, it will suffice to assume that the pressure drop in the Huka mudstones at any given time is approximately one-third of the field average (really measured in the liquid part of the Waiora formation).

Pritchett, et al. [1976] report data on formation compressibilities (C_m) obtained from hydrostatic and triaxial tests in the laboratory. In general, the values for C_m measured in the laboratory ($C_{m\ Huka} = 0.25$ $(kb)^{-1}$; $C_{m\ Waiora} = 0.024$ $(kb)^{-1}$) are far too small to account for the observed vertical movement at Wairakei (Pritchett, et al. [1976]). The reservoir engineering calculations discussed in the preceding chapters clearly demonstrate that the reservoir behavior at Wairakei is governed by fractures, formation heterogeneities, and other large scale features such as faults. For such a system, it is reasonable to assume that the compaction (subsidence) behavior will be quite different from that predicted on the basis of laboratory measurements of C_m. One possible procedure for obtaining apparent in situ compressibilities is to back-calculate them from the observed pressure drop rates and the observed subsidence rates.

Figure 7.2 (from Stillwell, et al. [1975]) is a map of the Wairakei field showing both the areas of principal production and principal subsidence. Within the subsidence area and somewhat to the south of the center of the region is "Benchmark A-97", located at about the one-third (subsidence) amplitude contour near the main highway. Figure 7.3 shows, as a function of total

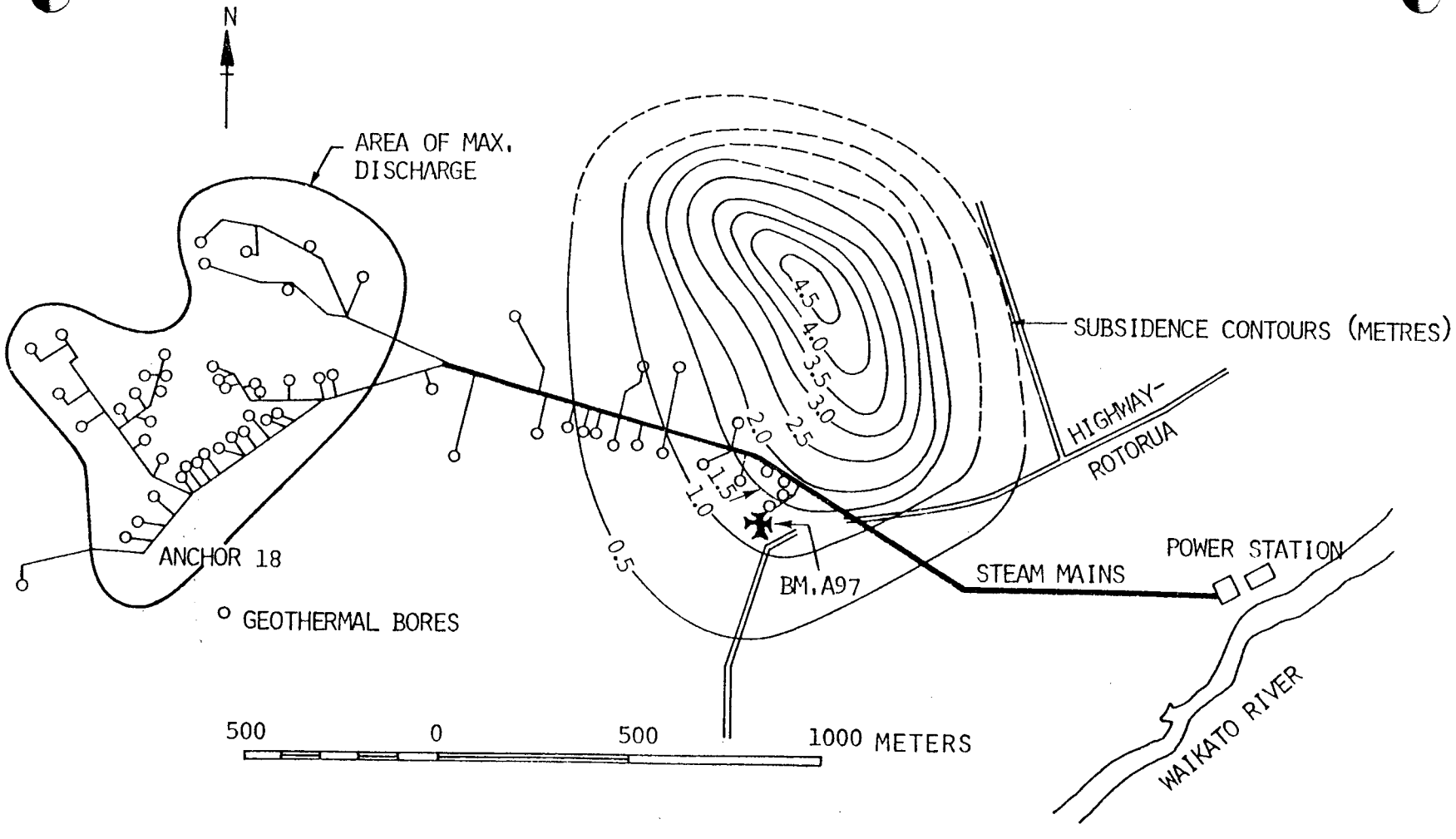

Figure 7.2. Total subsidence in meters at Wairakei during period 1964-1974 [Stillwell, et al., 1975].

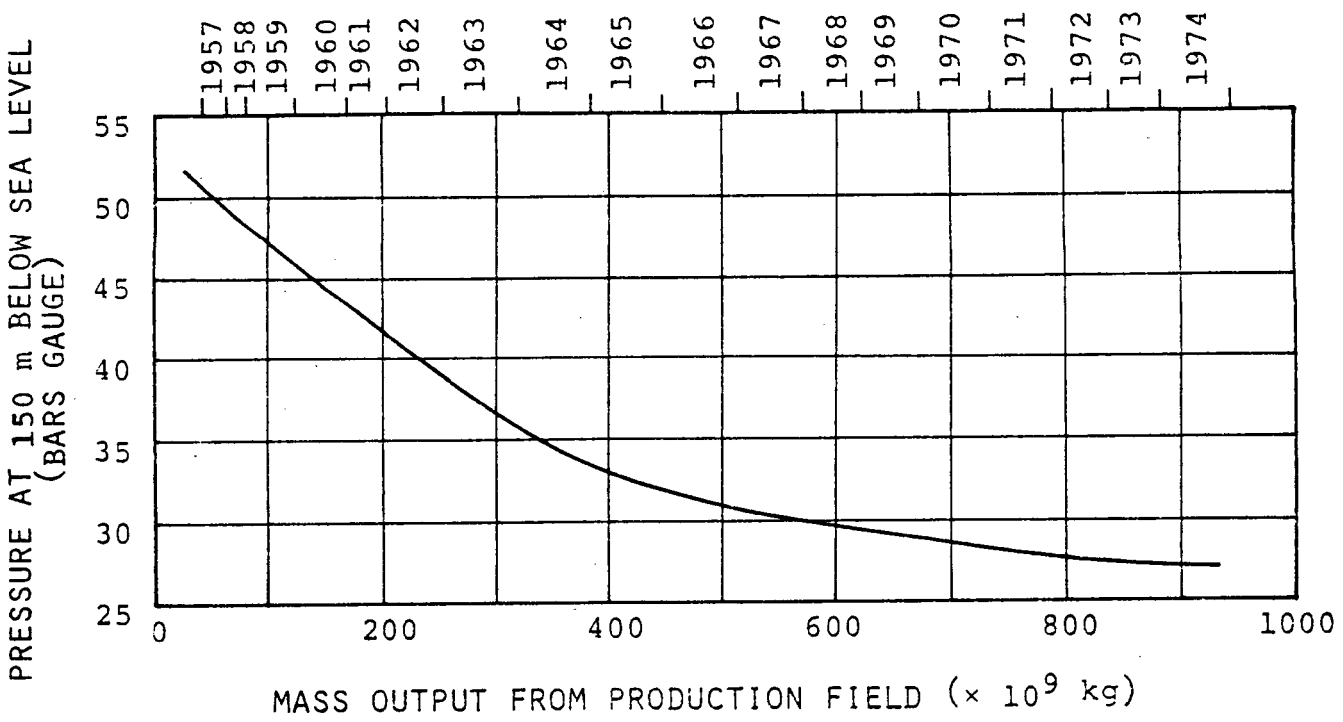

Figure 7.3. Pressure versus mass of fluid produced at Wairakei [Stillwell, et al., 1975].

fluid mass produced, the fluid pressure in the reservoir at 150 m below sea level; Figure 7.4 shows, on the same scale, the total vertical surface subsidence at Benchmark A-97. At early times, the pressure in the reservoir drops rapidly, but later on the pressure drops more and more slowly. The slope of the Benchmark A-97 subsidence versus total production curve, however, actually increases somewhat with time. At present, and for the past several years, the subsidence rate at Wairakei has remained essentially constant whereas the rate of pressure drop has declined continuously.

In Figure 7.5, the reservoir pressure drop is plotted as a function of the downward movement of Benchmark A-97 as deduced from the data presented in Figures 7.3 and 7.4. The "dots" denote time -- 1 January of the year indicated in each case. This plot strongly suggests that nonlinear ground movement processes are operating at Wairakei. At early times, the slope of this curve is 36 bars/meter of subsidence -- at present, the slope is 2.4 bars/meter, lower by a factor of 15 (It should be noted that these slopes are for subsidence -- approximately one-third maximum subsidence amplitude -- measured at Benchmark A-97. The corresponding slopes for the center of the subsidence bowl would be 12 bars/meter at early times and 0.8 bars/meter at present.) The apparent increase in rock compressibility at Wairakei with time is typical of many reservoirs (for a case study of an oil/gas reservoir see Merle, et al. [1976]). The nonlinear behavior can be explained if one assumes that the deforming material passes from a state of preconsolidation to one of normal consolidation (Merle, et al.

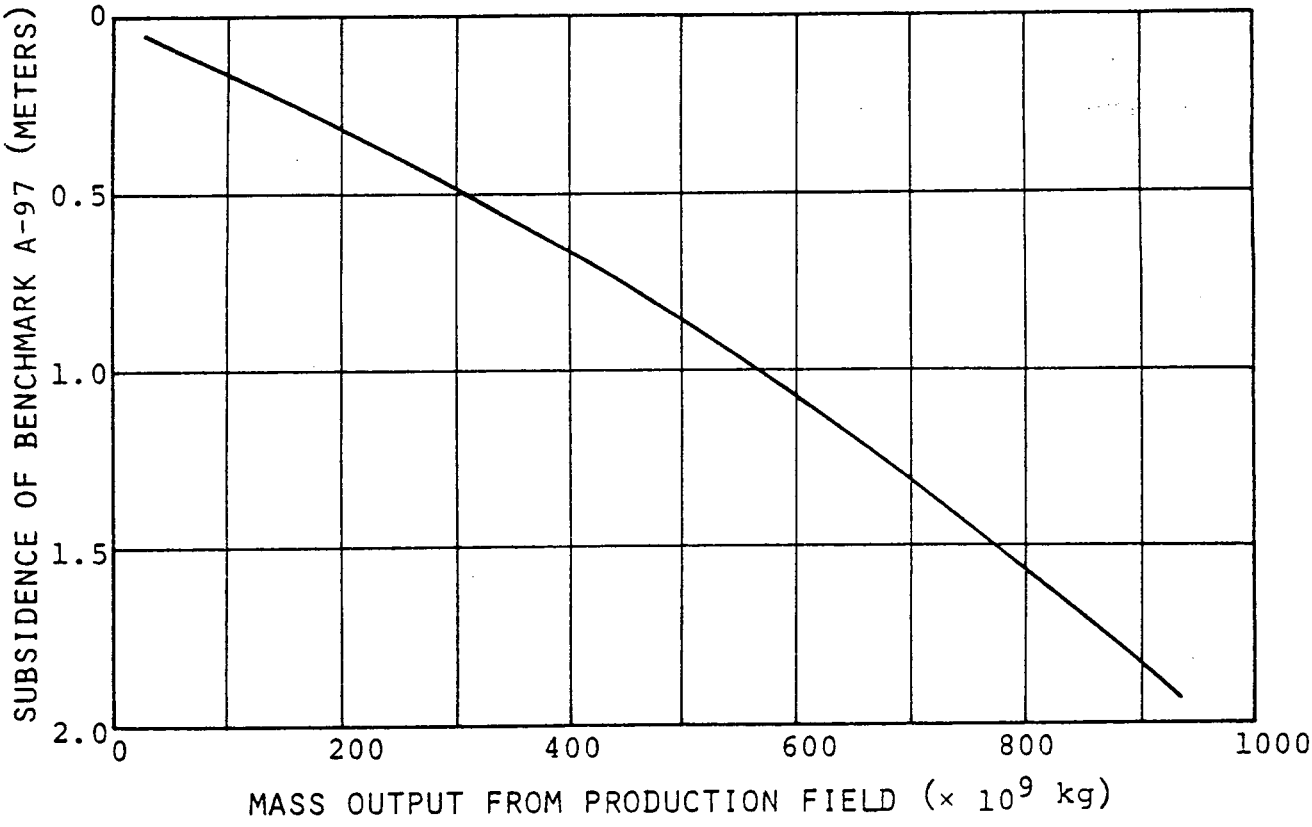

Figure 7.4. Subsidence at Benchmark A-97 versus mass of fluid produced at Wairakei [Stillwell, et al., 1975].

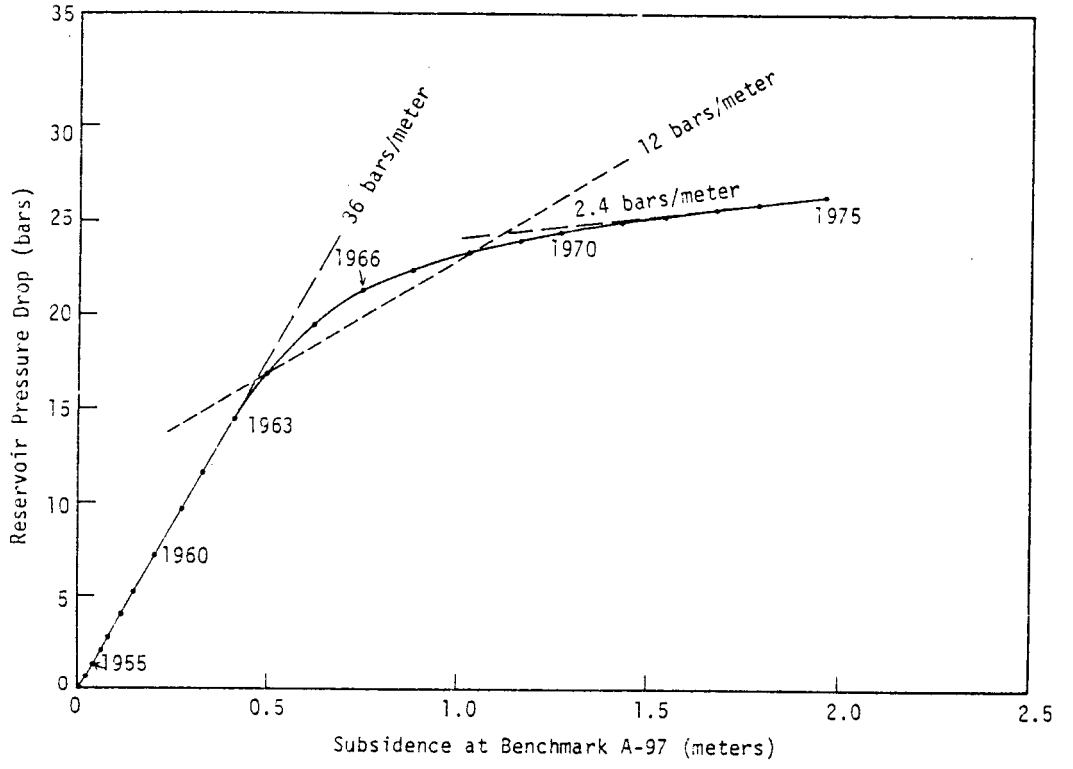

Figure 7.5. Wairakei subsidence data - reservoir pressure drop versus subsidence at Benchmark A-97.

[1976]; Narasimhan and Goyal [1979]). (Stated somewhat differently, the material exhibits a relatively low compressibility for (P_c-P_f) less than $(P_c-P_f)^*$, where $(P_c-P_f)^*$ denotes the maximum effective stress experienced by the material at some time in its geologic past. With continued fluid production, P_f decreases and eventually (P_c-P_f) exceeds $(P_c-P_f)^*$ at which point the material starts exhibiting a higher compressibility.) At Wairakei (see Figure 7.5), the formation appears to pass from a state of preconsolidation to normal consolidation around the beginning of 1964.

In order to calculate formation compressibility from the observed subsidence - pore pressure behavior, it is necessary to make certain further assumptions regarding the vertical distribution of total measured compaction. Pritchett, et al. [1976] assumed that approximately 90 percent of the compaction occurs in the Waiora formation. Although the exact thickness (h) of the Waiora formation in the region of maximum subsidence is not known (no deep wells have been drilled in this area), it does not in all likelihood exceed 1000 m. Given $\Delta h/\Delta p$ and h, formation compaction can be calculated from the following relation:

$$C_m = \frac{1}{h}\frac{\Delta h}{\Delta p}$$

If we take h_{Waiora} = 1000 m, then we obtain:

$$C_{m/Waiora} = \frac{0.9}{1000\ 12}\ \text{bars}^{-1} = 0.075\ (\text{kb})^{-1}\ \text{at early times}$$

$$= \frac{0.9}{1000\ (0.8)}\ \text{bars}^{-1} = 1.125\ (\text{kb})^{-1}\ \text{at late times}$$

Narasimhan and Goyal [1979] have also examined the subsidence behavior at Wairakei. The purpose of their study was "to make a preliminary study of the ground subsidence observed over the geothermal field at Wairakei, New Zealand and to find whether the field observations can be reasonably explained in terms of the well known geotechnical principles of consolidation." The "preliminary model, then, studies the effect of heterogeneity and plasticity on the subsidence phenomenon." More specifically, Narasimhan and Goyal assume that (1) most of the reservoir compaction occurs in the Huka mudstones, (2) the pressure drop in the Huka mudstones is approximately the same as that obtaining in the deeper Waiora formation and (3) the thickness of Huka mudstones in the region of maximum subsidence is 200 m. With these assumptions, Narasimhan and Goyal obtain the following values for Huka compressibilities:

$$C_{m/Huka} = \frac{1}{200\ (12)}\ \text{bars}^{-1} \sim 0.5\ \text{kb}^{-1} \text{ at early times}$$

$$= \frac{1}{200\ (0.8)}\ \text{bars}^{-1} \sim 5\ \text{kb}^{-1} \text{ at late times}$$

In actuality, the pressure drop in the Huka mudstones is only one-third of that in the Waiora aquifer. Also, in the area of maximum subsidence the Huka mudstones are only about 100 m thick. This implies that the compressibility values used by Narasimhan and Goyal should be raised by a factor of six. Thus

$$C_{m/Huka} \sim 3\ \text{kb}^{-1} \text{ at early times}$$

$$\sim 30\ \text{kb}^{-1} \text{ at late times}$$

The late time compressibilities (or virgin curve compressibilities) calculated by both Pritchett, et al. [1976] and Narasimhan and Goyal [1979] are extremely high; such large rock compressibilities have neither been measured in the laboratory nor observed in the field.*

Since the rock compressibilities required to explain the observed subsidence amplitude are far too large to be plausible, the question arises if the postulated subsidence mechanism (i.e., reduction in porosity with a drop in fluid pressure) is correct. Any model of subsidence, to be acceptable, should explain not only the subsidence amplitude but also the spatial distribution of ground deformation. At Wairakei, the area of principal subsidence encompasses the eastern part of the principal production area; no subsidence has been measured in the western half of the Wairakei field. Also, the region of maximum subsidence lies outside (although within the resistivity boundary of the Wairakei geothermal field) the production area. In their preliminary phenomenological study Narasimhan and Goyal [1979] assume that the zone of maximum subsidence coincides with the maximum thickness of Huka Falls formation (These authors use an idealized graded thickness of Huka Falls formation varying from 40 m

* In a personal communication to the present authors, Narasimhan and Goyal have taken issue with this view. Narasimhan and Goyal state that the present authors "fail to recognize that Huka Falls is a relatively shallow sandstone of lacustrine origin deposited during the interglacial periods. Geologically it is relatively young. Therefore, one should not be surprised if the in situ compressibility in fact proves to be far higher than the authors may want to believe. A porosity as high as 20 percent of the Huka Falls formation, as assumed by the authors in their simulation, makes our point even stronger."

in the principal production area to 200 m in the zone of maximum subsidence.). Available geologic evidence does not however appear to support this assumption. Figure 7.6 shows the subsidence and production areas superimposed on the isopachs for the Huka Falls formation. We also show in Figure 7.6 the control wells (Nos. 32, 33, 36 and 2A) used to infer the Huka Falls formation thickness in the eastern part of the Wairakei geothermal field. Clearly, the observed ground deformation does not correlate with the thickness of the Huka Falls formation. The control wells 2A, 32, 22 and 36 are relatively shallow wells and have not encountered the base of the Waiora formation; thus we have no direct knowledge of the deeper geologic structure in this part of the field. However, given the general geologic continuity between the Wairakei and Tauhara regions, there exists little reason at present to assume that the observed ground deformation can be correlated with the thickness of the Waiora formation as assumed by Pritchett, et al. [1976].

The foregoing discussion illustrates the difficulties associated with trying to explain the subsidence behavior at Wairakei by the simple pore collapse mechanism.* We are at present inclined to reject pore collapse/crack closure as the principal mechanism responsible for the observed ground deformation at

* As suggested by Narasimhan and Goyal, the pore collapse mechanism can be made to reproduce the observed subsidence history by assuming that the formation compressibility C_m is spatially varying. Such an approach, while feasible in principle, is however unlikely to yield either any understanding of the causative mechanisms or provide a reliable predictive model.

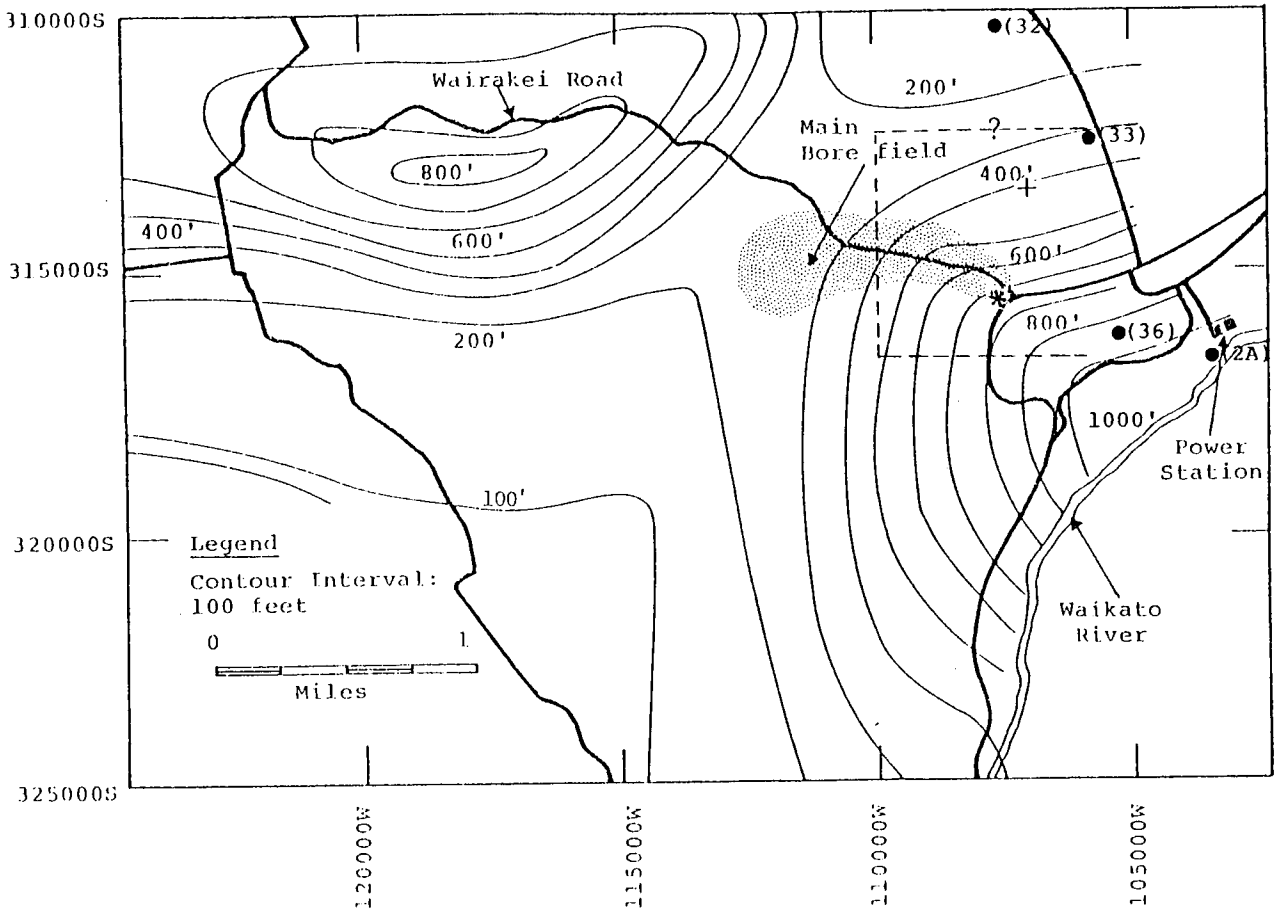

Figure 7.6. The region of maximum subsidence (dashed line) superposed on the isopach of the Huka Falls formation, in feet. Note that the northern limit of the subsidence region (indicated by --?--) has not been delineated by measurements. * - Benchmark A-97; + - center of subsidence bowl; ● (10) - control wells.

SSS-R-80-4313

Wairakei. In attempting to come up with an alternate mechanism, we note that the center of the major subsidence bowl lies rather close to the resistivity boundary for the Wairakei geothermal field. The resistivity boundary, in this part of the field, appears to coincide with the hydrologic boundary of the field (The evidence for this comes principally from the observed pressure response in well 33. Well 33 appears to have little, if any, connection to the field.). We also note here that in the early days of the development of the Wairakei geothermal field, there existed two zones at Wairakei (the present region of maximum subsidence, and a region near Karapiti) which were subsiding rapidly. The zone at Karapiti - an area of natural thermal activity about 2 miles south of the production field - was the most rapidly subsiding part of the field until about 1963, when the subsidence rate decreased to the same rate as for the surrounding ground surface. Around 1960, the subsidence rate at benchmark A97 began to increase and over the next several years the zone of rapid subsidence immediately north of the eastern production field (i.e., the present zone of large subsidence) was delineated. In any event, we wish to emphasize here that the earlier zone of subsidence at Karapiti, like the present region of maximum subsidence, lies close to the margin of the geothermal field.

The fact that maximum subsidence occurs near the edge of the geothermal field suggests that local phenomena are responsible for the observed ground deformation. One possible mechanism is aseismic slippage along pre-existing buried faults in response to local changes in fluid pressure. If the fault acts as a barrier to fluid migration (i.e., the fault acts as a sealing boundary),

then production on one side of the fault can lead to greater pore pressure decline on the producing side of the fault than on the other side. This differential pore pressure decline can cause movement on the fault which will be manifested at the surface as differential movement across the surface trace of the fault. Such behavior has been observed at several oil/gas fields along the Texas Gulf Coast. Fluid (oil and gas) production from the Saxet field (Texas) has resulted in a 6-foot scarp along a segment of the surface extrapolation of a regional growth fault. In the Chocolate Bayou Field, subsidence increases near an extrapolated fault (see Gustavson and Kreitler [1976] for a detailed discussion of the subsidence behavior along the Texas Gulf Coast).

Since at present the deep geologic structure in the region of maximum subsidence is not well defined, the suggestion that aseismic slip on a buried fault is responsible for the observed subsidence behavior must be regaded as speculative. This hypothesis is, however, not far-fetched in view of the facts that (1) the Wairakei region is traversed by many faults some of which have no surface manifestation, and (2) the maximum subsidence occurs near the hydrologic boundaries of the field (A hydrologic boundary must in some sense relate to the local geologic structure such as a region of low permeability or a sealing fault). In any event, it is our belief that the subsidence behavior at Wairakei is intimately tied with local subsurface geology. The present knowledge of subsurface geology in the subsidence region is, however, too poor to permit a definitive evaluation of the mechanism or mechanisms responsible for subsidence at Wairakei. The modeling of subsidence response must follow rather than precede an understanding of the underlying mechanisms.

VIII. CONCLUSIONS AND RECOMMENDATIONS

As discussed in the previous section, subsidence at Wairakei is probably controlled by discontinuous effects of undetermined character, rather than by continuum behavior such as pore collapse. This latter model is apparently inappropriate for Wairakei, owing both to the unrealistically high rock compressibilities required to explain the observed deformation and to the apparent lack of correlation between the subsidence pattern and the known stratigraphy of the region. Since no evidence exists which permits the identification of the physical mechanism responsible for the observed subsidence at Wairakei, the expenditure of additional effort to simulate the behavior based on various speculative phenomenological models is not warranted. Such an approach, while feasible, is unlikely to cast light on the fundamental physical phenomena involved. Unless more field data becomes available (such as might arise were drilling to be undertaken in the subsiding region), the basic cause for the observed ground motion will remain obscure.

As regards information of interest for more conventional reservoir engineering (such as history-matching of production, pressure drop, discharge enthalpy and the like, and forecasts of future performance), the situation is much more encouraging. As described in Chapter VI, a reasonably successful two-dimensional (vertical) simulation has been carried out, which incorporates the effects of subsurface geological structure, surface and deep recharge, and other

realistic effects. This simulation produced a very good match to the observed pressure history; measured discharge enthalpies are also reasonably well reproduced, except that computed values are slightly high at late times.

Predictive calculations using this two-dimensional model indicate that, if mass production rates are maintained at approximately the present level reservoir pressure in the future will remain essentially constant. Discharge enthalpies will continue to decline, however, at an average rate of five to ten BTU/pound/year. Thus, the eventual demise of the Wairakei geothermal power system will probably come about due to thermal degradation rather than reservoir depletion in the classical sense. Quantitatively, this forecast may be too optimistic since, as noted above, the two-dimensional model overestimates late-time discharge enthalpies somewhat. This shortcoming can probably be overcome by inclusion of three-dimensional effects, in particular declines in temperature to the north and south of the borefield.

It is indeed unfortunate that it was impossible to complete the three-dimensional work and obtain a good history match. Obviously, the next step is to complete this work. Predictive calculations may then be carried out with a high level of confidence to examine alternate future production strategies and devise optimum exploitation techniques.

REFERENCES

Banwell, C. J. [1955], "Physical Investigations," in Geothermal Steam for Power in New Zealand (L.I. Grange, compiler), D.S.I.R. Bull. 117.

Bixley, P. F [1977], "Land Subsidence in the Wairakei Geothermal Field," unpublished manuscript.

Bolton, R. S. [1977], Private Communication to J. W. Pritchett.

Bolton, R. S. [1970], "The Behavior of the Wairakei Geothermal Field During Exploitation," Proc. U. N. Symp. on the Dev. and Util. of Geothermal Resources, Pisa, Geothermics Special Issue 2, pp. 1426-1449.

Brownell, D. H., Jr., S. K. Garg and J. W. Pritchett [1977], "Governing Equations for Geothermal Reservoirs," Water Resources Research, 13, pp. 929-934.

Dawson, G. B. and D. J. Dickinson [1970], "Heat Flow Studies in Thermal Areas of the North Island of New Zealand," Proc. U. N. Symp. on the Dev. and Util. of Geothermal Resources, Pisa, Geothermics, Special Issue 2, pp. 466-474.

Fisher, R. G. [1964], "Geothermal Heat Flow at Wairakei During 1958," N.Z.J. Geol. Geophys., 7, pp. 172-184.

Garg, S. K. [1978], "Pressure Transient Analysis for Two-Phase (Liquid Water/Steam) Geothermal Reservoirs," SPE preprint No. 7479.

Grange, L. I. [1937], The Geology of the Rotorua-Taupo Sub-division, Rotorua and Kaimanawa Divisions, D.S.I.R., Bull. 37.

Grant, M. A. [1977], "Broadlands - A Gas Dominated Geothermal Field," in Geothermics, Vol. 6, pp. 9-29.

Grindley, G. W. [1974], "Wairakei, Tauhara Geothermal Fields," Part D, Sections 3.20 and 3.21, Minerals of New Zealand, N.Z.G.S. Report 38.

Grindley, G. W., D. E. Rishworth and W. A. Watters [1966], "Geology of the Tauhara Geothermal Field, Lake Taupo," D.S.I.R. Geological Survey Geothermal Report No. 4.

Grindley, G. W. [1965], The Geology, Structure and Exploitation of the Wairakei Geothermal Field, Taupo, New Zealand, D.S.I.R. Bull. n.s. 75.

Grindley, G.W. [1957], "Geothermal Power," in Science in New Zealand, (F. R. Callaghan, Editor), Reed, Wellington.

Gustavson, T. C. and C. W. Kreitler [1976], "Geothermal Resources of the Texas Gulf Coast - Environmental Concerns Arising from the Production and Disposal of Geothermal Waters," University of Texas at Austin, Bur. Econ. Geology, Circular 76-7.

Hatton, J. W. [1970], "Ground subsidence of a Geothermal Field During Exploitation, Proc. U. N. Symp. on the Dev. and Util. of Geothermal Resources, Pisa, Geothermics, Special Issue 2, pp. 1294-1296.

Healy, J. [1965], "Geology of the Wairakei Geothermal Field," Proc. Eighth Commonwealth Mining and Metallurgical Congress, Australia and New Zealand, New Zealand Section.

Mercer, J. W. and C. R. Faust [1979], "Geothermal Reservoir Simulation III: Application of Liquid- and Vapor-Dominated Hydrothermal Techniques to Wairakei, New Zealand," Water Resources Research, 15 (in press).

Mercer, J. W., G. F. Pinder and I. G. Donaldson [1975], "A Galerkin Finite-Element Analysis of the Hydrothermal System at Wairakei, New Zealand," J. Geophys. Res., 80, pp. 2608-2621.

Merle, H. A., C. J. P. Kentie, C. H. C. van Opstal and G. M. E. Schneider [1976], "The Bachaquero Study - A composite Analysis of the Behavior of the compaction Drive/Solution Gas Drive Reservoir," Journal of Petroleum Technology, pp. 1107-1115.

Narasimhan, T. N. and K. P. Goyal [1979], "A Preliminary Simulation of Land Subsidence at the Wairakei Geothermal Field in New Zealand," Summaries Fifth Workshop Geothermal Reservoir Engineering, Stanford University, Stanford, 1979.

Pritchett, J. W. [1979], "Vertical Two-Phase Flow in Geothermal Reservoirs," Systems Science and Software, Report SSS-R-80-4341.

Pritchett, J. W., S. K. Garg, D. H. Brownell, Jr., L. F. Rice, M. H. Rice, T. D. Riney and R. R. Hendrickson [1976], "Geohydrological Environmental Effects of Geothermal Power Production -- Phase IIA," Systems, Science and Software, Report SSS-R-77-2998.

Pritchett, J. W., L. F. Rice and S. K. Garg [1978], "Reservoir Engineering Data: Wairakei Geothermal Field, New Zealand," Systems, Science and Software, Report SSS-R-78-3597.

Rishworth, D. E. [1967], "Interim Correlations of Tauhara Monitor Holes," D.S.I.R. Geothermal Circular DEHR/2.

Sorey, M. [1978], "Wairakei Models," New Zealand Department of Scientific and Industrial Research, unpublished manuscript.

Stillwell, W. B., W. K. Hall and J. Tawhai [1975], "Ground Movement in New Zealand Geothermal Fields," Proc. Second U. N. Symp. on the Dev. and Use of Geothermal Resources, San Francisco, pp. 1427-1434.